PORTABLE CHEMICAL ANALYZERS FOR QUANTITATIVE ANALYSIS OF RENAL DYSFUNCTION MARKERS IN HUMAN URINE

ARJNARONG MATHAWEESANSURN

A THESIS SUBMITTED IN PARTIAL FULFILLMENT OF THE REQUIREMENT FOR
THE DEGREE OF DOCTOR OF PHILOSOPHY IN APPLIED CHEMISTRY
DEPARTMENT OF CHEMISTRY FACULTY OF SCIENCE
KING MONGKUT'S INSTITUTE OF TECHNOLOGY LADKRABANG
2019

KMITL-2019-SC-D-010-029

PORTABLE CHEMICAL ANALYZERS FOR QUANTITATIVE ANALYSIS OF RENAL DYSFUNCTION MARKERS IN HUMAN URINE

ARJNARONG MATHAWEESANSURN

A THESIS SUBMITTED IN PARTIAL FULFILLMENT OF THE REQUIREMENT FOR
THE DEGREE OF DOCTOR OF PHILOSOPHY IN APPLIED CHEMISTRY
DEPARTMENT OF CHEMISTRY FACULTY OF SCIENCE
KING MONGKUT'S INSTITUTE OF TECHNOLOGY LADKRABANG
2019

KMITL- KMITL-2019-SC-D-010-029

Thesis Title	Portable chemical analyzers for quantitative analysis of renal dysfunction markers in human urine
Student Name	Mr. Arjnarong Mathaweesansurn
Student ID	56605002
Degree	Doctor of Philosophy (Applied chemistry)
Department	Chemistry
Year	2018
Thesis Advisor	Asst. Prof. Dr. Nathawut Choengchan

Abstract

In this work, two portable chemical analyzers for quantitative analysis of renal dysfunction markers were presented. The first prototype was developed based on using a smart mobile phone embedded with an application for measurement of urinary albumin. Detection reaction of albumin is based on its association with tetrabromophenolphthalein ethyl ester in the presence of acetate buffer (pH 3.1) and Triton X-100. The prototype was composed of mobile phone, sample cassette and test paper. The test paper was designed to contain the standard colorimetric strip and the space for situating of sample cassette. Analytical workflows were started by transferring sample and reagents into the cassette. The cassette was shaken (2 min) and then placed onto the test paper. The images of standard colorimetric strip and sample were simultaneously captured under the same illumination by the mobile phone's camera. The color intensity of the developed product was evaluated and converted to the albumin concentration via the application. The urinary albumin concentrations were validated with the results obtained by the spectrophotometric method. By means of the Bland–Altman plot, the results were not significant different. Average recovery and RSD values were observed at 98 ± 1 % and 2.5 %, respectively. This implies that this analyzer provided high accuracy and high precision.

The second prototype was the portable LED spectrometer which was fabricated for measurement of urinary creatinine and uric acid. For determination of creatinine, detection principle is based on aggregation of gold nanoparticles (AuNPs) in the presence of creatinine which results in color change of the AuNPs solution from red-wine to purple. The AuNPs was synthesized accordingly to the modified Turkevich method using the reused-gold leaf as a starting material instead of standard gold (III) salt for more cost-effective preparation. The results showed that the properties of the gold leaf-prepared AuNPs were the same as the ones prepared

from standard gold (III) salt. Colorimetric response of the AuNPs was linear to the standard creatinine concentration up to 200 mg L^{-1} with good linearity (r^2 > 0.99). The limit of detection ($y_B + 3S_B$) was 0.23 mg L^{-1}. Good recoveries (102.2 ± 3.7 %) and fast analysis time (3 min) were achieved. The proposed method was applied to human urine samples and the results were compared to the results obtained by the HPLC method. By means of the Bland-Altman plot, there was no evidence of significant difference among the compared methods. This implies that the proposed method is high accuracy. For determination of uric acid, the colorimetric reaction between uric acid and phosphotungstate where the blue-colored product is developed, is employed as a detection reaction. Working range from 4.46 to 62.44 mg dL^{-1} was obtained with good linearity (r^2 > 0.99). The method also provided high precision (RSD: < 5.7 %) and high accuracy (Average recovery: 92.8 ± 2.7 %). The limit of detection ($y_B + 3S_B$) was found at 2.33 mg dL^{-1}. The uric acid concentrations, determined by the proposed method and by the spectrophotometric method were not significant difference by the Bland-Altman plot. These indicated that the developed method was suitable for real use.

Keywords: mobile phone-based analyzer, LED spectrometer, albumin, creatinine, uric acid, urine.

Acknowledgments

First of all, I would like to give my sincere thanks to my major advisor, Asst. Prof. Dr. Nathawut Choengchan from Department of Chemistry, Faculty of Science, King Mongkut's Institute of Technology Ladkrabang for his kindness and supports throughout my Ph.D. study.

I would like to thank Asst. Prof. Dr. Nuanlaor Ratanawimarnwong, a thesis external examiner from Department of Chemistry, Faculty of Science, Srinakharinwirot University, for her valuable guidance and scientific comment. I would also like to thank my thesis advisory committees including, Asst. Prof. Dr. Wiboon Praditweangkum, Asst. Prof. Dr. Ekarat Detsri and Asst. Prof. Dr. Saowapak Teerasong from Department of Chemistry, Faculty of Science, King Mongkut's Institute of Technology Ladkrabang, for their useful suggestions for my thesis.

I would like to acknowledge Assoc. Prof. Dr. Chutima Matayatsuk Phechkrajang and Miss Putthiporn Khongkaew, from Department of Pharmaceutical Chemistry, Faculty of Pharmacy, Mahidol University and Mr. Sorawit Jitnok, from Ladkrabang hospital for their kindness on doing validation experiments.

I would also like to acknowledge Asst. Prof. Dr. Noppadol Maneerat and Mr. Santikon Amnuayphol, from Department of Control Engineering, Faculty of Engineering, KMITL, for their contributions in the development of mobile application and LED spectrometer.

I would like to acknowledge Graduate School, Srinakharinwirot University for awarding a gold medal for my work, 'Albumin Smart Test', in the 32th National Graduate Research Conference. I also would like to acknowledge Wat Sothorn Wararam Worawihan for donating of reused gold leaf.

Financial and Instrumental supports from Department of Chemistry, Faculty of Science, King Mongkut's Institute of Technology Ladkrabang and FIRST Labs @ KMITL as well as Applied Analytical Chemistry Research Unit are acknowledged.

All contributions from my friends and colleagues in Applied Analytical Chemistry Research Unit are also acknowledged. Finally, I would like to thank my family for their eternal love and care throughout my life.

Mr. Arjnarong Mathaweesansurn

Contents

List of Tables

List of Figures

Abbreviations / Symbols

HSA	Human serum albumin
TBPE	Tetrabromophenolphthalein ethyl ester
AuNPs	Gold nanoparticles
PVA	Polyvinyl alcohol
SPR	Surface Plasmon Resonance
LSPR	Localized Surface Plasmon Resonance
LED	Light emitting diode
nm	Nanometer
mg	Milligram
dL	Deciliter
SD	Standard deviation
RSD	Relative standard deviation
r^2	Coefficient of determination
LOD	Limit of detection
LOQ	Limit of quantitation

Chapter 1
Introduction

1.1 Research Motivation

Instrumental method of analysis is one kind of the methods for quantitative analysis. There are a large numbers of the instrumental methods that have been developed for environmental monitoring of pollutants, quality control of food/beverages and clinical diagnosis. The important advantage of the instrumental method is that it provides precise and accurate results. However, there are some drawbacks of the instrumental method. In Thailand, as well as the other developing countries, most of the equipment are imported, cost of the instruments are therefore highly expensive (compared to the classical methods). The method also requires high skill and well-training user. Some instrumental methods employed long analysis time, especially, separation techniques. In addition, dimension of the instrument is usually bulky and this leads the method to be applied for only laboratory use. Application to 'in-situ' analysis/monitoring is restricted. Therefore, in this work, we aim to develop the methods for quantitative analysis based on using the 'in-house' and 'portable' analyzer for the sake of rapid analysis and cost-effectiveness. The analyzers were developed for some clinical applications which are summarized in the following issues:

1.1.1 Mobile phone-based analyzer for measurement of urinary albumin

Albumin is a protein synthesized by the liver and is one of the most abundant proteins in blood fluid or plasma. Molecular size of albumin is too large to pass through kidney's filters. Usually, the albumin concentration in urine is very low excepting in case of renal dysfunction such as diabetic nephropathy. Therefore, the content of albumin in urine can be used as a marker for indication of kidney damage. Urinary albumin concentration of lower than 30 mg L^{-1} is regarded as normal. The concentration that fall in the range of 30 – 300 mg L^{-1} is denoted as 'microalbuminuria' which is relevance to preliminary stage of kidney failure. The concentration of greater than 300 mg L^{-1} is considered as 'albuminuria' or 'proteinuria' which represents severe stage.

The turbidimetric immunoassay method is commonly used to measure urinary albumin in hospital laboratory. The advantages of this method are high selectivity, precision and high accuracy. However, this method is complicated and consumed long analysis time. In addition, dimension of the instrument is too cumbersome to be employed for point-of-care testing.

In this work, the simple and rapid method using a smart mobile phone or tablet, installed with an application program was therefore developed as an analyzer for quantitative analysis of urinary albumin. Detection reaction is based on the association reaction between albumin and tetrabromophenolphthalein ethyl ester (TBPE) in which greenish-blue-colored product is developed. The smart device was employed with a sample cassette and a standard colorimetric strip. Optical images of the tested urine sample in the cassette and the standard colorimetric strip were simultaneously captured. The color intensity of the sample was quantitated by 'self-calibration' approach.

1.1.2 A LED spectrometer for measurement of urinary creatinine and uric acid

Creatinine is a metabolite formed from creatine and phosphocreatine and it is excreted in urine by kidney at a relatively constant rate. The creatinine concentration in urine is an important parameter for kidney diagnosis. The normal ranges of creatinine concentration in urine are 3.6 to 27 mmol L^{-1} and 3.3 to 22.5 mmol L^{-1} for men and women, respectively. Uric acid is the end product of the degradation of purines and excreted into urine. In patients with reduced glomerular filtration rate (GFR), urinary uric acid levels are lower than normal person. In recent year, it has been proposed that uric acid cause of chronic kidney disease and possibly in acute kidney injury. Normally, uric acid is excreted in urine in the range of 150 to 200 mg dL^{-1}. Therefore, creatinine and uric acid levels in urine are markers for kidney disease and quantitative measurements of their contents in urine are very important.

The common methods for determination of creatinine and uric acid are the colorimetric Jaffé method and the colorimetric-enzymatic method, respectively. Even though both of the methods are simple, the bulky spectrophotometer is exploited which is not applicable for point-of-care testing.

In this work, a portable LED spectrometer for individual determination of creatinine and uric acid in urine was developed for the sake of point-of-care application. The detection of creatinine is based on the aggregation of gold nanopartices (AuNPs) by creatinine, where the color of the nanoparticles solution is converted from wine-red to blue. However, cost of tetrachloroauric acid ($HAuCl_4$) which is a starting material for AuNPs preparation is very expensive. The net price of tetrachloroauric acid is much expensive e.g., 197 USD/g (99.9 %) or 174 USD/g (49 %). This work then explores use of an alternative material for synthesis of AuNPs. Gold leaf is selected as its cost is much cheaper and it is commercially available in religions supply store in all over Thailand. For uric acid, the reaction between uric

acid and phosphotungstic acid in the presence of sodium carbonate was chosen as detection principle because of its simplicity.

1.2 Objectives of the study

1) To develop a mobile phone – based device for urinary albumin analysis.
2) To fabricate a portable LED spectrometer for quantitative measurement of creatinine and uric acid in urine.

1.3 Scopes of the study

1) Development of mobile phone/tablet – based devices for urinary albumin analysis.

Firstly, detection reaction of albumin was studied by spectrophotometer. Then, the urinary albumin test kit and mobile phone/tablet application were designed and developed. Next, effect of chemical and physical parameter effecting sensitivity of the albumin determination were studied for selection of the optimal condition. Analytical performances of the test kit were evaluated. Finally, the developed method was applied to analysis of urinary albumin. The method was validated against UV - visible spectrophotometer.

2) Development of portable spectrometer for quantitative measurement of creatinine and uric acid in urine.

The detection reaction of creatinine and uric acid were studied. The detection of creatinine is based on the aggregation of the AuNPs by creatinine. AuNPs was synthesized from reused traditional gold leaf that was digested by aqua regia. Optimal conditions for digestion of the gold leaf were also investigation. The detection of uric acid is based on reaction between uric acid and phosphotungstic acid in the presence of sodium carbonate. Then, a portable LED spectrometer was fabricated and applied as detector to measurement of creatinine and uric acid. Then, the developed analyzer was applied to analysis of creatinine and uric acid in human urine and compared results with UV-visible spectrophotometer.

1.4 Benefits of the study

1) A rapid and accurate mobile phone – based analyzer for urinary albumin analysis was achieved.

2) A portable LED spectrometer for quantitative measurement of creatinine and uric acid in human urine was successfully developed.

Chapter 2
Theory and Literature Reviews

2.1 Markers in human urine for clinical diagnosis of renal dysfunction

2.1.1 General information of albumin

Albumin is one of the most important proteins. It is the most abundant protein in human blood plasma and is produced in the liver. It comprises about 50 % of total plasma protein. Molecular weight of albumin is a 65–70 kDa [1]. Structure of human serum albumin is depicted in Figure 2.1.

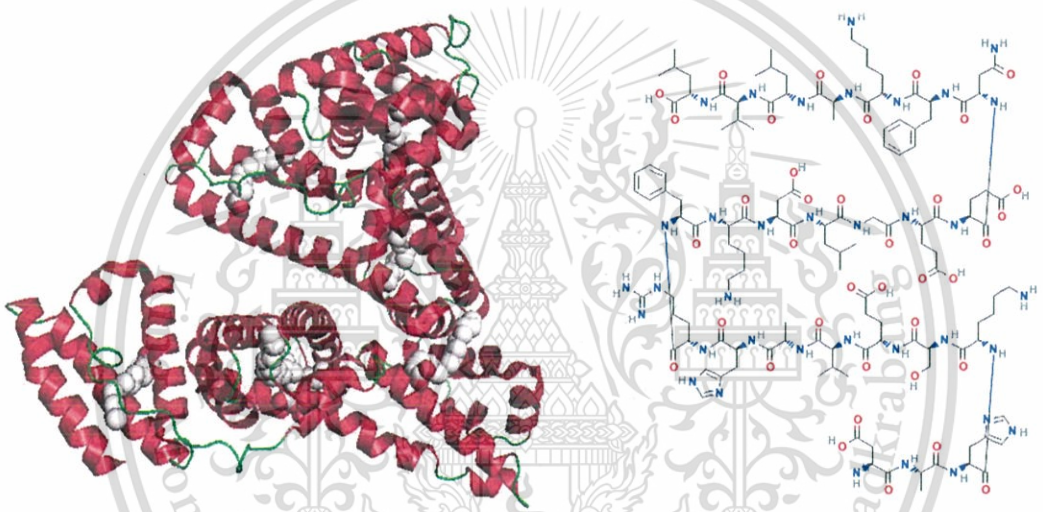

Figure 2.1 3D-Structure (A) and chemical structure (B) of human serum albumin [2]

Serum albumin provides the colloid osmotic pressure that regulates passage of water and diffusible solutes through the capillaries. Albumin serves in the transport of fatty acids, hormones, steroids, metals, vitamins and drugs. Albumin has a negative charge at normal blood pH (7.35 - 7.45) and attracts and retains cations, especially Na^+ in the vascular compartment. Because of its negative charge, albumin is also able to furnish some of the anions needed to balance the cations of the plasma [3].

Usually, albumin is not found in urine except in cases of renal dysfunction such as diabetic nephropathy. Diabetic nephropathy refers to kidney disease that is specific to diabetes. Although kidney biopsy is required to diagnose diabetic glomerulopathy definitively, in most cases, careful screening of diabetic patients can identify people with diabetic nephropathy without the need for kidney

biopsy. Diabetic nephropathy is based in part on the finding of elevated urinary albumin excretion, which is divided into: (1) microalbuminuria (the urinary albumin excretion between 30 and 300 mg L^{-1}), a modest elevation of albumin thought to be associated with stable kidney function, and (2) macroalbuminuria (values above 300 mg L^{-1} of albuminuria), a higher elevation of albumin associated with progressive decline in glomerular filtration rate (GFR), an increase in systemic blood pressure, and a high risk of kidney failure [4]. There are five stages in the development of diabetic nephropathy [5].

Stage I: Hyper filtration. In this stage, GFR is either normal or increased. The size of the kidneys is increased by approximately 20% and renal plasma flow is increased by 10% - 15%, while albuminuria and blood pressure remain within the normal range.

Stage II: Silent stage. This stage starts approximately two years after the onset of the disease and is characterized by kidney damage with basement membrane thickening and mesangial proliferation. There are still no clinical signs of the disease. GFR returns to normal values. Many patients remain in this stage until the end of their life.

Stage III: Incipient or the microalbuminuria stage (albumin 30 - 300 mg L^{-1}). This is the first clinically detectable sign of glomerular damage. It usually occurs five to ten years after the onset of the disease. Blood pressure may be increased or normal. Approximately 40% of patients reach this stage.

Stage IV: Overt nephropathy or macroalbuminuria stage. Albuminuria develops (albumin > 300 mg mg L^{-1}), GFR decrease 12 - 15 mL/min/year, and blood pressure increases above normal values.

Stage V: End stage renal disease (ESRD) (GFR < 15 mL/min). Approximately 50% of the patients with ESRD require kidney replacement therapy.

In the initial stages of diabetic nephropathy, increased kidney size and changed doppler indicators may be the early morphological signs of renal damage, while albuminuria and GFR are the best indicators of the degree of the damage. At this stage, the kidney may leak more serum albumin than normal in the urine (Figure 2.2).

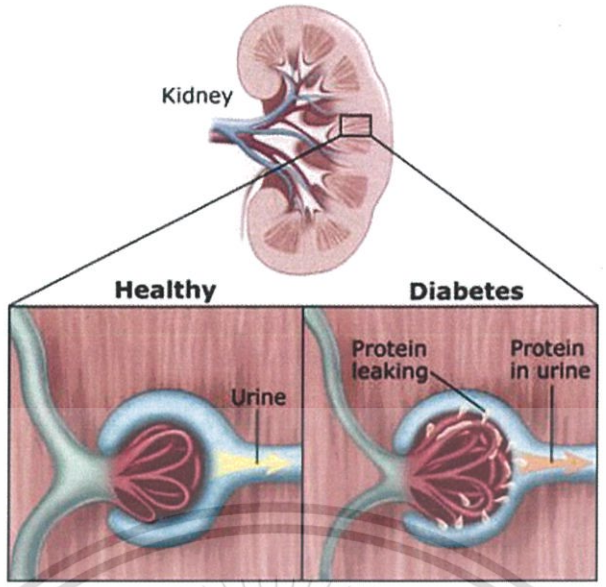

Figure 2.2 Effect of diabetes to kidney [6].

2.1.2 General information of creatinine

Creatinine is a non-protein nitrogenous substance with molecular weight of 113.12 g/mol, which is metabolite formed from creatine and phosphocreatine in muscle and it is usually excreted from the body through glomerular filtration into at a relatively constant rate. Chemical structure of creatinine is shown in Figure 2.3.

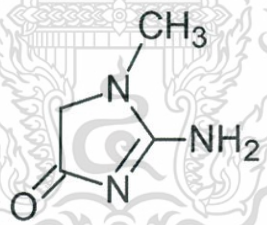

Figure 2.3 Chemical structure of creatinine

The amount of creatinine per unit of muscle mass is constant. The normal ranges of excreted creatinine level in urine are 390 to 2590 mg L^{-1} and 280 to 2170 mg L^{-1} for men and women, respectively [7]. If the filtration in the kidney is deficient, creatinine blood levels rise and creatinine urine levels drop.

<u>Causes of abnormally level of creatinine [8]</u>

1) Prerenal due to decreased renal perfusion (shock, endotoxemia, hypovolemia, dehydration, and cardiovascular disease).
2) Renal azotemia (acute or chronic)
3) Postrenal azotemia due to a urinary obstruction or nephrolithiasis.

Therefore, excreted creatinine level in urine is an important marker for renal disease that is useful in the diagnosis and treatment of renal diseases, in monitoring renal dialysis and also as a calculation basis for other urinary analytes.

2.1.3 General information of uric acid

Uric acid is a heterocyclic organic compound with a molecular weight of 168.11 g/mol. It is the end product of the catabolism of purines that are from foods and excreted into urine. Chemical structure of creatinine is illustrated in Figure 2.4.

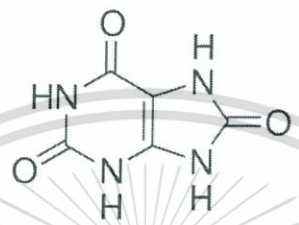

Figure 2.4 Chemical structure of uric acid

Normally, uric acid is excreted in urine in 150 to 200 mg dL^{-1} [9]. The kidneys eliminate approximately two-thirds, while the gastrointestinal tract eliminates one-third of the uric acid load. Almost all uric acid is filtered from glomerulus and excreted in urine. In renal dysfunction, uric acid excretion is lower than the normal value, leading to hyperuricemia which is an excess of uric acid in the blood and lacking of uric acid in the urine. Additionally, hyperuricemia is also a key risk factor for the development of gout, hypertension, hyperlipidemia, diabetes and obesity [10].

2.2 Urine specimen collection [11]

Urine has utilized as a source for measuring health and an important tool for clinical diagnosis due to the frequency and volume of urine and the ease of its collection.

Urine is commonly collected for laboratory analysis for diagnosing disease and monitoring the progression of disease. Urine samples are also used for a range of research purposes, such as monitoring human exposure to environmental contaminants and developing biomarkers of effects based on recent advances in genomics, proteomics, and metabolomics. Types of urine collections depend on the analyte and the purpose of urinalysis, which the collection types vary by time and the way in which they are collected.

2.2.1 Random urine specimen

Random urine specimen or a spot urine sample is the one that is collected at any time of day (or night). There is no patient preparation and no guidelines on hydration are needed prior to sample collection. Random urine specimen is used for routine. However, the random urine specimen for clinical diagnosis need to report a result as a ratio *e.g.* protein - creatinine, because the ratio compare urinary protein concentration relative to urinary creatinine concentration, urinary dilution or concentration does not affect its value.

2.2.2 First – morning urine specimen collection

A first - morning urine specimen collection is the type which an urine is collected after urine has been accumulated in the bladder overnight. The European urinalysis guidelines recommend that the urine be allowed to collect in the bladder for a minimum of 4 h. As a result of the prolonged urine accumulation in the bladder, urinary analytes are more concentrated and the detection of these elements is enhanced. This method is utilized for human chorionic gonadotropin for the detection of pregnancy, nitrates and proteins and it can also be used for routine screening and cytological analysis.

2.2.3 Timed-urine specimen collection

Timed urine collections are collected at a specified time in the 24 - hour period with respect to another activity such as following ingestion of a meal, following the first morning collected of the day, medications or sleeping.

2.2.4 A 24 - hour urine specimen collection

A 24 - hour urine specimen collection is the type which all urine produced during a 24-hour period is collected. It is necessary to measure the total amount of solutes excreted in a 24-hour period, a strictly timed 24-hour specimen is required, because many solutes exhibits diurnal variations.

2.3 Mobile phone – based analyzer for measurement of urinary albumin

2.3.1 Color model

Colors are important for daily life of human. These colors are numerically represents using a mathematical formula to ease data processing and help humans select colors. . This mathematical representation is known as color model, which is a system for measuring colors that can perceive by human, and a process of combining different values as a set of primary colors.

2.3.1.1 RGB color model

The RGB color model is the model that assembles the primary light spectra of Red (R), Green (G), and Blue (B) together in various combinations to produce new spectrum of colors as shown in Figure 2.5. The RGB color model is used in various technologies producing color images, such as conventional photography and the display of images in electronic systems.

The RGB color space could be represented as a cube by normalized RGB color values in the range (x_R , y_G , z_B) with gray values on the main diagonal of the black values (0,0,0) and on the opposite corner the white values (255,255,255) [12].

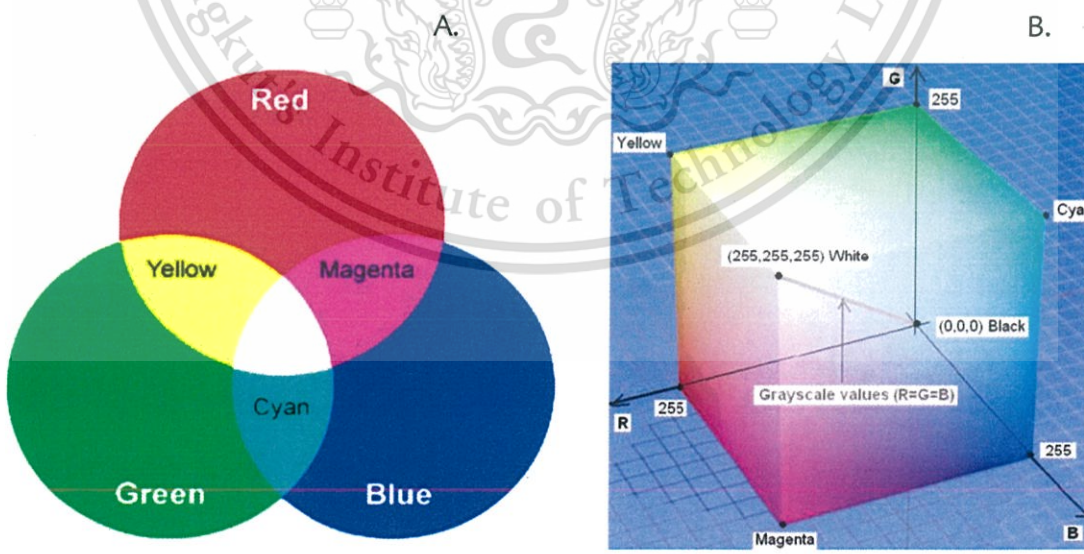

Figure 2.5 RGB color model: The primary color (A) and the primary color cube (B) [12].

2.3.1.2 HSV color model

The HSV color model is based on the idea of human visual system. The HSV color model uses the classifying descriptors hue, saturation and value (brightness). Hue (H) is a numerical representation of color. Saturation (S) is the purity or shade of a color (the degree of white color embedded in specific color). Value (V) represents color brightness or lightness, which these parameters value in the range 0 to 1.

The HSV color model is derived from the red, green, and blue intensity values and uses conical coordinates for the representation of RGB points (Figure 2.6). An important feature of this color model is the representation of the cognitive color information in a single parameter which is the H parameter. In this way, the color coordinate H from this space can be considered as a qualitative signal, independent of variations in color intensity coming from concentration and optical path.

Equations 1-3 display the calculations in order to convert from RGB to HSV [13].

$$H = \begin{cases} \left(\dfrac{G - B}{max_{channel} - min_{channel}} + 0\right) / 6 ; & \text{if } max = R \\ \left(\dfrac{B - R}{max_{channel} - min_{channel}} + 0\right) / 6 ; & \text{if } max = G \\ \left(\dfrac{R - G}{max_{channel} - min_{channel}} + 0\right) / 6 ; & \text{if } max = B \end{cases} \quad (1)$$

$$S = \frac{max_{channel} - min_{channel}}{max_{channel}} \quad (2)$$

$$V = max_{channel} \quad (3)$$

Here, R, G, and B are the red, green, and blue color intensities, respectively. Max and min are the maximum and minimum values of R, G, and B.

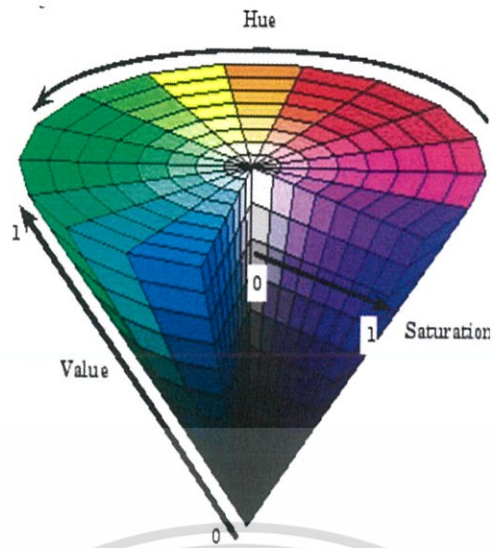

Figure 2.6 HSV color model [12]

2.3.2 Chemistry of detection principle [14]

For quantitative determination of albumin, a reaction consists of two steps. In the first step, tetrabromophenolphthalein ethyl ester (TBPE•H) dissolved in the micelle formed by adding Triton X-100 ($(TBPE^{\bullet}H)_m$). Consequently, the protein in acid solution (HSA^{x+}) is exchanged with H^+ in the micelle. The maximum absorption wavelength of the $(HSA^{x+}\cdot(TBPE^-)_x)_m$ associate was found to be at 605 nm. The micelle extraction of TBPE - protein into Triton X-100 at pH 3.1, the color development occurs according to the following Equations (4) and (5).

$$TBPE{\cdot}H + \text{Triton X-100} + \text{buffer (pH 3.1)} \longrightarrow (TBPE\cdot H)_m \qquad (4)$$

The micelle solution at pH 3.1 in the absence of albumin shows the yellow – green color.

$$x(TBPE\cdot H)_m + HSA^{x+} \longrightarrow (HSA^{x+}\cdot(TBPE^-)_x)_m + xH^+ \qquad (5)$$

The color of micelle solution at pH 3.1 in the presence of albumin was converted to blue.

2.4 A LED spectrometer for measurement of urinary creatinine and uric acid

2.4.1 LED spectrometer [15]

The LED spectrometer is a photometric detector used to measure absorbance. The absorbance of a compound is one of its most useful physical characteristics, both as a means of identification (qualitative analysis) and of estimation (quantitative analysis). If there is absorption in the visible and that absorption occurs in the red then the substance will be seen as green since red and green are complementary colors (Figure 2.10).

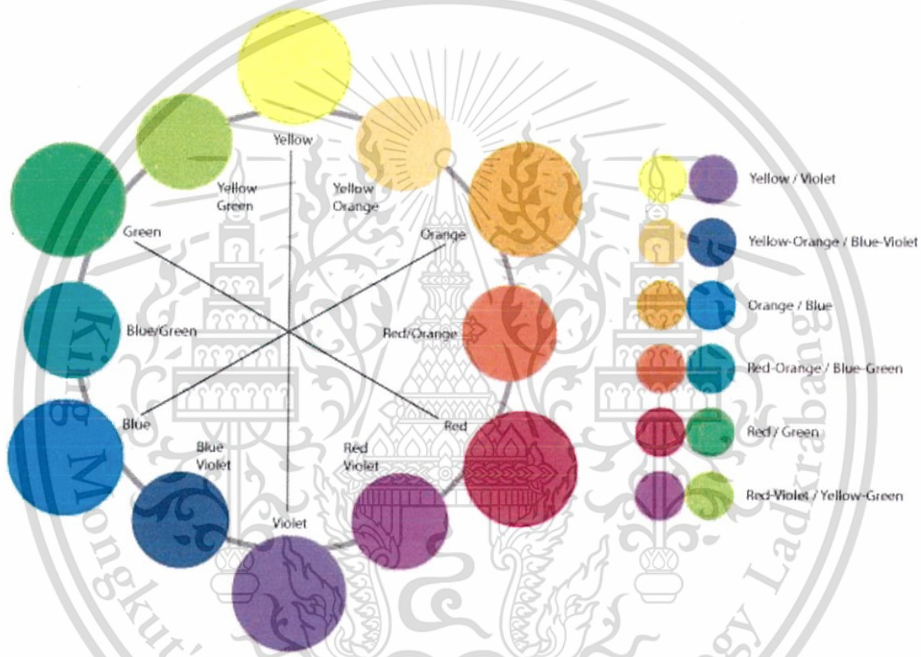

Figure 2.7 Complementary colors

For analytical purposes, two main propositions define the laws of light absorption as the following details.

The LED spectrometer consists of a light source (Red, Green, Blue LED bulbs), phototransistor as a detector and an amplifier. A compound absorbs some of the light that falls upon them, the energy from the radiation being used to excite electrons to higher energy levels. The absorbance (A) of a solution of the compound at a particular wavelength is described by the Beer–Lambert law (equation 8) which is widely used in quantitative analysis.

1) Lambert's Law.

The proportion of incident light absorbed by a transparent medium is independent of the intensity of the light (provided that there is no other physical or chemical change to the medium). Therefore successive layers of equal thickness will transmit an equal proportion of the incident energy. Lambert's law is expressed by equation 6.

$$T = \frac{I}{I_0} \tag{6}$$

Where I is the intensity of the transmitted light, I_0 is the intensity of the incident light, and T is the Transmittance.

It is customary to express transmittance as a percentage:

$$\%T = \frac{I}{I_0} \times 100 \tag{7}$$

2) Beer's Law.

The absorption of light is directly proportional to both the concentration of the absorbing medium and the thickness of the medium in the light path. A combination of the two laws (known jointly as the Beer-Lambert Law) defines the relationship between absorbance (A) and transmittance (T).

$$A = -\log \frac{I}{I_0} = \log \frac{1}{T} = \varepsilon bc \tag{8}$$

Where A is absorbance (no unit of measurement), ε is molar absorptivity (L^{-1} mol^{-1} cm^{-1}), b is path length (cm) and c is molar concentration (mol L^{-1})

The LED spectrometer gives information as a voltage. The absorption by the compound, other processes reduce the intensity of light that passes through the cuvette, so it is essential to take a 'background' reading for the solvent and the cell, which corresponds to I_0. The circuit does not send out 0 V, although it has no light falls on the detector. Hence, the making correction by subtracting the voltage at zero light (V_{zero}) from all readings is necessary. The photometer exhibits a linear relationship between incidents light and the voltage ratio described in equation (9).

$$\frac{I}{I_0} = \frac{I_{sample}}{I_{solvent}} = \frac{V_{sample} - V_{zero}}{V_{solvent} - V_{zero}} \tag{9}$$

The absorbance is calculated by combining equations (8) and (9) into (10).

$$A = -\log \frac{I}{I_0} = -\log \left(\frac{V_{sample} - V_{zero}}{V_{solvent} - V_{zero}} \right) \quad (10)$$

Where V_{zero} is output voltage when there is no light falls on the detector which is ont equal to 0, V_{sample} is output voltage when a sample absorbs the light that sample dissolved in the solvent and $V_{solvent}$ is output voltage of the solvent while there is no sample dissolved.

2.4.2 Gold nanoparticles [16]

Gold nanoparticles (AuNPs) have long been considered to exhibit unique physical and chemical properties different from those of the bulk. One of the most fascinating aspects is their optical properties. AuNPs strongly absorb light in the visible region as a result of the Surface Plasmon Resonance. The resonance wavelength depends on the nanoparticle size and shape as well as the dielectric constant of the surrounding medium. The optical property of AuNPs leads to many uses as sensor and colorimetric techniques.

AuNPs can be prepared by both "top down" and "bottom up" approaches. For "top down" procedures, a bulk state Au is systematically broken down to generate AuNPs of desired dimensions. In this case, particle assembly and formation is controlled by a pattern or matrix. However, the "top down "method is limited concerning the control of the size and shape of particles as well as further functionalization. In another hand, in the "bottom up" strategy, the formation of AuNPs originates from individual molecules, because it involves a chemical or biological reduction. The formation of AuNPs proceeds through a number of consecutive stages: formation of individual atoms; nucleation and formation of an initial atomic cluster; cluster growth to a certain size; and the stabilization of AuNPs. The sizes and dispersity of the formed AuNPs and also their stability in time are regulated by varying the nature of the stabilizer and its amount.

2.4.2.1 Methods of synthesis of gold nanoparticles

(1) Turkevich method

The most often used method for the preparation of AuNPs is the Turkevich method, based on the reduction of chloroauric acid by sodium citrate, and also its various modifications. To prepare AuNPs, the $HAuCl_4$ solution is boiled, and

the trisodium citrate dihydrate is then quickly added under vigorous stirring. After a few minutes, the wine-red colloidal suspension is obtained. In the synthesizing process, reaction occurring and the intermediates formed are described in equation (11) – (14) [17].

The initial step of the multiple - step process, with reactions occurring in series and parallel, is the oxidation of citrate, which yields dicarboxy acetone:

$$(^{-}OCCH_2)_2C(OH)CO^{-} \longrightarrow (^{-}OCCH_2)_2C{=}O + CO_2 + H^{+} + 2e^{-} \quad (11)$$

The second step is the reduction of auric salt to aurous salt:

$$AuCl_3 + 2e^{-} \longrightarrow AuCl + 2Cl^{-} \quad (12)$$

The next step is the disproportionation of aurous species to gold atoms:

$$3AuCl \longrightarrow 2Au^{0} + AuCl_3 \quad (13)$$

The overall stoichiometry of the reaction can be represented as

$$2AuCl_3 + 3(^{-}OCCH_2)_2C(OH)CO^{-} \longrightarrow 2Au^{0} + 3(^{-}OCCH_2)_2C{=}O + 6Cl^{-} + 3H^{+} + 3CO_2 \quad (14)$$

The size of the AuNPs can be controlled by varying the ratio between the concentration of sodium citrate (in this case it is both the reductant and the stabilizer) and chloroauric acid. The average diameter of the AuNPs decreases with increasing citrate concentration in the reaction mixture. The illustration of AuNPs synthesis using the Turkevich method is demonstrated in Figure 2.8

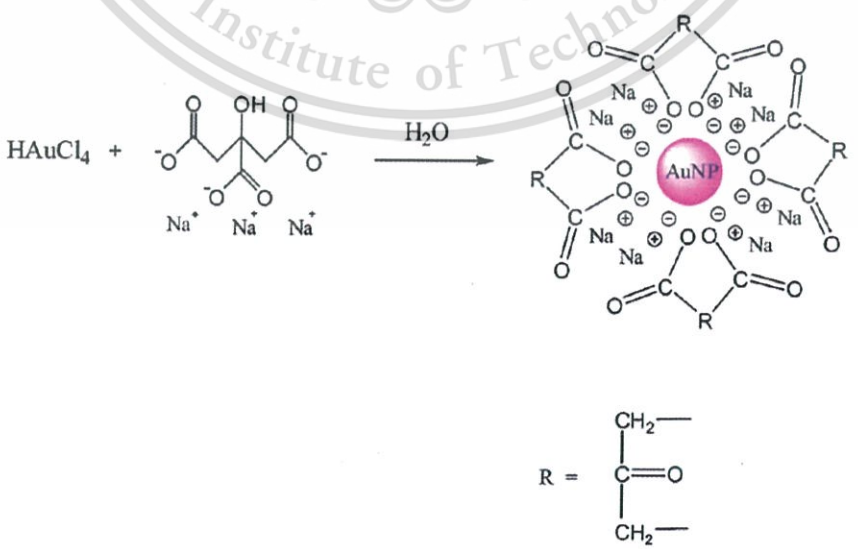

Figure 2.8 AuNPs synthesis using the Turkevich method [16].

(2) Brust - Schiffrin method [16]

The two-phase Brust-Schiffrin method is the first method able to prepare the thiolate-stabilized AuNPs. Its high impact is due to (i) facile synthesis in ambient condition; (ii) relative high thermal and air stability of the prepared AuNPs in this way; (iii) repeated isolation and re-dissolution without aggregation or decomposition; (iv) control of the small size (less than 5 nm) with narrow dispersity; (v) relatively easily functionalization and modification by ligand substitution.

In the AuNPs preparation, the $HAuCl_4$ are reduced by sodium borohydride ($NaBH_4$) in an organic solvent in the presence of thiol capping ligands using either a two-phase liquid/liquid system or a suitable single-phase solvent. Typically, tetrachloroaurate (III) is transferred from aqueous phase to toluene using tetraoctyl ammonium bromide (TOAB) as the phase-transfer reagent and reduced by $NaBH_4$ in the presence of dodecanethiol (DDT). Smaller average core sizes were obtained with larger thiol/gold mole ratios, and fast reductant addition and cooled solutions produced smaller and more monodisperse particles. The nanoparticles can be thoroughly dried and then redispersed in organic solvents without any aggregation or decomposition. The synthesis of AuNPs by the Brust-Schiffrin method as illustrated in Figure 2.9

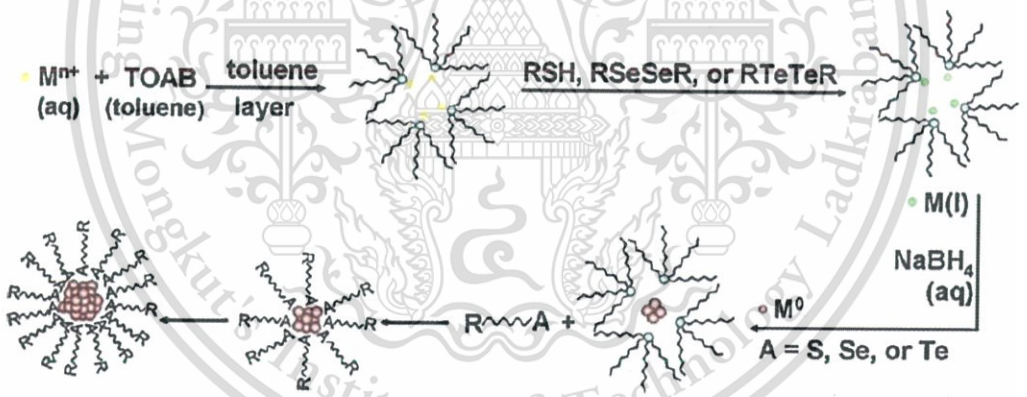

Figure 2.9 Mechanism for AuNP synthesis by the Brust-Schiffrin method [16].

2.4.2.2 Surface Plasmon Resonance of gold nanoparticles [18]

Noble-metal elements, including copper, silver and gold, exhibit metal shine due to free electrons. When the light electromagnetic wave shines on a metal, it is resonant with free electrons on the surface. The resonant free electrons produce an electromagnetic wave that is transmitted to the metal exterior (such as reflected light). The reflection efficiency of silver is 97%, but it is not in color. The white color is also called silver white. Gold yellow is the mixture of metal shine and yellow color that absorbs the wave apart from green light, while strongly reflecting

visible light in the green to red light region. Thus, the naked eye sees the color of gold as yellow. AuNPs and silver NPs (AgNPs) exhibit strong visible absorption bands that differ from the color of the bulk metals. In nanoscale, metal nanoparticles have different physical and chemical properties from the bulk. One of these is the optical properties.

The unique optical properties of AuNPs are determined by the phenomenon of Surface Plasmon Resonance (SPR) (as applied to nanoparticles, SPR is sometimes named Localized Surface Plasmon Resonance). The resonance condition is established when the frequency of light matches the natural frequency of valence electrons oscillating against from this restoring force.

"Surface Plasmon Resonance", the word plasmon corresponds to the quantum of energy associated with an eigenfrequency of a plasma oscillation. In general, plasma is a gas where electric charges are free to move under the influence of electromagnetic or gravitational forces. In the case of metals, the conduction electrons play the role of free charges since they are detached from their ionic core and can be excited by an electromagnetic wave such as an optical beam. The oscillation of the electrons and the oscillation of the electromagnetic field are intrinsically linked. These modes are sometimes termed by their corresponding quasiparticles: polaritons, when the phenomenon is considered from the point of view of electrical charges, and plasmon when it is studied from the electromagnetic point of view. Therefore plasmon waves correspond to the coupling of two waves: the mechanical oscillations of charges and the electromagnetic oscillations of the electric field.

In solid state physics, the plasmon represents the collective oscillation of a free charge in a metal, and may be considered as a kind of plasma wave. The positive electrical charge in the metal is fixed and the free electron is free to move around it. An applied external electric field, as from a light source, causes the free electrons at the surface of the metal to vibrate collectively, giving rise to surface plasmons. Since electrons are also particles with an electric charge, when they vibrate they also generate an electric field, and when the electric field from the vibration of free electrons and the applied external electric field (e.g., electromagnetic waves) resonate the resulting phenomenon is referred to as a Surface Plasmon Resonance that takes place at the surface of the metal. However, if light irradiates a solution that contains dispersed metal nanoparticles smaller than the wavelength of light, then depending on the electric field of light, the deviation produces a free electron at the surface of the metal. As a result, the weak or thick portions of the electric field appear on the nanoparticle surface and can be

considered as a kind of polarization. Such Localized Plasmon Resonance is called Localized Surface Plasmon Resonance (LSPR) (Figure 2.10).

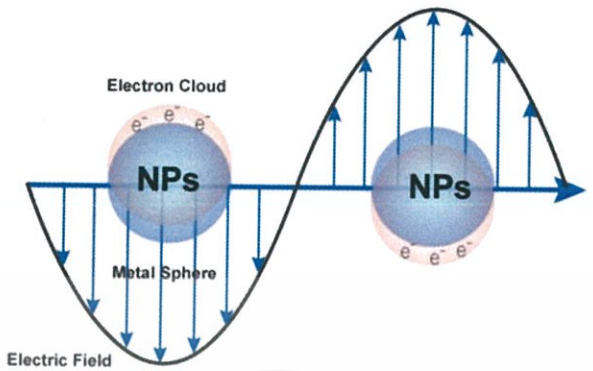

Figure 2.10 Schematic illustrations of Localized Surface Plasmon Resonance in spherical nanoparticles. [19]

2.4.3 Chemistry of detection principle

2.4.3.1 Detection principle for the creatinine measurement

Detection principle for the creatinine analysis is based on the aggregation of the polyvinyl alcohol - stabilized AuNPs in the presence of creatinine. The mechanism of the interaction between the AuNPs and creatinine is illustrated in Figure 2.11. Based on the Turkevich method, reduction of Au (III) by citrate ions to become the citrate-capped AuNPs is obtained (step 1). By the post-modification, facile exchange between the weakly bound surface citrate ions and PVA is occurred (step 2). This leads the colloidal gold to be suspended in the solution without self-aggregation. However, the non-covalent interaction of the AuNPs and PVA is weak because the polymer forms physically adsorb to the particles. In the presence of creatinine, the ring nitrogen of hybrid aromatics exhibit much stronger binding affinity to the AuNPs. The cross-linking reaction between creatinine and the AuNPs is therefore easily achieved via the coordination interaction between the three nitrogen atoms and the AuNPs (step 3). This promotes aggregation of the nanoparticles and results in the color of AuNPs solution gradually change from wine-red to blue when the standard creatinine concentrations increase.

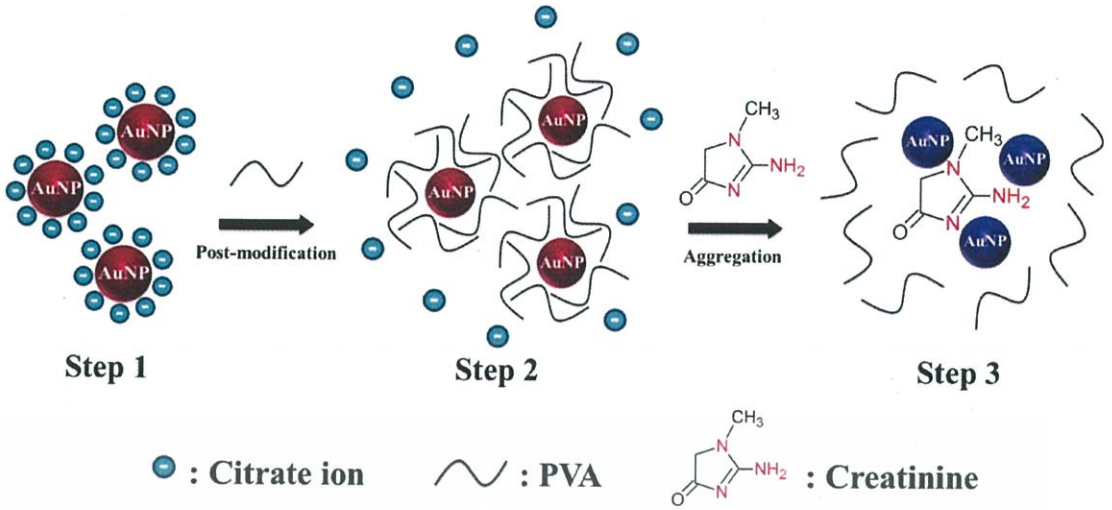

Figure 2.11 Schematic illustration of the colorimetric AuNPs sensor to detect creatinine.

2.4.3.2 Detection principle for uric acid measurement

The detection reaction for uric acid is presented as the following simple equation (15) [20].

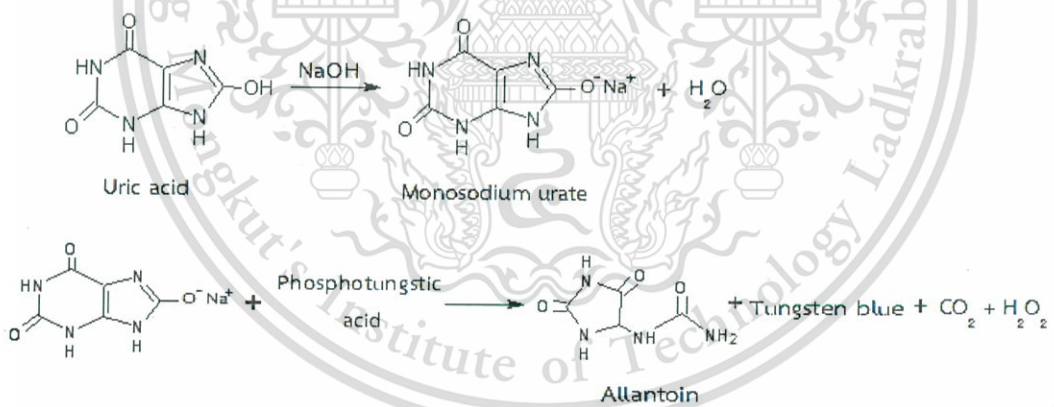

(15)

Urate is oxidized to allantoin and carbondioxide by a phosphotungst acid regent in alkaline medium. Phosphotungstic acid is reduced in this reaction to tungsten blue which is measured at 700 nm.

2.5 Literature Reviews

2.5.1 Quantitative analysis of albumin

There are many publications study on the development of analytical methods for measurement of albumin level. Some interesting publications are listed as the following details.

S. Turek [21] proposed a turbidity reaction for determination of albumin in blood serum. The turbidity was occurred by the specific reaction of serum albumin with its corresponded antibody and comes about when the serum was diluted with Mcilvaine buffer (phosphate-citrate buffer in the range of pH 3.9 - 4.4). It was significantly enhanced by warming the solution. The reaction is suitable as a screening-test of albumin.

G. L. Luque *et al.* [22] developed a sensor for the quantification of albumin based on the incorporation of copper microparticles within a carbon nanotubes paste electrode (CNTPE-Cu). A square wave voltammogram between −0.20 and 1.00 V was obtained after holding the CNTPE-Cu at −0.10 V for 10 min in a stirred solution of albumin. The voltammetric parameters were the following: frequency of 25 Hz, pulse amplitude of 25 mV, staircase step 10 mV and scan rate of 0.250 V s^{-1}. The linear range for albumin was 5.0 - 25.0 mg mL^{-1} with high precision (%RSD = 4.0 %).

J. H. Contois *et al.* [23] evaluated the performance characteristics of the HPLC assay and compared results with a turbidimetric immunoassay for detection of urinary albumin. The HPLC assay was linear to 963 mg L^{-1} with a limit of detection of 6.1 mg L^{-1}. From the results, the albumin concentrations were higher by HPLC than by the turbidimetric immunoassay.

C. Jiang and L. Luo [24] proposed a spectrofluorometric method for determination of human serum albumin (HSA) using doxycycline (DC) - europium (Eu^{3+}) as a fluorescent probe. In a buffer solution of pH 10.2, HAS can remarkably enhance the fluorescence intensity of the DC - Eu^{3+} complex at 612 nm and the enhanced fluorescence intensity of Eu^{3+} is proportional to the concentration of HSA. The linear ranges for HSA were 0 - 9.2 and 9.2 - 34.5 µg mL^{-1} with limits of detection of 64 and 115 ng mL^{-1}, respectively.

T. Sakai *et al.* [25] employed flow injection analysis (FIA) with TBPE·H with Triton X-100 for determination of protein in patient urine. The detection system was based on the ion association formation between human serum albumin (HSA) and TBPE·H in the micelle formed by Triton X-100. An absorbance of product was measured at 610 nm. The calibration curve was linear in the range of 0.15 – 12.0 mg dL^{-1} of HSA with r^2 = 0.998. The limit of detection was 0.05 mg dL^{-1}.

K. Watla-iad *et al.* [14] employed SIA system with spectrophotometric detections for determination of protein and glucose. Tetrabromophenolphthalein ethyl ester (TBPE) in the presence of Triton X-100 at pH 3.2 was used as a chromogenic reagent for albumin-TBPE associate formation. An absorbance of the blue product was monitored. Linear ranges were up to 10 mg dL^{-1} human serum albumin (HSA) with a limit of detection of 0.3 mg dL^{-1}.

2.5.2 Quantitative analysis of creatinine

Several analytical methods have been reported for the determination of creatinine. Some outstanding publications are presented as the summary below.

G. A. Moss *et al.* [26] reported kinetic enzymatic method for determination of creatinine in serum. Creatinine amidohydrolase is used to measure serum creatinine in a totally enzymatic procedure. Creatine, produced by hydrolysis, is acted upon by creatine kinase, and then by pyruvate kinase and lactate dehydrogenase, to result in a change in absorbance at 340 nm. The amount of creatinine present is related to the rate of change in A_{340} and is determined from a standard curve. Absorbance and concentration are linearly related to 100 mg L^{-1}. Analytical recovery of creatinine added to either normal or abnormal sera averaged 102%.

J. Ogawa *et al.* [27] described the enzymatic measurement of creatinine in both serum and urine. The method is based on a microbial creatinine degradation pathway via *N*-methylhydantoin. By using two enzymes, *N*-methylhydantoin amidohydrolase and *N*-carbamoylsarcosine amidohydrolase, the hydrogen peroxide is produced and reacts with peroxidase. The purple color product is obtained and measured. Linear ranges were up to 1.0 mmol L^{-1}. The recoveries were found in range 107 - 110%.

Even though the above mentioned methods provide high specificity and high accuracy, the enzyme reagents are expensive and non-stable. Other methods for determination of creatinine have been developed.

R. T. Ambrose *et al.* [28] employed cation-exchange chromatography for separation of creatinine from other species in serum. A 50 cm x 2.1 mm stainless-steel HPLC column packed with a strong cation-exchange material was used. The 20 mmol L^{-1} of lithium acetate at pH 4.68 and 7.1 were used as eluents. The flow rate was 1.20 mL min^{-1}. The absorbance of creatinine in eluent was monitored at 234 nm. The limit of detection of the method was 0.01 μmol L^{-1}.

P. S. T. Yuen *et al.* [29] presented the High Performance Liquid Chromatography method for determination of creatinine in mouse serum. Creatinine was determined in serum by acetonitrile deproteinization, followed by isocratic,

cation exchange HPLC. The 5.0 mmol L^{-1} of sodium acetate, pH 5.1 was used as mobile phase (flow rate of 1 ml/min). A 100 x 4.1-mm PRP-X200 cation exchange column was utilized. The creatinine was measured by monitoring the absorbance at 234 nm.

Although these methods provide high accuracy and precision, their instruments are expensive, or the analytical procedures are complicated and time-consuming. The common method for the measurement of creatinine is the Jaffé method [30], where the orange complex is developed by the reaction between creatinine and alkaline picrate [31, 32]. While this approach is simple, it is less selective and can be interfered by urine matrices. Additionally, picric acid is a kind of poisonous and explosive chemical. Nowadays, in Thailand, ordering of this chemical from local suppliers must be requested for permission by The Ministry of Defense.

To date, metal nanoparticles have been considered to exhibit unique physical and chemical properties different from those of the bulk state or atoms. Gold nanoparticles (AuNPs) are probably the most outstanding metal nanoparticles because of the advantages of their size-dependent optical properties and high extinction coefficient. Its distinct optical property is the clearly color change from wine-red to blue after aggregation of the particles. This offers the use of AuNPs for colorimetric assay in various applications [33, 34] including creatinine determination with the benefits of excellent sensitivity and simplicity.

Y. He *et al.* [35] presented the method for determination of creatinine using citrate-stabilized AuNPs. The detection is based on a direct cross-linking reaction that occurs between creatinine and AuNPs that causes aggregation of AuNPs and results in a color change from wine red to blue. The calibration curve was linear in the range of 0.1 –20.0 mmol L^{-1}. The detection limit is 80 μmol L^{-1}.

P. G. Sutariya *et al.* [36] proposed a new method using AuNPs based colorimetric sensing system by using calix [4] arene functionalized AuNPs (pSDSC4–AuNPs) assembly for creatinine detection. The AuNPs and p-tert-butylcalix [4] arene were synthesized by microwave assisted method. The detection is based on the negative groups of pSDSC4 which adsorb on the surface of AuNPs, the SO_3^- groups provide the hydrogen binding site for the creatinine. The linearity range is 10 – 100 n mol L^{-1}. The detection limit of the method is 2.16 nmol L^{-1}.

J. Sittiwong *et al.* [37] proposed the use of label-free AuNPs for determination of creatinine in human urine after a sample preparation by extraction of creatinine on sulfonic acid functionalized silica gel. With the extraction method, the interferences were eliminated. This method can be applied to determination of creatinine in human urine with acceptable accuracy and precision.

2.5.3 Quantitative analysis of uric acid

K. Lorentz and W. Berndt [38] presented an enzymic method for determination of uric acid. Detection is based on quantitative development of hydrogen peroxide by uricase and following oxidation of a chromogenic O_2 acceptor by peroxidase. An absorbance of product can be measured between 510 and 550 nm. Although the conventional method provides high accuracy and selectivity, cost of analysis is quite expensive because enzyme reagents and spectrophotometer are exploited.

N. Gochman and J. M. Schmitz [39] described use of uricase – peroxidase system for determination of uric acid. Hydrogen peroxide is generated when uric acid is oxidized by uricase. The generated hydrogen peroxide is measured by 3-methyl-2-benzothiazolinone hydrazone and N,N-dimethylaniline, in the presence of peroxidase where a stable indamine dye was produced. The method provided high sensitive and high selective.

For non-enzymatic method, M. N. Islam *et al.* [40] proposed the paper based method for urinary determination. The detection principle is based on the reaction of ferric chloride with potassium ferricyanide in the presence of uric acid. The Prussian blue color product is developed. The method provided calibration curve with a linear detection range of 0 – 500 mg d L^{-1}.

R. G. Martinek [41] proposed the method for determination of uric acid in biological fluid. Uric acid has the ability to reduce phosphotungstic acid to form a blue color. The method provided linearity curve in range of 2 – 18 mg dL^{-1}.

R. J. Henry [42] presented a method for using alkaline phosphotungstate for the uric acid determination and comparison with the spectrophotometric uricase method. The calibration curve was linear in the range of 20.0 – 100.0 mg dL^{-1}. The correlations between the results from this methods and the method with specific uricase, this method provided the results better than enzymatic method.

2.5.4 Smart phone application for quantitative analysis

Nowadays, the improvement of electronics and information technology has brought about the revolution of personal computers to smart mobile devices. With the rapid advancement of cell phones and tablets embedded with digital cameras and central processing units, simple mobile devices are reported as a portable analyzer for many applications.

S. Sumriddetchkajorn *et al.* [43] proposed a mobile-platform based colorimeter embedded with a self-referencing analysis for converting the color level of water to its corresponding chlorine concentration. The key idea relies on a two-dimensional (2D) color analysis in a portable closed chamber. 2D color analysis with

self-referencing is performed via the arrangement of both the reference material and the glass bottle in such a way that they both fit in the field of view of the mobile-device's camera. In this way, one color image inherently contains two image regions, one from the reference material and another from the glass bottle. Consequently, a specific color ratio from these two image regions is used for specifically converting the water color inside the glass bottle into its corresponding chlorine concentration.

Y. Intaravanne *et al.* [44] proposed a mobile device-based rice leaf color analyzer called ''BaiKhao'' (means rice leaf in Thai). The key idea is to simultaneously capture and process the two-dimensional (2D) data of the color image from the rice leaf and its surrounding reference, thus eliminating expensive external components and alleviating the environmental fluctuation but yet achieving a high color-reading accuracy.

A. F. Coskun *et al.* [45] proposed a digital sensing platform, termed Albumin Tester, running on a smart-phone that images and automatically analyses fluorescent assays confined within disposable test tubes for detection of albumin in urine. This Albumin Tester is mechanically installed on the existing camera unit of a smart-phone, where test and control tubes are inserted from the side and are excited by a battery powered laser diode. The fluorescent images of the sample and control tubes were captured and digitally processed within one second through an android application running on the same cellphone for quantification of albumin concentration. The method takes 5 min per sample. The detection limit of the sensing platform is lower than 10 $\mu g\ mL^{-1}$.

A. Soni *et al.* [46] developed a smart phone based hand-held optical biosensor for determination of urea in saliva. The test paper was prepared by immobilization of urease enzyme along with a pH indicator on a filter paper based strip. The strip changed color upon the reaction with urea present in saliva. The calibration curve of the method was obtained with a linear detection range of 10 – 260 $mg\ dL^{-1}$. The detection limit of the method is 10.4 $mg\ dL^{-1}$.

2.5.5 LED spectrometer for chemical analysis

Currently, there are a large numbers of the instrumental methods that have been developed for clinical diagnosis. However, there are some drawbacks of the instrumental method such as highly expensive and requiring high skill user. In addition, dimension of the instrument is usually bulky and this leads the method to be applied for laboratory use. Application of the instrumental method to 'point-of-care' analysis is therefore restricted. In many resource limited countries and laboratories, there is a need for a low cost analytical instrument that could provide both qualitative and quantitative analysis.

Nowadays, there is a strong interest in the development of hand-held instruments. The size of instruments is shrinking from bench-top size to pocket-size. The cost is decreasing, whereas the performance is still acceptable. A spectrophotometer is generally exploited as detector for determination of the analysts by measuring the light absorption. However, a conventional spectrophotometer is large and complex which not suitable 'point-of-care' analysis [47]. The device and accessories are also expensive.

Recently, the light emitting diode (LED) was successfully developed with wavelengths from IR to the UV range. The LED is more stable, longer life time, smaller than other light sources, a wide range of selections of available wavelengths and low power consumption [48]. Therefore, it is extensively used as light sources for the development of small size spectrometer.

D. R. Albert *et al.* [49] developed a prototype of the spectrophotometer. a LEGO blocks was used for constructing the prototype module and LED was used as light source. The construction of homemade spectrophotometer can be simple and inexpensive.

T. S. Yeh *et al.* [48] described a fabrication of a low cost LED based spectrometer. This LED based spectrometer could be operated as a stand-alone instrument or under PC control via serial link. When compared the results with the commercial spectrophotometer, the LED spectrometer provided performance that is not significantly different.

G. Veras *et al.* [50] proposed a portable and low-cost spectrophotometer. The instrument combines the use of a compact disc (CD) media as diffraction grid and white light-emitting diode (LED) as radiation source. The proposed device was successfully applied to determination of food colorants. Good precision in the analyte concentrations was obtained by using the device. The relative standard deviation (R.S.D.) was lower than 1.0%.

Chapter 3
Research methodology

3.1 Chemicals and apparatus

3.1.1 Chemical

Name	Chemical formula	Purity (%)	Company
Human serum albumin	-	95.0	Aldrich, USA
Tetrabromophenolphthaline ethyl ester potassium salt	$C_{22}H_{13}Br_4KO_4$	90.0	Aldrich, USA
Absolute ethanol	C_2H_5OH	99.9	Carlo Erba, Italy
Triton X-100	-	-	Aldrich, USA
Glacial acetic acid	$C_2H_4O_2$	99.8	Carlo Erba, Italy
Sodium Acetate	$C_2H_3O_2Na$	99.0	Sigma-Aldrich, USA
Poly (vinyl alcohol), (M.W. 9,000-10,000)	$[CH_2CH(OH)]_n$	99.0	Sigma-Aldrich, USA
Sodium citrate tribasic dihydrate	$C_6H_5Na_3O_7 \cdot 2H_2O$	-	Sigma-Aldrich, USA
Tetrachloroauric (III) acid trihydrate	$HAuCl_4 \cdot 3H_2O$	99.9	Sigma-Aldrich, USA
Hydrochloric acid	HCl	37.0	Carlo Erba, Italy
Nitric acid	HNO_3	65.0	Carlo Erba, Italy
Creatinine	$C_4H_7N_3O$	98.0	Sigma-Aldrich, USA
Uric acid	$C_5H_4N_4O_3$	99.0	Sigma-Aldrich, USA
Monosodium phosphate	$NaH_2PO_4 \cdot 2H_2O$	-	AJAX FINECHEM, New zealand
Disodium phosphate	Na_2HPO_4	-	Carlo Erba, Italy
Phosphotungstic acid	$H_3[P(W_3O_{10})_4]_x \cdot H_2O$	-	Loba Chemie, India
Sodium carbonate anhydrous	Na_2CO_3	-	Quality Reagent Chemical, New zealand

3.1.2 Apparatus

1) Volumetric flask
2) Erlenmeyer flask
3) Micropipette
4) Beaker
5) Test tube
6) pH meter – FiveEasyPlus™ FEP20, USA
7) Hotplate – IKA® C-MAG HS7, Malaysia
8) Vortex mixer - Gennie Z Vortex, USA
9) UV - visible spectrophotometer – Jasco FP-8000, USA
10) Illuminance meter – LX-1330B, Sinometer, China
11) Deionized water system - ZENEER UP 900, Human Corporation, Korea
13) Samsung Galaxy S5, Samsung, South Korea
14) Samsung tablet 10.1, Samsung, South Korea
15) Transmission electron microscope, FEI-TECNAI T20 G^2, Netherlands

3.2 Research methodology

3.2.1 Mobile phone – based analyzer for measurement of urinary albumin

All standards and reagents used were of analytical reagent grade. Deionized-distilled water was used throughout all the experiments.

3.2.1.1 Chemical preparation

1) 250 mg L^{-1} of albumin standard stock solution

250 mg L^{-1} of albumin standard stock solution was prepared by dissolving 0.0125 g of solid powder of human serum albumin in 50.00 mL of water. The prepared solution was stored at 4 °C until use.

2) Working albumin standard solution

5 mg L^{-1} of albumin standard solution was freshly prepared by pipetting 0.20 mL of the albumin standard stock solution into 10.00 mL volumetric flask and diluting to the mark with DI water. The concentrations of 50, 100, 150 and 200 mg L^{-1} were prepared by pipetting 2.00, 4.00, 6.00, 8.00 mL of the albumin standard stock solution, respectively.

3) 2×10^{-4} mol L^{-1} of tetrabromophenolphthalein ethyl ester potassium salt

2×10^{-4} mol L^{-1} of tetrabromophenolphthalein ethyl ester potassium salt was prepared by dissolving 0.0140 g of TBPE in 5.0 mL of 99.9 % ethanol. Into this solution, 2.0 mL of Triton X-100 was added. The solution was then made up with ethanol to 100.0 mL.

4) 0.1 mol L^{-1} of acetate buffer (pH 3.1)

0.1 mol L^{-1} of acetate buffer (pH 3.1) was prepared by adding 0.1 mol L^{-1} sodium acetate in 0.1 mol L^{-1} acetic acid. This solution was adjusted to a final pH of 3.0 by using either 0.1 mol L^{-1} of HCl or NaOH.

5) Urine sample

Urine samples were spot collected from normal volunteers. Aliquot of 0.1 mL of urine sample was pipetted into 10.00 mL volumetric flask and diluted to the mark with DI water.

3.2.1.2 Experiment

1) Study on detection reaction of albumin using UV - visible spectrophotometer

0.50 mL of albumin standard solution was pipetted into a test tube, followed by adding 0.5 mL of 2.0×10^{-4} mol L^{-1} TBPE in 2.0 % v/v Triton X-100 and 1.5 mL of 0.1 mol L^{-1} acetate buffer (pH 3.0). The solution was mixed through a Gennie Z Vortex mixer and was kept standing for incubation (2 min). The solution was then transferred into a 10-mm pathlength quartz cuvette. Absorption spectrum (400 – 700 nm) was monitored using a UV-Vis. spectrophotometer.

2) Study on kinetic of reaction

0.50 mL of albumin standard solution was pipetted into a test tube, followed by adding 0.5 mL of 2.0×10^{-4} mol L^{-1} TBPE in 2.0 % v/v Triton X-100 and 1.5 mL of 0.1 mol L^{-1} acetate buffer (pH 3.0). The solution was mixed through a Gennie Z Vortex mixer. The solution was then transferred into a 10-mm pathlength quartz cuvette. Absorbance reading at 605 nm was recorded for 30 minute using a UV-Vis. spectrophotometer.

3) Development and verification of the printed standard colorimetric strip

The printed reference colors were developed from the standard reference solutions that were prepared by mixing of the standard working solutions of albumin (1, 10, 20, 30, 40 and 50 mg L^{-1}) with 2.0 x 10^{-4} mol L^{-1} TBPE in the presence of 2.0 % v/v Triton X-100 and acetate buffer (pH 3.1).

Firstly, spectra and absorbance readings at 605 nm of the mixing solutions were monitored. The mixed solutions were then transferred into the plastic spot plate. The image of the spot plate was captured by the mobile device's camera and was downloaded into personal computer. The sensing area (129 x 129 pixels) of each image of standard reference solution in the spot plate was digitally processed using Mathlab for evaluation of the H parameter.

The results were designated as the color indices for printing a pattern of the reference colors in the standard colorimetric strip.

4) Apparatuses and analytical workflows

Figure 3.1 illustrates key apparatuses exploited for quantitative determination of albumin in urine by the developed mobile phone-based analyzer. The smart mobile device in Figure 3.1A is Samsung Galaxy S5 (Samsung, South Korea) embedded with Android 5.0 operation system. Its specifications are full HD (1920 x 1080 pixel) main display, 16 M pixel digital camera and 2.5 GHz processing unit. Our developed application (15 MB) namely 'Albumin smart test' or 'AST app' was installed into the mobile phone. Figure 3.1B shows the sample cassette that is adapted from a commercially available contact lens container. One cassette is composed of two holders which are employed for accommodating control and test urine samples. Dimension of each holder is 2.2 cm diameter and 1.3 cm depth. The test paper in Figure 3.1C, is made of a 270-gram, white uniformly photo paper. Two zones are assigned on the paper sheet. Zone 'A' is standard colorimetric strip and zone 'B' is space for situating sample cassette. The standard colorimetric strip was made by printing the reference colors (illustrated as (a) to (f) in Figure 3.1C) onto the photo paper using a 2605HP color laser printer.

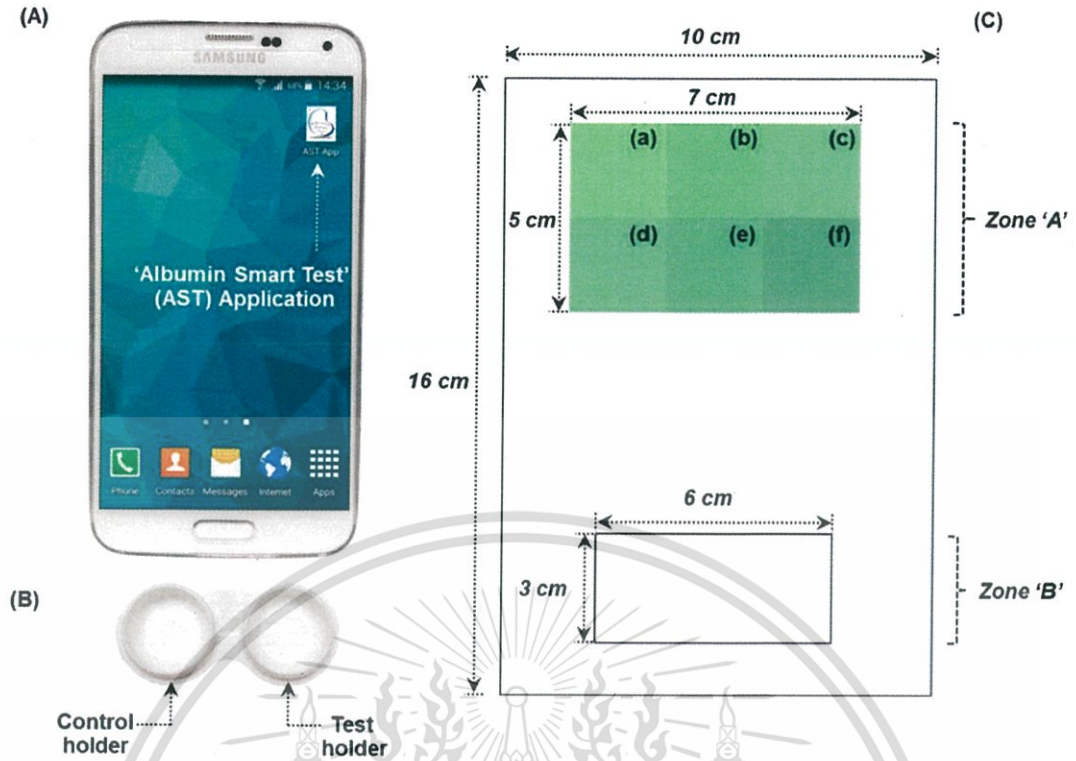

Figure 3.1 The apparatuses exploited with the mobile phone-based analyzer for quantitative determination of urinary albumin. (A) Smart mobile phone, (B) Sample cassette and (C) Test paper which contains Zone "A" and Zone "B". Zone "A": Standard colorimetric strip that composes of printed reference colors representation of (a) 1 mg L^{-1}, (b) 10 mg L^{-1}, (c) 20 mg L^{-1}, (d) 30 mg L^{-1}, (e) 40 mg L^{-1} and (f) 50 mg L^{-1} standard albumin. Zone "B": Space for situating the sample cassette.

5) Steps of measurement by mobile phone application

Analytical workflows for the albumin measurement are summarized in Figure 3.2. The measurement is started from transferring of an aliquot of 0.5 mL of diluted urine sample and 0.5 mL of 2.0×10^{-4} mol L^{-1} TBPE and 1.5 mL of 0.1 mol L^{-1} acetate buffer (pH 3.1) into the holders as shown in Figure 3.2A. Both holders are covered with their lids and the solutions are mixed by gently shaking of the cassette (Figure 3.2B).

After kept standing for incubation (2 min), the lids are opened (Figure 3.2 C). The cassette is situated onto the test paper. The application is run to capture images of standard colorimetric strip and urine sample by touching the camera icon on the screen of the mobile device.

Parameters of the camera of the mobile phone are fixed (ISO: 100, aperture: 2.2 and shutter speed: 1/33). Prior to capture, it is necessary to align the mobile device in order that the images of the standard colorimetric strip and the

sample cassette are fixed inside the red frames (See Figure 3.2E). The acquired images are then automatically processed for converting color intensity into its corresponding albumin concentration. All measurement processes are completed within 3 min.

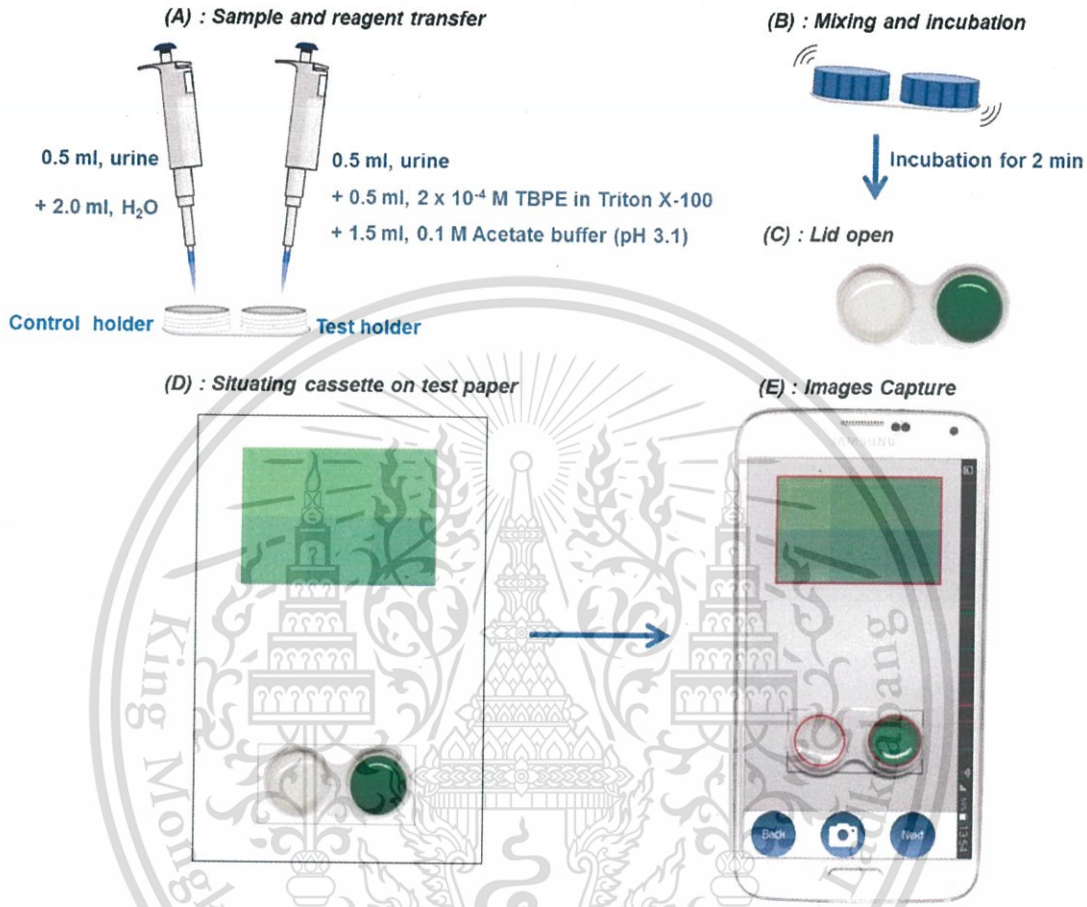

Figure 3.2 The analytical workflows for the albumin measurement in urine sample by the mobile phone-based analyzer. (A): Transferring of sample and reagents into the sample cassette, (B): Mixing and incubation, (C): Opening lids of the sample cassette, (D): Placing the sample cassette in the test paper and (E): Capturing the images.

6) Study on effect of illumination on image processing

The application was tested for standard albumin concentrations (1, 10 and 30 mg L^{-1}) with inside laboratory (500 lx), inside building (2,000 lx) and outside building (3,500 lx).

An aliquot of 0.5 mL of albumin standard solution was pipetted into both tested and control holders, followed by adding 0.5 mL of 2.0 x 10^{-4} mol L^{-1} TBPE and 1.5 mL of 0.1 mol L^{-1} acetate buffer (pH 3.0) into the tested holder only. The cassette was covered with its lids for mixing with gently shaking. After kept

standing at an interval time of 2 min for incubation, the lids were opened. The cassette was placed onto the standard colorimetric strip and captured images using the application.

7) Validation

- Precision

Percent relative standard deviation (% RSD) was considered for precision of the method. The application was tested for standard albumin concentrations (10, 30 and 50 mg L^{-1}). This was done by five replicates.

- Accuracy

Accuracy was studied by evaluation on analytical recovery (%). 50 mg L^{-1} spiked sample solution was prepared by pipetting 0.10 mL of urine sample into 10.00 mL volumetric flask, followed by adding 2.00 mL of 250 mg L^{-1} albumin standard solution and diluting to the mark with DI water. For the concentrations of 10, 20, 30 and 40 mg L^{-1} were prepared by pipetting 2.00, 0.40, 0.80, 1.20 and 1.60 mL of the albumin standard stock solution, respectively. The measurement for all the prepared solutions is described in section 3.2.1.2 (5).

8) Application to human urine

The developed mobile phone analyzer was applied to the determination of albumin in 50 urine samples that were spot collected from volunteers of various ages (30 to 60 year-old) with no known history of diabetic nephropathy. The samples were just 100-fold diluted without any pretreatment. The results determined by our mobile phone were compared with results obtained using the validating spectrophotometric method by means of the Bland–Altman plot.

9) Spectrophotometric determination of urinary albumin

0.50 mL of urine sample was pipetted into a test tube, followed by adding 0.5 mL of 2.0×10^{-4} mol L^{-1} TBPE in 2.0 % v/v Triton X-100 and 1.5 mL of 0.1 mol L^{-1} acetate buffer (pH 3.0). The solution was mixed through a Gennie Z Vortex mixer and was kept standing for incubation (2 min). The solution was then transferred into a 10-mm pathlength quartz cuvette. Absorption spectrum (400 – 700 nm) was monitored using a UV-Vis. spectrophotometer.

3.2.2 Preliminary performance test of a LED spectrometer

3.2.2.1 Chemical preparation

1) 100 mg L^{-1} of ammonium ferrous sulfate solution

100 mg L^{-1} of ammonium ferrous sulfate stock solution was prepared by dissolving 0.0351 g of solid powder of ammonium ferrous sulfate in DI water. 0.05 mL of sulfuric acid was then added. The solution was transferred to 50.00 mL volumetric flask and diluted to the mark with DI water.

2) 0.5 % w/v of ortho–phenanthroline

0.5 % w/v of ortho–phenanthroline solution was prepared by dissolving 0.2500 g of solid powder of ortho–phenanthroline in 50.00 mL of DI water.

3) 10.0 % w/v of hydroxylamine hydrochloride

10.0 % w/v of hydroxylamine hydrochloride solution was prepared by dissolving 2.5000 g of solid powder of hydroxylamine hydrochloride in 25.00 mL of DI water.

4) Working standard solutions of ferrous

1.0 mg L^{-1} of ferrous standard solution was prepared by pipetting 0.25 mL of the ammonium ferrous sulfate stock solution into 25.00 mL volumetric flask. Then, 0.25 mL of 10 % w/v hydroxylamine hydrochloride and 0.50 mL of 0.5 % w/v ortho–phenanthroline were added. The solution was diluted to the mark with DI water. The concentrations of 2.0, 3.0, 4.0 and 5.0 mg L^{-1} were prepared by pipetting 0.50, 0.75, 1.00 and 1.25 mL of the ammonium ferrous sulfate stock solution, respectively.

5) Working standard solutions of ethanol

Working standard solutions of ethanol (5.0, 10.0, 20.0, 30.0 and 40.0 % v/v) were freshly prepared by pipetting stock standard of 99.8 % ethanol (1.25, 2.50, 5.00, 7.50, 10.00 and 12.50 mL) into 25.00 mL volumetric flask and diluting to the mark with DI water.

6) 0.03 mmol L^{-1} of potassium dichromate

0.03 mmol L^{-1} of potassium dichromate solution was prepared by dissolving 0.8830 g of solid powder of potassium dichromate in 100.00 mL of 1.5 mol L^{-1} sulfuric acid. The solution was transferred to 50.00 mL volumetric flask and diluted to the mark with DI water

7) Working standard solutions of uric acid

5.0 mg L^{-1} of uric acid standard solution was prepared by pipetting 0.5 mL of the uric acid standard stock solution into 10.00 mL volumetric flask and diluting to the mark with DI water. The concentrations of 10.0, 30.0, 50.0 and 70.0 mg dL^{-1} were prepared by pipetting 1.00, 3.00, 5.00 and 7.00 mL of the uric acid standard stock solution, respectively.

8) 40.0 % (w/v) of phosphotungstic acid solution

40 % (w/v) of phosphotungstic acid solution was prepared by dissolving 4.0000 g of phosphotungstic acid in water. The solution was then made up with DI water to 10.00 mL in volumetric flask.

9) 2.0 % (w/v) of sodium carbonate solution

2.0 % (w/v) of sodium carbonate solution was prepared by dissolving 0.5000 g of sodium carbonate in water. The solution was then made up with DI water to 25.00 mL in volumetric flask.

3.2.2.2 Experiment

1) Performance test for red bulb

The chemical reaction between ethanol and potassium dichromate was chosen. 4.0 mL of 0.03 mmol L^{-1} of potassium dichromate solution was pipetted into a test tube. 1.0 mL of the working standard solutions of ethanol was then pipetted into the test tube. The absorbance readings were recorded by the LED spectrometer and the UV - visible spectrophotometer.

2) Performance test for green bulb

The chemical reaction between uric acid and phosphotungstic acid was selected. 5.0 mL of the working uric acid standard solution was transferred to a test tube. The 3.0 mL of 2 % (w/v) sodium carbonate solution and 3.0 mL of 40 % (w/v) phosphotungstic acid solution were then added. The absorbance readings

were recorded at 1 min after adding the phosphotungstic acid solution by the LED spectrometer and the UV - visible spectrophotometer.

3) Performance test for blue bulb

The chemical reaction between ferrous and ortho–phenanthroline was selected. The working ferrous standard solution was transferred into a 10-mm pathlength quartz cuvette. The absorbance readings were recorded by the LED spectrometer and the UV - visible spectrophotometer.

3.2.3 A LED spectrometer for measurement of urinary creatinine

3.2.3.1 Chemical preparation

1) Aqua regia

An aqua regia solution was prepared by mixing of concentrated hydrochloric acid (37 %) and nitric acid (65 %) at 3:1 volume ratio.

2) 1.0 mol L^{-1} of sodium hydroxide

1.0 mol L^{-1} of sodium hydroxide was prepared by dissolving 2.00 g of sodium hydroxide in 50.00 mL of DI water.

3) 1.0 mmol L^{-1} of standard tetrachloroauric acid

1.0 mmol L^{-1} of tetrachloroauric acid solution was prepared by dissolving 0.0394 g of tetrachloroauric (III) acid trihydrate in 100.00 mL of DI water.

4) 38.8 mmol L^{-1} of sodium citrate

38.8 mmol L^{-1} of sodium citrate was prepared by dissolving 0.5705 g of trisodium citrate dehydrate in 50.00 mL of DI water.

5) 2.0 % (w/v) of sodium citrate

2.0 % (w/v) of sodium citrate stock solution was prepared by dissolving 1.0000 g of sodium citrate in 50.00 mL of DI water.

6) 8.0 % (w/v) of polyvinyl alcohol

8.0 % (w/v) of polyvinyl alcohol stock solution was prepared by dissolving 4.0000 g of polyvinyl alcohol in 50.00 mL of DI water.

7) 1,000 mg L^{-1} of creatinine standard solutions

1,000 mg L^{-1} of creatinine stock standard solutions was prepared by dissolving 0.0500 g of creatinine in 50.00 mL of DI water. The prepared solution was stored at 4 °C until use.

8) Working creatinine standard solutions

1.0 mg L^{-1} of creatinine standard solution was prepared by pipetting 0.01 mL of the creatinine standard stock solution into 10.00 mL volumetric flask and diluting to the mark with DI water. The concentrations of 5, 10, 20, 50, 100 and 200 mg L^{-1} were prepared by pipetting 0.05, 0.10, 0.20, 0.50, 1.00 and 2.00 mL of the creatinine standard stock solution, respectively.

3.2.3.2 Experiment

1) Digestion of the reused traditional gold leaf

An accurate weight of 0.1000 g of the reused gold leaf was digested with 5.0 mL of 70 % (v/v) aqua regia at 75 °C with continuous stirring (20 min). The solution was then set aside to room temperature and filtered through WhatmanTM No 2. The filtrate was made up to 50.00 mL with DI water.

2) Synthesis of gold nanoparticles

2.1) From the digested gold leaf

The digested gold leaf solution was adjusted to pH 2.0 using 1.0 mol L^{-1} sodium hydroxide and was heated to 95 °C. The solution of 1.2 % (w/v) sodium citrate was then rapidly added under vigorous stirring. The solution was continuously boiled for 15 min. After cooling, aliquot of 0.5 mL of 2.0 % (w/v) PVA was added into this solution. The gold nanoparticles solution is kept at 4 °C.

2.2) From the standard tetrachloroauric acid solution

The 100 mL of 1.0 mmol L^{-1} $HAuCl_4$ was boiled. To the boiling solution, 7.00 mL of 38.8 mmol L^{-1} sodium citrate was added under vigorous stirring. The mixture was continuously heated for 15 min. The solution was then taken from hot plate and continuously stirred at room temperature.

2.3) From the standard gold sheet solution

The digested gold sheet solution was adjusted to pH 2.0 using 1.0 mol L^{-1} sodium hydroxide and was heated to 95 °C. The solution of 1.2 % (w/v) sodium citrate was then rapidly added under vigorous stirring. The solution

was continuously boiled for 15 min. After cooling, aliquot of 0.5 mL of 2.0 % (w/v) PVA was added into this solution. The gold nanoparticles solution is kept at 4 °C.

3) Effect of pH of the digested gold leaf solution

The effect of pH of the digested gold leaf solution was studied in pH range of 2.0, 3.0, 4.0 and non-adjusted (pH = 1.4). The pH of digested gold leaf solution was adjusted using 1.0 mol L^{-1} sodium hydroxide and was heated to 95 °C. The solution of 1.2 % (w/v) sodium citrate was then rapidly added under vigorous stirring. The solution was continuously boiled for 15 min. After cooling, aliquot of 0.5 mL of 2.0 % (w/v) PVA was added into this solution. The gold nanoparticles solution is kept at 4 °C.

4) Effect of the concentrations of sodium citrate

The digested gold leaf solution was adjusted to pH 2.0 using 1.0 mol L^{-1} sodium hydroxide and was heated to 95 °C. Sodium citrate solution (1.0, 1.2, 1.4, 1.6 and 1.8 % (w/v)) was then rapidly added under vigorous stirring. The solution was continuously boiled for 15 min. After cooling, aliquot of 0.5 mL of 2.0 % (w/v) PVA was added into this solution. The gold nanoparticles solution is kept at 4 °C.

5) Effect of the concentrations of polyvinyl alcohol

The digested gold leaf solution was adjusted to pH 2.0 using 1.0 mol L^{-1} sodium hydroxide and was heated to 95 °C. The solution of 1.2 % (w/v) sodium citrate was then rapidly added under vigorous stirring. The solution was continuously boiled for 15 min. After cooling, aliquot of 0.5 mL of PVA (2.0, 4.0, 6.0 and 8.0 % (w/v)) was added into this solution. The gold nanoparticles solution is kept at 4 °C.

6) Comparison of the characteristics of the AuNPs prepared from reused gold leaf, tetrachloroauric acid and gold sheet

TEM images of the AuNPs, prepared from gold leaf, standard tetrachloroauric acid and standard gold sheet were captured. Their characteristics in term of morphology, Au^0 content, stability and toxicity of starting materials were compared.

7) Colorimetric response of the reused traditional gold leaf-prepared AuNPs to creatinine

An aliquot of 1.0 mL of the gold leaf-prepared AuNPs was pipetted into test tube, followed by adding 5.0 mL of 10 mmol L^{-1} phosphate buffer (pH 6.0) and 0.05 mL of standard creatinine solution. The solution was mixed through a Gennie Z Vortex mixer and was incubated (3 min) at ambient temperature. The solution was then transferred into a 10-mm pathlength quartz cuvette. The Surface Plasmon band was monitored from 400 to 800 nm.

8) Effect of reaction time

An aliquot of 1.0 mL of the gold leaf-prepared AuNPs was pipetted into test tube, followed by adding 5.0 mL of 10 mmol L^{-1} phosphate buffer (pH 6.0) and 0.05 mL of standard creatinine solution. The solution was mixed through a Gennie Z Vortex mixer and was incubated (1, 3, 5 and 10 min) at ambient temperature. The solution was then transferred into a 10-mm pathlength quartz cuvette. The Surface Plasmon band was monitored from 400 to 800 nm.

9) Selectivity study

An aliquot of 1.0 mL of the gold leaf-prepared AuNPs was pipetted into test tube, followed by adding 5.0 mL of 10 mmol L^{-1} phosphate buffer (pH 6.0) and 0.05 mL of either the small organic compounds containing nitrogen solution or the other substances potentially existed in urine (albumin, uric acid and ascorbic acid). The solution was mixed through a Gennie Z Vortex mixer and was incubated (1, 3, 5 and 10 min) at ambient temperature. The solution was then transferred into a 10-mm pathlength quartz cuvette. The Surface Plasmon band was monitored from 400 to 800 nm.

10) Determination of creatinine using the LED spectrometer

An aliquot of 1.0 mL of the gold leaf-prepared AuNPs was pipetted into test tube, followed by adding 5.0 mL of 10 mmol L^{-1} phosphate buffer (pH 6.0) and 0.05 mL of standard creatinine solution. The solution was mixed through a Gennie Z Vortex mixer and was incubated (3 min) at ambient temperature. The solution was then transferred into a 10-mm pathlength quartz cuvette. The red and blue LED bulbs were chosen as a light source for monitoring of the absorption at 650 and 530 nm, respectively.

11) Validation

- Precision

% RSD was considered for precision of the method. The reproducibility was studied by a series of ten repetitive measurements of 10 and 200 mg L^{-1} creatinine.

- Accuracy

Accuracy was studied by evaluation on analytical recovery. 10 mg L^{-1} spiked sample solution was prepared by pipetting 0.10 mL of urine sample into 10.00 mL volumetric flask, followed by adding 0.10 mL of 1,000 mg L^{-1} creatinine standard solution and diluting to the mark with DI water. For the concentrations of 50 and 200 mg L^{-1} were prepared by pipetting 0.50 and 2.00 mL of the creatinine standard stock solution respectively. The measurement for all the prepared solutions is described in section 3.2.2.2 (10).

- LOD and LOQ

The limit of detection (LOD) and the limit of quantitation (LOQ) were calculated by calibration curve method using the following equations:

$$LOD = y_B + 3S_B \quad (16)$$

$$LOQ = y_B + 10S_B \quad (17)$$

Where y_B is intercepts of regression line and S_B is standard deviation of intercepts of regression line.

12) Application to human urine

The 16 urine samples were spot collected from volunteers and were 100-fold diluted with water prior to analysis. The sample solutions were prepared by pipetting 0.10 mL of urine sample into 10.00 mL volumetric flask and diluting to the mark with DI water. The measurement for all the prepared solutions is described in section 3.2.2.2 (10).

13) HPLC method (The validating technique)

The sample solutions were prepared by pipetting 1.00 mL of the collected urine sample into 10.00 mL volumetric flask and diluting to the mark with DI water. The prepared solutions were determined by HPLC method using the following condition:

Parameter	Optimal conditions
Column	Symmetry® C18 ,5µm, 3.9x150 mm
Injection volume	20 uL
Mobile phase	20mM Ammonium dihydrogen orthophosphate phosphate, pH 7.4
Flow rate	0.8 mL min^{-1}
Detector	PDA 190-800 nm (detect at 231 nm)

3.2.4 A LED spectrometer for measurement of urinary uric acid

3.2.4.1 Chemical preparation

1) 100 mg dL^{-1} of uric acid standard solutions

100 mg dL^{-1} of uric acid stock standard solutions was prepared by dissolving 0.1000 g of uric acid in water. Into this solution, 3.0 mL of 1.0 mol L^{-1} sodium hydroxide was added. The solution was then made up with DI water to 100.00 mL in volumetric flask.

2) Working standard solution of uric acid

5.0 mg L^{-1} of uric acid standard solution was prepared by pipetting 0.5 mL of the uric acid standard stock solution into 10.00 mL volumetric flask and diluting to the mark with DI water. The concentrations of 10.0, 30.0, 50.0 and 70.0 mg dL^{-1} were prepared by pipetting 1.00, 3.00, 5.00 and 7.00 mL of the uric acid standard stock solution, respectively.

3) 40.0 % (w/v) of phosphotungstic acid solution

40 % (w/v) of phosphotungstic acid solution was prepared by dissolving 4.0000 g of phosphotungstic acid in water. The solution was then made up with DI water to 10.00 mL in volumetric flask.

4) 2.0 % (w/v) of sodium carbonate solution

2.0 % (w/v) of sodium carbonate solution was prepared by dissolving 0.5000 g of sodium carbonate in water. The solution was then made up with DI water to 25.00 mL in volumetric flask.

3.2.4.2 Experiment

1) Study on the detection principle of uric acid by UV - visible spectrophotometer

Aliquot of 5.0 mL of the uric acid working standard solution was transferred to a test tube. The 3.0 mL of 2 % (w/v) sodium carbonate solution and 3.0 mL of 40 % (w/v) phosphotungstic acid solution were then added. The absorption spectra in range 400 – 1000 nm were monitored at 1 min after adding the phosphotungstic acid solution via UV - visible spectrophotometer.

2) Colorimetric detection of uric acid by LED spectrometer

Aliquot of 5.0 mL of the uric acid working standard solution was transferred to a test tube. The 3.0 mL of 2 % (w/v) sodium carbonate solution and 3.0 mL of 40 % (w/v) phosphotungstic acid solution were then added. The absorbance readings were recorded at 1 min after adding the phosphotungstic acid solution via the LED spectrometer. (Note that the red LED bulb was used as a light source for all experiments involving the absorbance measurement by LED spectrometer.)

3) Effect of phosphotungstic acid concentration

Aliquot of 5.0 mL of the uric acid working standard solution was transferred to a test tube. The 3.0 mL of 2 % (w/v) sodium carbonate solution and 3.0 mL of phosphotungstic acid solution (20, 40, 60 and 80 % (w/v)) were then added. The absorbance readings were recorded at 1 min after adding the phosphotungstic acid solution via the LED spectrometer.

4) Effect of sodium carbonate concentration

Aliquot of 5.0 mL of the uric acid working standard solution was transferred to a test tube. The 3.0 mL of sodium carbonate solution (2, 6, 10, 14 % (w/v)) and 3.0 mL of 80 % (w/v) phosphotungstic acid solution were then added. The absorbance readings were recorded at 1 min after adding the phosphotungstic acid solution via the LED spectrometer.

5) Appropriate time for measurement

Aliquot of 5.0 mL of the uric acid working standard solution was transferred to a test tube. The 3.0 mL of 2 % (w/v) sodium carbonate solution and 3.0 mL of 80 % (w/v) phosphotungstic acid solution were then added. The absorbance readings were monitored for 5 min after adding the phosphotungstic acid solution via the LED spectrometer.

6) Selectivity study

Aliquot of 5.0 mL of either of glucose, creatinine, cysteine and oxalic acid solution was transferred to a test tube. The 3.0 mL of 2 % (w/v) sodium carbonate solution and 3.0 mL of 80 % (w/v) phosphotungstic acid solution were then added. The absorbance readings were monitored at 1 min after adding the phosphotungstic acid solution via the LED spectrometer.

7) Validation

- Precision

% RSD percent was considered for precision of the method. The reproducibility was studied by a series of six repetitive measurements of 4.46 to 62.44 mg dL^{-1} uric acid.

- Accuracy

Accuracy was studied by evaluation on analytical recovery. 5.0 mg dL^{-1} spiked sample solution was prepared by pipetting 0.10 mL of urine sample into 10.00 mL volumetric flask, followed by adding 0.50 mL of 100 mg dL^{-1} uric acid standard solution and diluting to the mark with DI water. For the concentrations of 30 mg dL^{-1} were prepared by pipetting 3.00 mL of the uric acid standard stock solution.

- LOD and LOQ

The LOD and the LOQ were calculated by using the following equations:

$$LOD = y_B + 3S_B \quad (18)$$

$$LOQ = y_B + 10S_B \quad (19)$$

Where y_B is intercepts of regression line and S_B is standard deviation of intercepts of regression line.

8) Application to human urine

The 10 urine samples were spot collected from volunteers and were 100-fold diluted with water prior to analysis. The sample solutions were prepared by pipetting 0.10 mL of urine sample into 10.00 mL volumetric flask and diluting to the mark with DI water. The measurement for all the prepared solutions is described in section 3.2.4.2 (2).

9) Spectrophotometric determination of urinary uric acid (The validating method)

The UV – visible spectrophotometric method was used as the validating method. The determination of the prepared sample solutions is described in section 3.2.4.2 (1).

Chapter 4
Results and Discussion

4.1 Mobile phone – based analyzer for measurement of urinary albumin

4.1.1 Study on detection reaction of albumin using UV – visible spectrophotometer

In this study, the association reaction between albumin and tetrabromophenolphthalein ethyl ester (TBPE) in the presence of Triton X-100 was chosen as detection reaction. The chemical reactions can be written as the following equations:

$$TBPE{\cdot}H + \text{Triton X-100} + \text{buffer (pH 3.1)} \longrightarrow (TBPE \cdot H)_m \qquad (19)$$

The micelle solution at pH 3.1 in the absence of albumin shows the yellow – green color.

$$x(TBPE \cdot H)_m + HSA^{x+} \longrightarrow (HSA^{x+} \cdot (TBPE^{-})_x)_m + xH^{+} \qquad (20)$$

The color of micelle solution at pH 3.1 in the presence of albumin was converted to blue.

The studied solutions were prepared by mixing of the standard working solutions of albumin (1, 10, 20, 30, 40 and 50 mg L^{-1}) with 2.0 x 10^{-4} mol L^{-1} TBPE in the presence of 0.2 % v/v Triton X-100) and acetate buffer (pH 3.1). The absorption spectra of the products were monitored in range of 400 to 700 nm. Results are shown in Figure 4.1.

The absorption spectra in Figure 4.1A show that the maximum absorption wavelength (λ_{max}) located at 605 nm. When standard albumin is increased, the absorbance reading is increased in the concentration range of 1 to 50 mg L^{-1} albumin. The linear calibration curve that plotted between the absorbance values at λ_{max} and the concentrations of standard albumin (Figure 4.1B) also showed good linearity (r^2 = 0.9998).

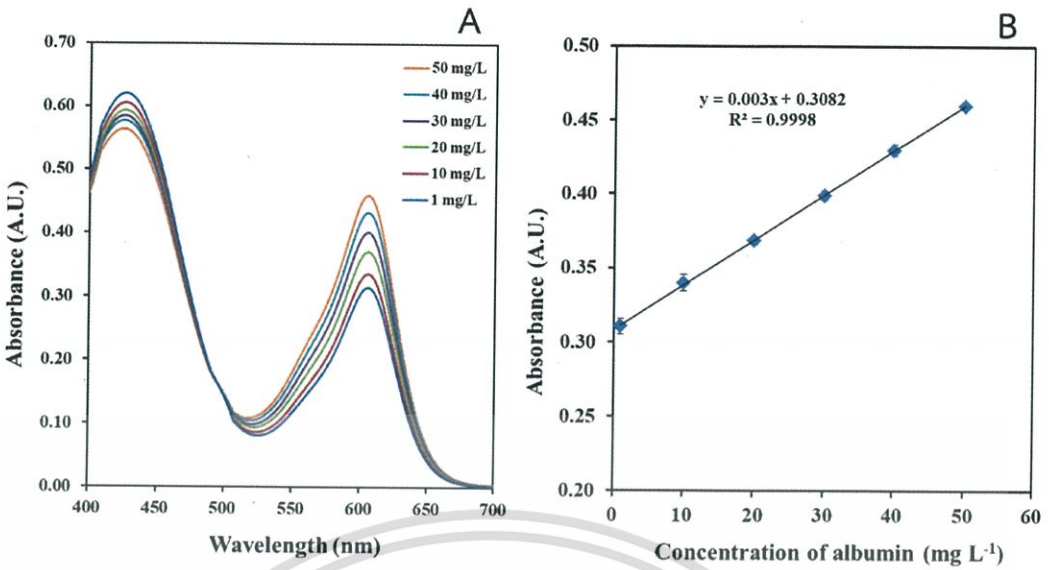

Figure 4.1 (A) Absorption spectra and (B) calibration line of the standard albumin solution (from 1 – 50 mg L^{-1}) were obtained.

4.1.2 Study on kinetic of the reaction

Kinetics of the detection reaction was studied for 30 min at the fixed wavelength (605 nm). The results are shown in Figure 4.2. After mixing the standard albumin solutions (1, 30 and 50 mg L^{-1}) with TPBE, the reaction reached equilibrium within 1 min. Hence, the reaction was suitable to utilize in this work for rapid analysis.

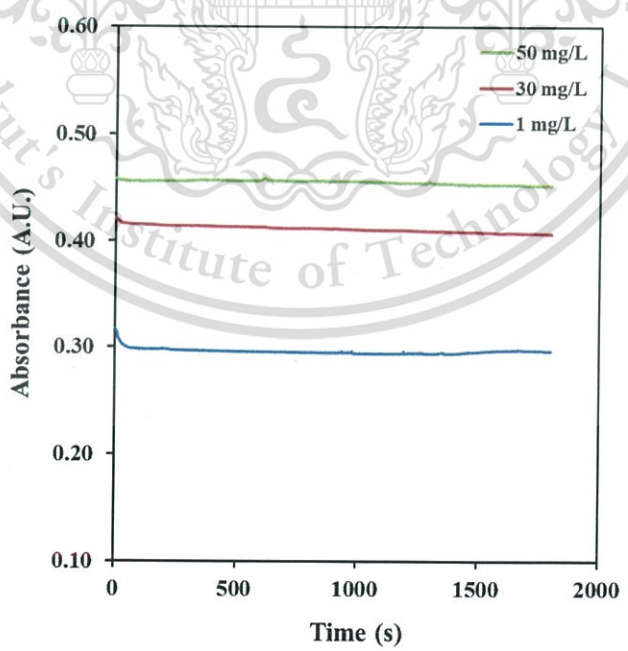

Figure 4.2 The kinetic curves of the reaction between albumin and TBPE in the presence of Triton X-100 obtained when standard albumin solutions (1, 30 and 50 mg L^{-1}) were studied.

4.1.3 Design of 'Albumin smart test' application and image processing

'Albumin smart test' application was designed using the Java-based program for Android operating system. Android was chosen because of its ease for programming and the benefit of being free license. Furthermore, Android currently leads the smart-phone operating system market with almost 75% of the devices [51]. Figure 4.3 displays four different screenshots of the developed application at different stages of image processing. User interface is displayed as shown in Figure 4.3A. The albumin test is initiated after touching "START". User manual is summarized in "HOW TO". The albumin concentrations for previous diagnoses are recorded in "HISTORY". This information is useful as regarding in term of long-term monitoring of microalbuminuria. General information of the application is concluded in "ABOUT". User can exit the application by touching "QUIT".

After touching on "START", the new window appears and the digital camera of the smart phone is power up as depicted in Figure 4.3B. The rectangular frame and the circular frames are exploited to confine the area of the standard colorimetric strip and the samples, respectively. User can conveniently adjust the distance and the orientation of the mobile phone in such a way that the images of the standard colorimetric strip and the samples are clearly observed within these frames (See Figure 4.3C). The distance between the digital camera and the objects can be therefore kept constant at every analysis under the same mobile device. Non precise measurement due to the position of the mobile phone is typically shifted or moved away from the objects can be eliminated.

The images of the standard colorimetric strip and the samples are simultaneously captured after touching the camera icon (Figure 4.3C). The acquired images are then digitally processed by touching "Next". The image (as JPEG format) with a size of 129 x 129 pixels of each printed reference color is consecutively calculated for its characteristic H (hue) parameter of the HSV color space using the embedded color analysis algorithm as proposed by K. Crantell *et. al* [13]. The H value is employed as a quantitative analytical parameter in this work as this value is the representation of the cognitive color information in a single parameter [52]. In addition, the H value is stable and easily obtained from the digital camera [13]. The results are exploited for construction of calibration equation against the albumin concentration ranging from 1 to 50 mg L^{-1}. The calibration equation is re-constructed at every measurement. For the next step, the area of the images of the samples (129 x 129 pixels) in the control and the test holders are evaluated for their H parameters. Result obtained by the test holder is subtracted by the one from the control holder for background correction of any perturbation arisen from color of urine sample. The result is converted to its corresponding albumin concentration by

the constructed calibration equation. Once the measurement is finished, summary of the result appears in the display of the mobile phone (Figure 4.3D). Two different types of labels, either "Normal" or "High Risk to microalbuminuria" is presented for the albumin concentration that fall within a range of lower or greater than 30 mg L^{-1}, respectively. An example of the result in Figure 4.3D is observed when urine sample collected from normal volunteer is analyzed. All imaging processes are accomplished within 5 sec. User can record the result by touching 'SAVE' or can repeat the measurement by touching 'BACK'.

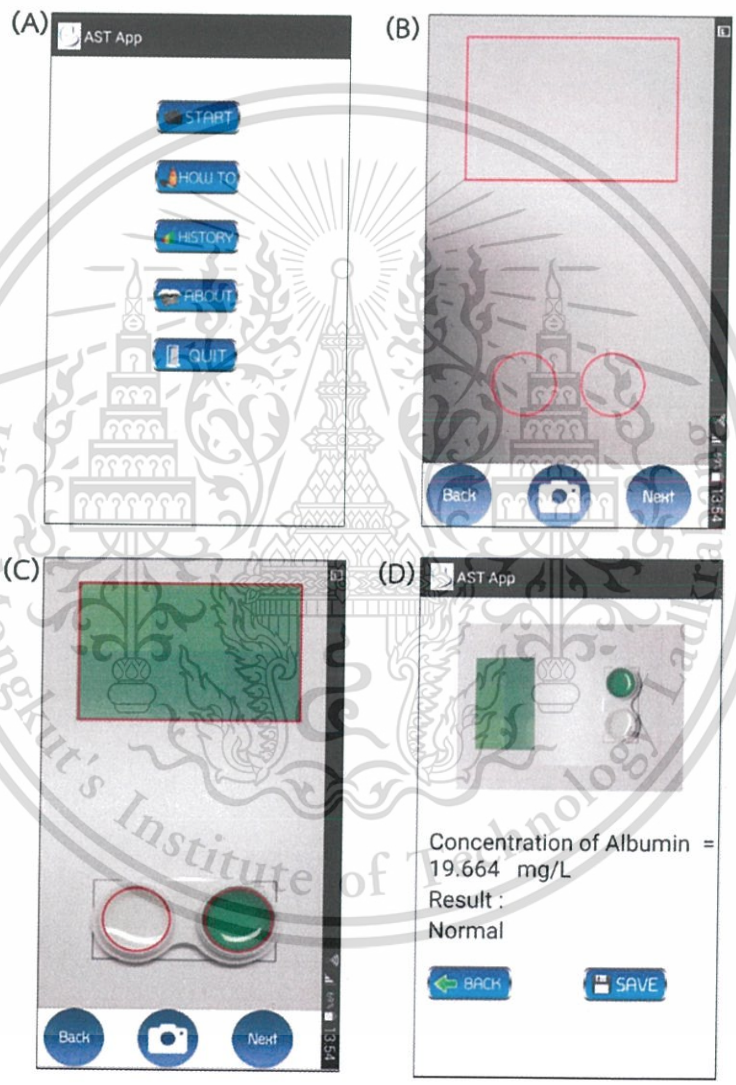

Figure 4.3 Screenshots of the "Albumin smart test" application at difference stages of the image processing. (A): User interface, (B): Power up the digital camera of the smart phone, (C): Simultaneously capturing the images of standard colorimetric strip and the sample and (D): Report on summary of the albumin test.

4.1.4 Development and verification of the printed standard colorimetric strip

Reliability of our developed method is strongly depended on the printed reference colors in the standard colorimetric strip since the H parameters of the printed reference color is employed for constructing the calibration equation. The printed reference colors (Figure 4.4) were developed from the standard reference solutions that were prepared by mixing of the standard working solutions of albumin (1, 10, 20, 30, 40 and 50 mg L^{-1}) with the color developing reagents and acetate buffer (pH 3.1).

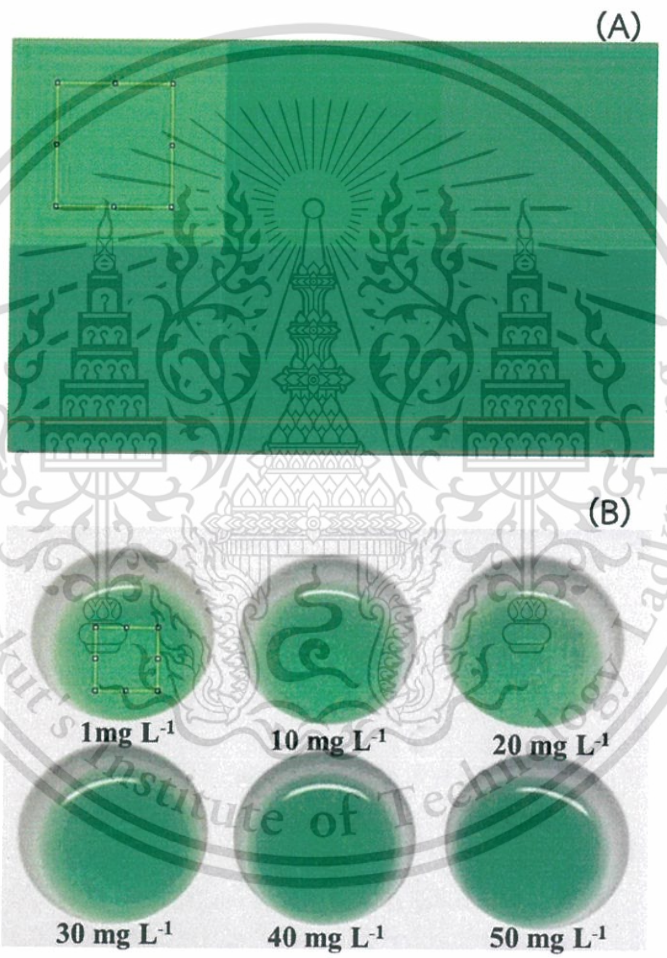

Figure 4.4 (A) and (B) Optical images of the printed reference colors on the test paper and the reference standard solution in the plastic spot plate, respectively. The sensing area (depicted as square) is 129 x 129-pixel.

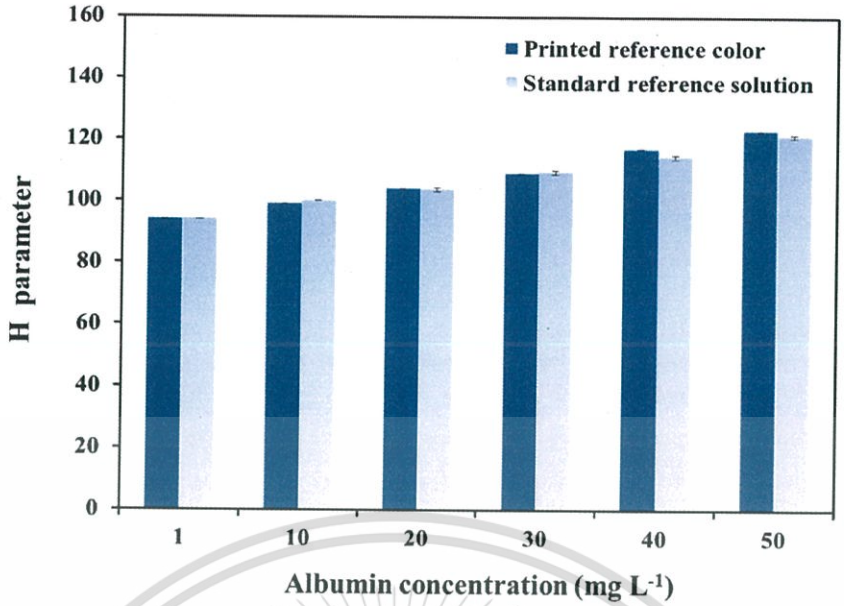

Figure 4.5 Comparison of the H parameters obtained by the printed reference colors and by the reference standard solution.

Criteria to verify the printed reference color is to compare its H parameter to the one obtained by the standard reference solutions (Figure 4.4B) that spectra and absorbance reading at 605 nm were monitored. The H parameter of each printed reference color was evaluated similarly to the H parameter obtained by the standard reference solution. The results in Figure 4.5 are not significant difference by the statistical paired t-test [53] (t_{stat} = -1.08, t_{cri} = 2.57, d.f. = 5). This implies that the printed reference colors of the standard colorimetric strip can be employed as the representation of the standard reference solutions for the quantification of albumin.

4.1.5 Advantage for self-calibration configuration

The 'Albumin smart test' and the test paper are designed in order that the standard colorimetric strip and the sample are simultaneously captured in a single shot. Integration of self-calibration configuration is therefore achieved. The most advantage is that effect of variation of illuminations can be minimized. To demonstrate this advantage, optical images of the mixed solutions between standard albumin (1, 10 30 and 50 mg L^{-1}) and the chromomeric reagents were captured and were analyzed by our mobile phone device at various illumination levels. As shown in Figure 4.6, the measured albumin concentrations are not difference for all illuminant conditions. The effect of variation of illumination is therefore negligible. This can lead our mobile phone-based to provide high versatility for measurement of the urinary albumin concentration in both typical indoor and outdoor illumination without requirement of any additional lighting control apparatus.

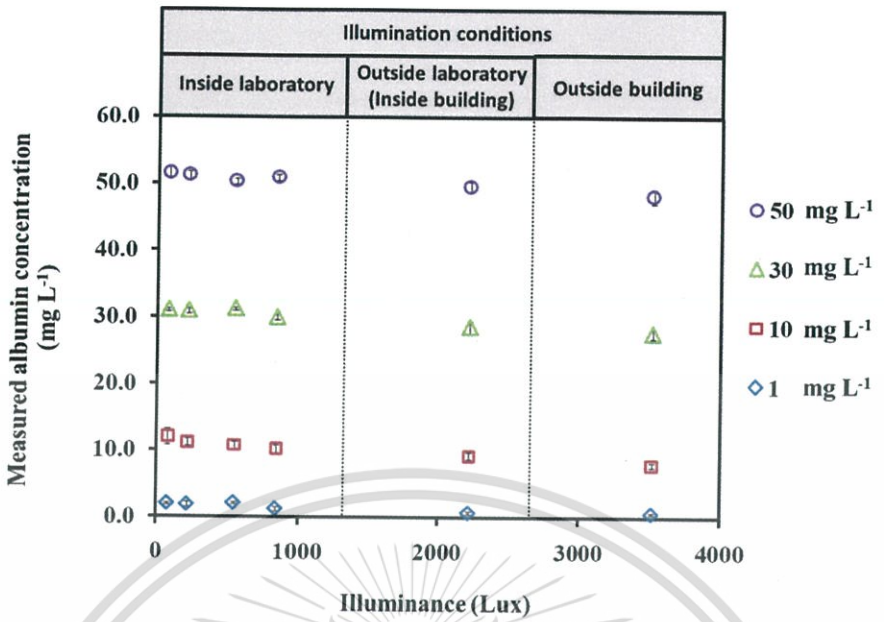

Figure 4.6 Effect of different illumination conditions.

4.1.6 Application to urine samples: validation and diagnosis of microalbuminuria

4.1.6.1 Precision

The precision is represented in term of relative standard deviation (RSD, %). The RSD was calculated from the standard albumin solutions (10, 30 and 50 mg L^{-1}) that were measured for five replicates. Table 4.1 shows the RSD of this method.

Table 4.1 Relative standard deviation (RSD, %) of the 'Albumin smart test' application (n = 5).

Std. albumin concentration (mg L^{-1})	Intraday		Interday	
	Found (mg L^{-1})	%RSD	Found (mg L^{-1})	%RSD
10	10.24 ± 0.13	1.22	11.18 ± 0.28	2.51
30	31.23 ± 0.29	0.93	30.06 ± 0.36	1.18
50	50.25 ± 0.46	0.91	50.52 ± 0.36	0.72

It is clearly observed from the results in Table 4.1 that RSD value is very low (< 3%). This confirms that our 'Albumin smart test' provides high precision.

4.1.6.2 Recovery

An experiment was carried out on 50 urine samples to evaluate the recovery of the method. Addition of albumin standards (10 to 50 mg L^{-1}) was made for a sample solution. The samples were analyzed by the mobile phone-based analyzer without any further dilution. The results given in Table 4.2 demonstrate that the method provides satisfactorily good recovery of the signal.

Table 4.2 Recovery study of standard albumin added to urine samples.

Sample	Original (Mean (mg L^{-1}) ± SD)**	Added (mg L^{-1})*	Found (Mean (mg L^{-1}) ± SD)**	Recovery (%)
S1	1.0 ± 0.08	10.6	11.4 ± 0.24	98.4
S2	1.0 ± 0.17		11.5 ± 0.45	98.6
S3	1.2 ± 0.19		11.8 ± 0.31	100.7
S4	1.1 ± 0.20		11.7 ± 0.28	100.5
S5	1.4 ± 0.09		11.3 ± 0.29	94.4
S6	1.1 ± 0.05	20.9	21.9 ± 0.10	99.7
S7	1.0 ± 0.01		21.6 ± 0.11	98.6
S8	1.2 ± 0.06		22.1 ± 0.24	100.3
S9	1.6 ± 0.09		21.8 ± 0.41	97.0
S10	0.9 ± 0.02		21.2 ± 0.39	97.3
S11	1.7 ± 0.39	31.4	32.1 ± 0.29	96.9
S12	1.3 ± 0.18		32.0 ± 0.16	97.9
S13	1.5 ± 0.28		32.3 ± 0.25	97.9
S14	1.2 ± 0.19		32.4 ± 0.41	99.1
S15	1.3 ± 0.30		31.9 ± 0.14	97.5
S16	1.1 ± 0.05	40.4	41.9 ± 0.29	101.2
S17	1.0 ± 0.01		41.7 ± 0.55	100.9
S18	1.2 ± 0.06		42.0 ± 0.70	101.0
S19	1.6 ± 0.09		41.5 ± 0.58	98.9
S20	0.9 ± 0.02		41.1 ± 0.35	99.6
S21	1.1 ± 0.05	51.7	52.0 ± 0.16	98.4
S22	1.0 ± 0.01		51.9 ± 0.35	98.4
S23	1.2 ± 0.06		52.4 ± 0.44	99.1
S24	1.6 ± 0.09		52.1 ± 0.23	97.6
S25	0.9 ± 0.02		51.8 ± 0.41	98.4

Note * Concentration of standard albumin added to urine sample solutions.

**Measurement was carried out in triplicates.

4.1.6.3 The Bland – Altman plot

The developed method was applied to the determination of albumin in 50 urine samples that were spot collected from volunteers of various ages (30 to 60 year-old) with no known history of CKD. The results determined by the mobile phone were compared with results obtained using the validating spectrophotometric method by means of the Bland–Altman plot [54] for validation study.

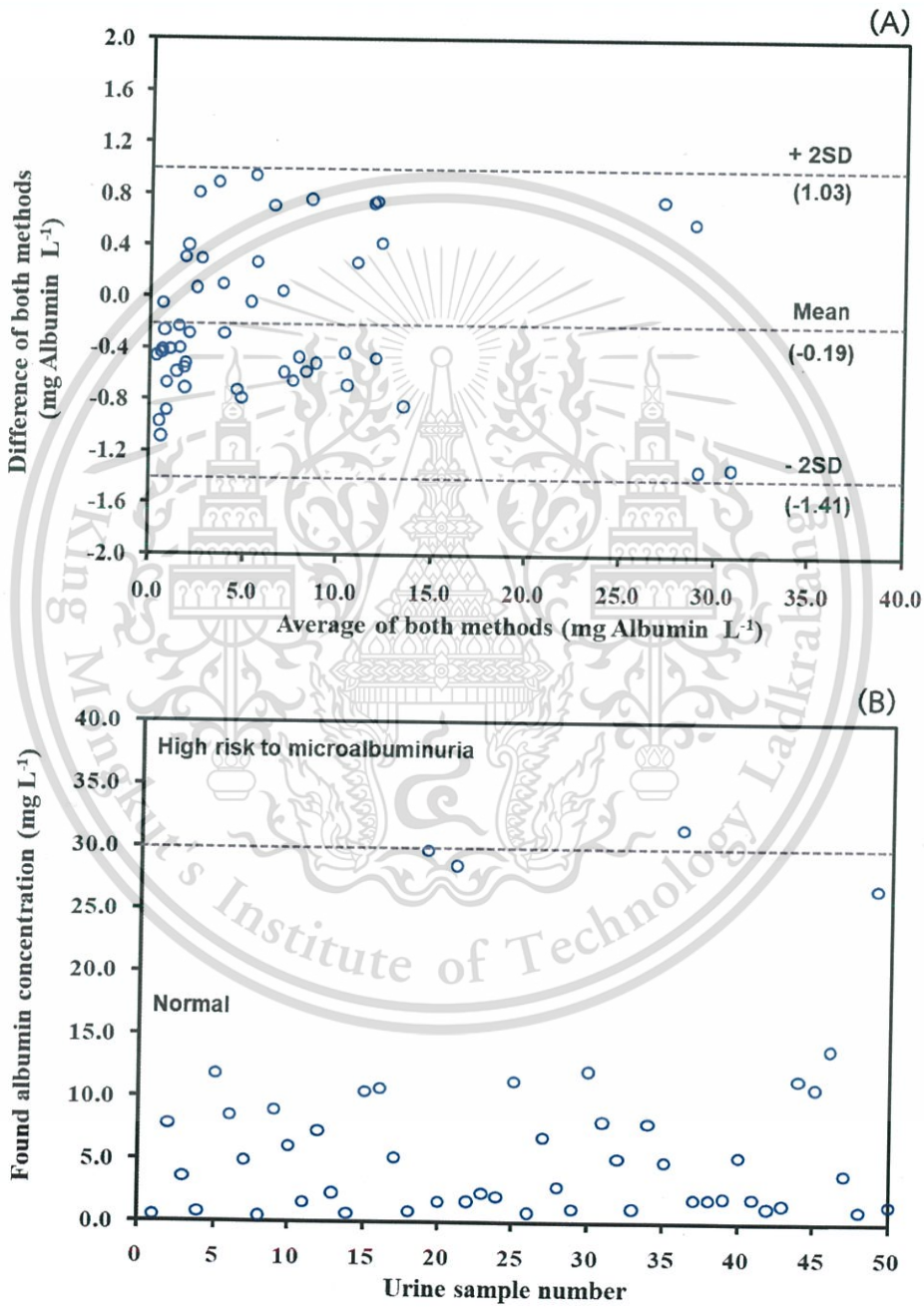

Figure 4.7 Validation and application to urine samples (n = 50 samples). (A) The Bland-Altman plot for comparison of the data obtained from the method with the validating spectrophotometric method. (B) Found albumin concentration, determined by this method.

Results in Figure 4.7A show that all data lay within ± 2SD of the mean of their differences, indicated that this method was equivalent to the validating method. Figure 4.7B shows that some volunteers are of high risk of microalbuminuria. It was observed by our personal interview that these volunteers suffered from hypertension and diabetes.

4.1.6.4 Comparison of the albumin content, determined by different mobile devices

The developed application program was installed into the other mobile devices. Comparison of the albumin content in urine samples, determined by different mobile devices is concluded in Table 4.3. By ANOVA test [45], the results are not significant difference (F_{stat} = 3.12, F_{crit} = 3.89). This implies that the developed application program is applicable for different devices and models.

Table 4.3 Comparison of the albumin content in urine samples, determined by different mobile devices.

Sample	Concentration of measured albumin[a] (Mean (mg L^{-1}) ± SD)		
	Device 1[b]	Device 2[c]	Device 3[d]
S1	31.2 ± 1.0	31.1 ± 0.5	30.6 ± 1.3
S2	31.0 ± 0.5	32.2 ± 0.8	30.1 ± 0.5
S3	32.4 ± 0.5	33.9 ± 1.4	31.3 ± 0.8
S4	31.9 ± 2.1	33.2 ± 0.4	32.4 ± 0.3
S5	31.8 ± 1.8	32.0 ± 1.0	31.2 ± 0.5

Note [a]Measurement was carried out in triplicates.
[b]Samsung Galaxy Tab. 10.1 (No.1).
[c]Samsung Galaxy Tab. 10.1 (No.2).
[d]Samsung Galaxy S5.

4.2 A LED spectrometer for measurement of urinary creatinine and uric acid

A LED spectrometer for measurement of urinary creatinine and uric acid was comprised of two main components. The first component is hardware which consisted of light source, a microcontroller and light detector. Another is software that loaded into microcontroller.

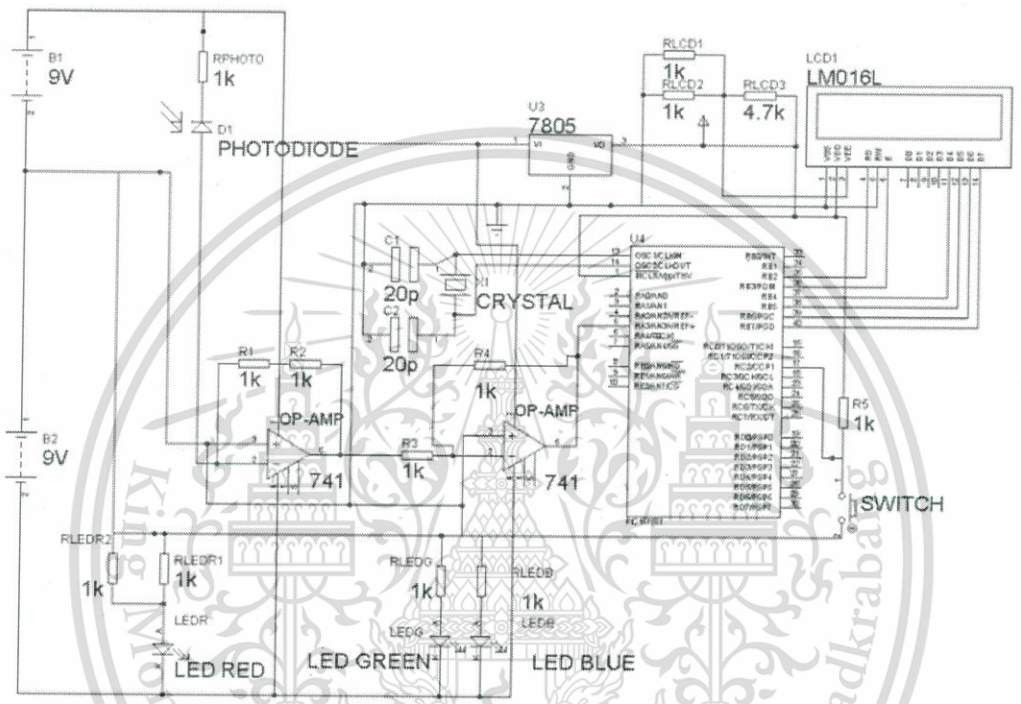

Figure 4.8 The electronic circuit design of the LED spectrometer.

Figure 4.8 illustrates the circuit design for the developed LED spectrometer. The photograph of the device and its compartments are illustrated in Figure 4.9. Dimension of the LED spectrometer is 9 x 20 x 8 cm^3 (width x length x height). Hardware are consisted of Red-Green-Blue LED bulbs, microcontroller (for evaluation of the absorbance based on Beer's law) and photo transistor (as light detector). The absorbance is displayed on an LCD screen.

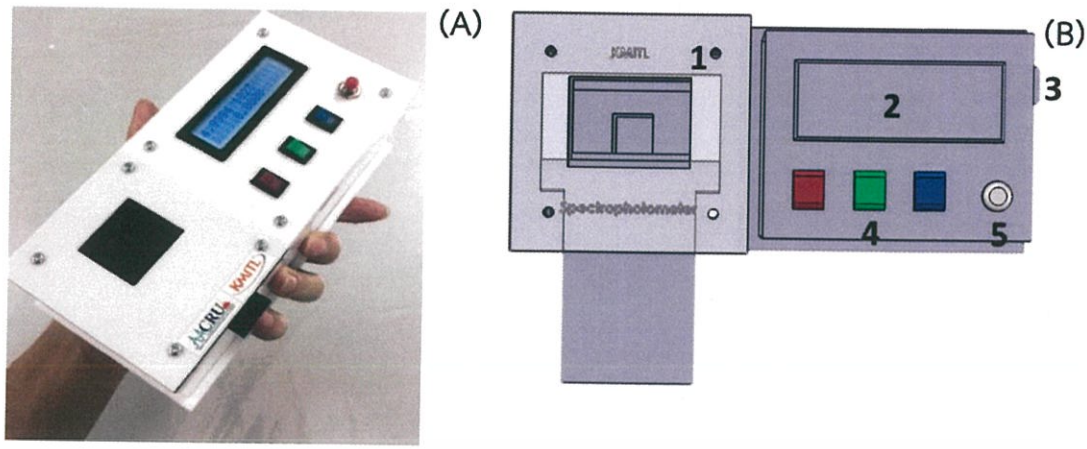

Figure 4.9 (A) Photograph of the LED spectrometer. (B) Components of the LED spectrometer which is consisted of (1) sample holder, (2) LCD display, (3) Switch on / off, (4) Buttons for Red-Green-Blue LED lamp, (5) Button for auto zero.

4.2.1 Preliminary performance test of a LED spectrometer

Slope and coefficient of determination obtained of the standard linear equation from linear plot when either the LED spectrometer or the UV - visible spectrophotometer were compared in order to consider in term of performance of the LED spectrometer and the UV - visible spectrophotometer.

The LED spectrometer was applied to measure the absorbance of three color products developed from different chemical reactions. The chemical reactions of ethanol and potassium dichromate, uric acid and phosphotungstic acid and Fe (II) and ortho–phenanthroline were selected for performance test of red, green and blue bulbs, respectively. Results are shown in Figure 4.10 A - C.

From the results, the slopes obtained by UV - visible spectrophotometer were not significant different to the slopes obtained by the LED spectrometer. The results of r^2 that observed by the LED spectrometer were ranged from 0.98 to 0.99 which are acceptable accordingly to Beer's law.

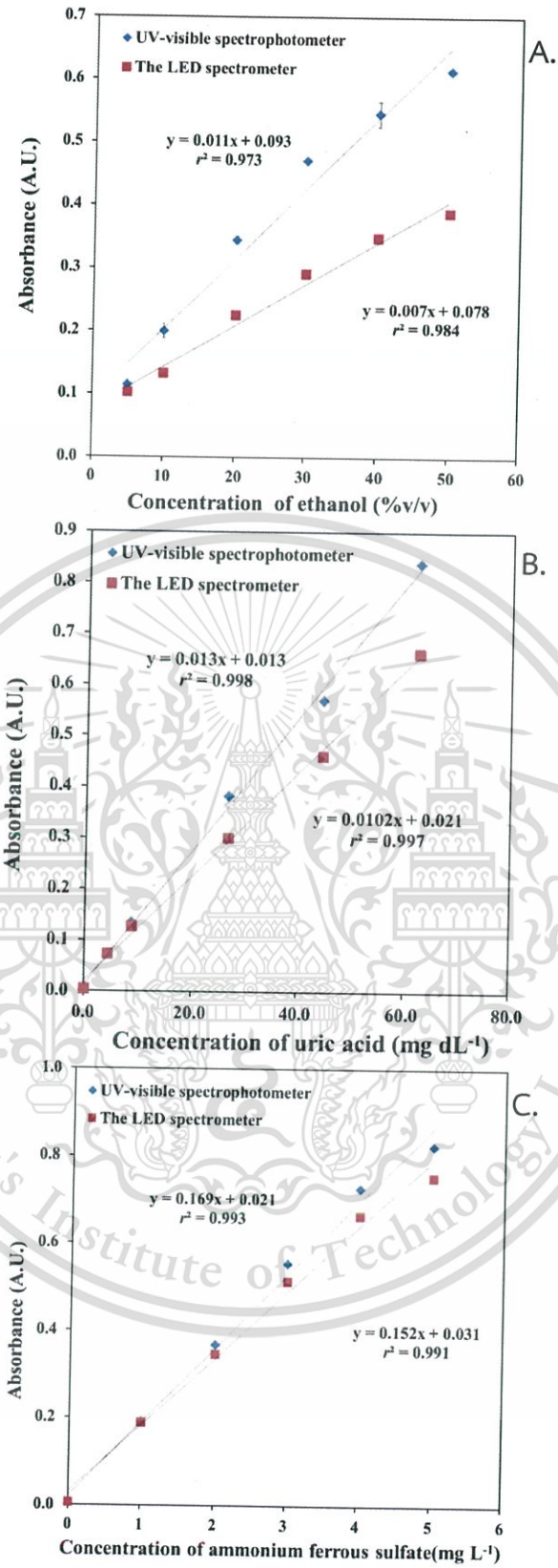

Figure 4.10 The linear plots between the concentration of various analytes and the absorbance readings obtained by LED spectrometer and UV - visible spectrophotometer. (A) Performance test for red bulb, (B) for green bulb and (C) for blue bulb.

4.2.2 A LED spectrometer for measurement of urinary creatinine

4.2.2.1 Digestion of the reused traditional gold leaf using the gold nanoparticles as colorimetric sensor

Gold is resistant to most acids, though it can dissolve in aqua regia (HCl/HNO_3, 3:1). HNO_3 dissolve gold to form Au (III). HCl react with Au (III) to produce tetrachloroauric acid ($HAuCl_4$) as written in the following equation (14) [55].

$$2Au(s) + 3HNO_3(aq) + 11HCl(aq) \longrightarrow 2HAuCl_4(aq) + 3NOCl(aq) + 6H_2O(l) \quad (14)$$

The parameters affecting the digestion of the reused traditional gold leaf, which are the concentration of aqua regia and the digestion time were investigated. Criterion for selection of the appropriate conditions is based on the product yield (%) which is calculated from the ratio of $[HAuCl_4]_{observed}$ to $[HAuCl_4]_{theoretical}$ (the following equation (15)).

$$\text{Yield (\%)} = \frac{[HAuCl_4]_{observed}}{[HAuCl_4]_{theoretical}} \times 100 \quad (15)$$

Where the $[HAuCl_4]_{observed}$ is the concentration of $HAuCl_4$ in the digested gold leaf solution which is evaluated using the linear calibration plot between the absorbance reading at 308 nm (the maximum absorption wavelength (λ_{max}) of $HAuCl_4$) against the concentrations of the standard $HAuCl_4$. The $[HAuCl_4]_{theoretical}$ is the concentration of $HAuCl_4$ which is stoichiometrically calculated based on use of equation (14).

Results in Figure 4.11A show that the λ_{max} of the digested gold leaf is located at 310 nm, where is very close to the λ_{max} of the standard $HAuCl_4$. This implies that $HAuCl_4$ were obtained after digestion. Both the absorbance readings and yields were increased, when the aqua regia concentrations were increased up to 70 % (v/v). Therefore, the concentration of 70 % (v/v) aqua regia was chosen. The absorbance readings and yields were also risen, when the digestion times were increased up to 30 min (Figure 4.11B). The digested time of 30 min was selected as compromising between the obtained yield and the consumed time. This digestion time was shortened from more than 2 hours, compared to the other reports [56, 57] with the comparable yield.

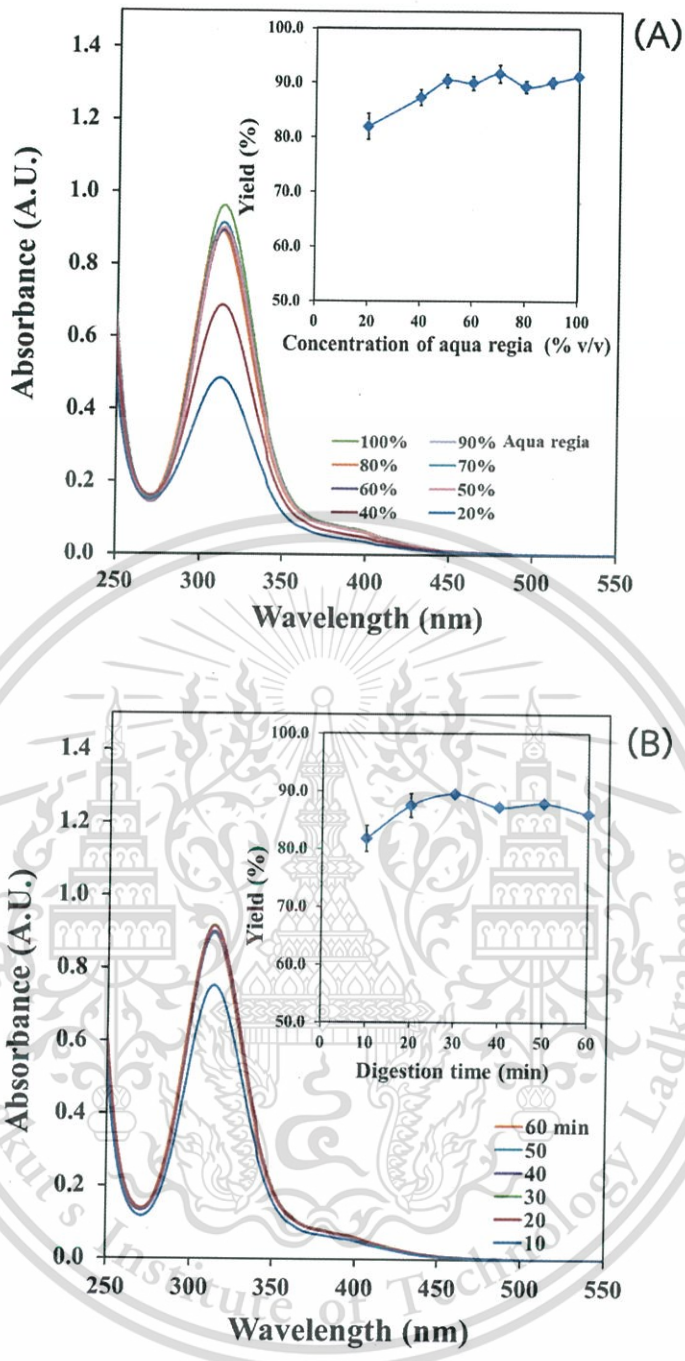

Figure 4.11 UV - visible absorption spectra of the digested gold leaf solutions obtained by (A) various concentrations of aqua regia (at fixed acid volume (5.0 mL) and digestion time (30 min)), and (B) various digestion times (at fixed acid volume (5.0 mL) and aqua regia concentration (70 % v/v)). Inset graphs are the product yield (%) at various concentrations of aqua regia and digestion times.

4.2.2.2 Chemical parameters affecting the synthesis of the reused traditional gold leaf-prepared AuNPs

The pH of the digested gold leaf solution, the concentrations of PVA and sodium citrate are the critical parameters which affect size, morphology and chemical properties of the synthesized AuNPs.

(1) Effect of pH of the digested gold leaf solution

The initial pH of the digested gold leaf solution is very important for using the solution as the precursor for synthesis of AuNPs. Results in Figure 4.12A indicate that the characteristic Surface Plasmon band of the AuNPs was not appeared when the original digested gold leaf solution (pH 1.4) was used as the precursor. Color of the prepared solution was still pale yellow and was not changed to wine-red (See inset photos of Figure 4.12A). This suggests that the AuNPs were not formed. This is because at low pH, the carboxyl group of sodium citrate is protonated to citric acid [58]. Reduction of Au (III) to become the Au^0 nanoparticles is not occurred. The pH of the digested gold leaf solutions were then adjusted to obtain the final pH of 2.0, 3.0 and 4.0 by using NaOH (1.0 mol L^{-1}) prior to use for synthesis. At pH 2.0, the narrowest Surface Plasmon band was located at 530 nm and color of the corresponded solution was turned to wine-red (Figure 4.9A). This means that Au (III) ions in the digested gold leaf solution were converted to Au^0 particles by citrate ions. The representative TEM image in Figure 4.12B also displays that the colloidal and spherical-shaped AuNPs are obtained. At higher pH values (pH 3.0 and 4.0), their Surface Plasmon bands were expanded with decreasing in the absorbance readings at 530 nm (Figure 4.12A). This is due to the hydrolysis of $AuCl_4^-$ is occurred in more alkaline solution and the species of $[AuCl_{4-n}(OH)_n]^-$ are produced. This hydrolyzed auric species are less reactive species and lead to broadening of Surface Plasmon bands [58-60]. Additionally, at higher pH, the auric species (Au(III), Au(I) and $[AuCl_{4-n}(OH)_n]^-$) can adsorb on surface of the formed gold seeds and this results in the ellipsoidal-shape AuNPs [60] as the representative TEM image demonstrated in Figure 4.12C. The pH value of 2.0 was therefore regarded as the suitable pH of the digested reused gold leaf solution.

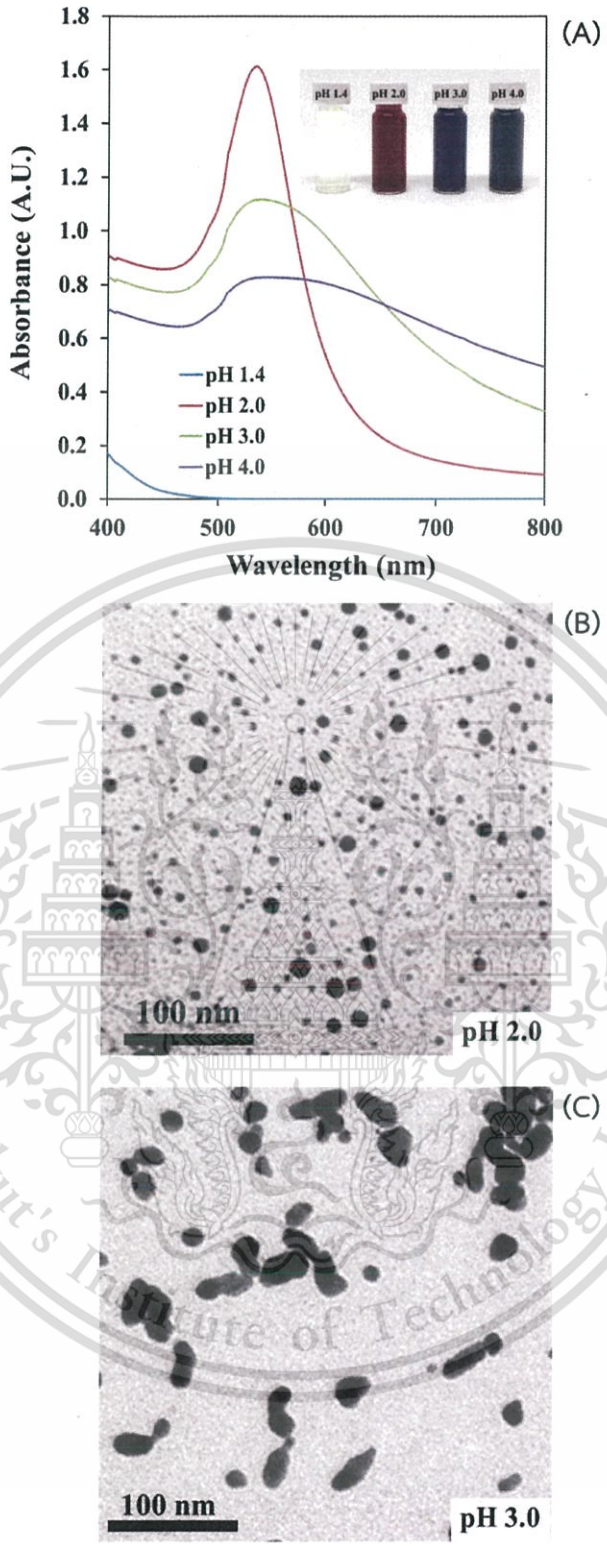

Figure 4.12 (A) Surface Plasmon bands obtained when the pH values of the digested gold leaf solutions are varied from 1.4 to 4.0. Inset photos represent colors of the as-prepared solutions at different pH values of the solutions. (B) and (C) are the TEM images of the reused gold leaf-prepared AuNPs at pH 2.0 and 3.0, respectively. The concentrations of citrate and PVA are fixed at 1.2 and 2.0 % (w/v), respectively.

(2) Effect of the concentrations of sodium citrate

The effect of the concentrations of sodium citrate was also investigated. Results in Figure 4.13 (A to D) indicate that when the concentrations of citrate were increased, the size of the particles was decreased. However, it is noticed that self-aggregation of the nanoparticles tends to occur when higher concentrations of the reductant are examined, and it is clearly observed at 1.8 % (w/v). This causes the solution color turn to more dense wine-red. This effect is promoted due to the compression of the double layers contributed by the high counter sodium ion concentration [17, 61]. It was also found that, at 1.6 and 1.8 % (w/v), precipitation of the particles was appeared after keeping the solution for > 48 hr. In this work, the concentration of 1.2 % (w/v) is chosen as the appropriate concentration because the colloidal AuNPs are obtained without any observation of self-aggregation (Figure 4.13B).

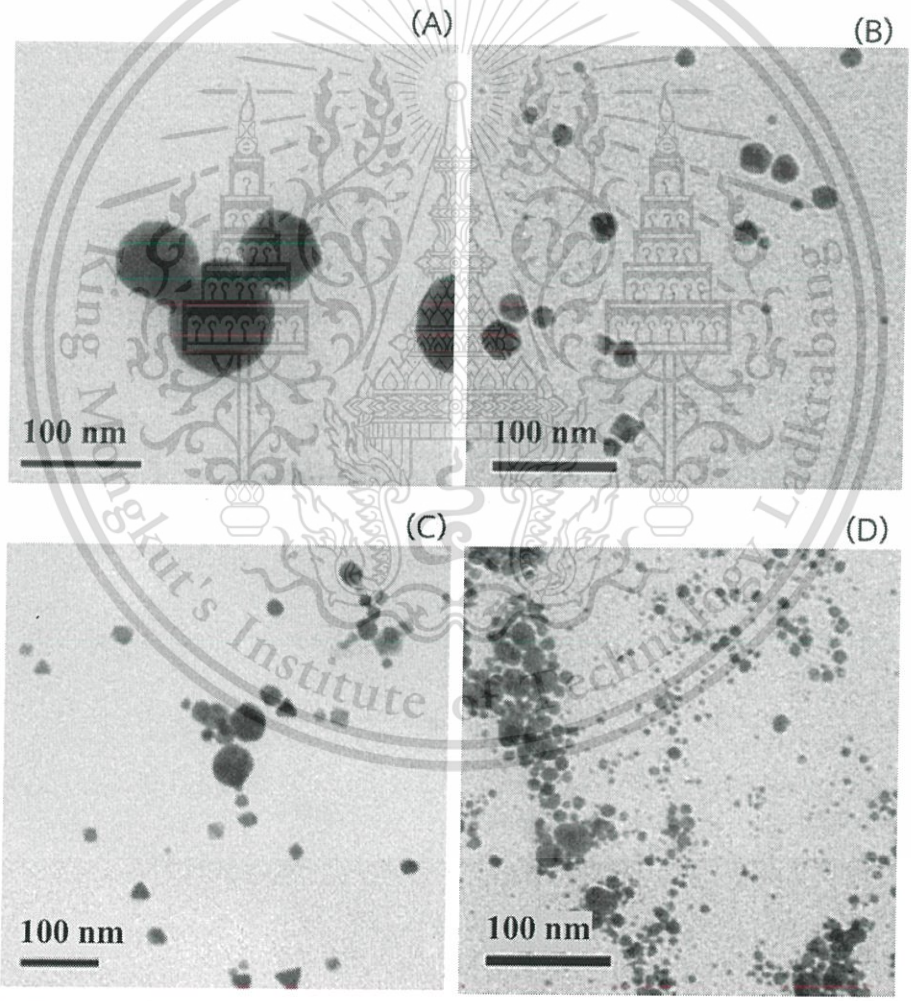

Figure 4.13 TEM images of the reused traditional gold leaf-prepared AuNPs obtained when (A) 1.1 (B) 1.2, (C) 1.5 and (D) 1.8 % (w/v) citrate are studied. The concentration of PVA is kept at 2.0 % (w/v).

(3) Effect of the concentrations of polyvinyl alcohol

Dispersed AuNPs are thermodynamically unstable because of their high surface energy, and they are subject to form the aggregates. A strategy to prevent the assembly of AuNPs is to conjugate the nanoparticles with water-soluble polymers to inhibit the contact between the individual AuNPs.

Result by the representative TEM image as displayed in Figure 4.14A shows that without using any stabilizer, the AuNPs precipitates are observed, and the solution becomes colorless. It is therefore necessary to add the stabilizer for enhancement of the long-term stability of the gold colloids. In this work, PVA, which is the non-ionic hydrophilic polymer, is selected for preventing the assembly of the AuNPs. Mixing of the AuNPs and PVA was carried out accordingly to the post-modification approach which is simple, and the preformed-AuNPs offer surface, where the exchange of the citrate ions with the polymer is easily attained [62].

At 2 % (w/v) PVA, the spherical-shaped AuNPs are suspended, and this results in the wine-red color solution as shown in Figure 4.14B. The stabilization mechanism of the AuNPs by PVA is based on the steric effect achieved by the adsorbing polymer onto the surface of particles. However, the nanoparticles tend to be self-aggregated at 8 % (w/v) PVA (Figure 4.14C). It is because when the polymer concentration is greater, it initiates bridging flocculation of the nanoparticles [63, 64]. The concentration of 2 % (w/v) PVA is therefore selected.

To confirm the modification, the transmission FT-IR spectra of the as-prepared AuNPs were studied. Results in Figure 4.15 allow extracting of the following observations: (i) the spectra of the PVA-stabilized AuNPs are similar to that of the pristine PVA, where the characteristic OH stretching bands emerge at 3200 - 3600 cm^{-1} and (ii) the intensity of this identical band increases when the PVA concentration increases from 1 to 2 % (w/v). This information confirms that the AuNPs are successfully modified with PVA.

. By the selected concentration, long-term stability of the as-prepared AuNPs is obtained without precipitation for at least 3 months (Figure 4.16).

Under the most appropriate conditions as mentioned above, the as prepared-AuNPs offer the spherical shape with an average size of 24.2 (± 2.3) nm. The concentration of these AuNPs is 0.83 nmol L^{-1}, which is calculated accordingly to Beer's law using an extinction coefficient of 8.42 x 109 M^{-1} cm^{-1} at 530 nm [65].

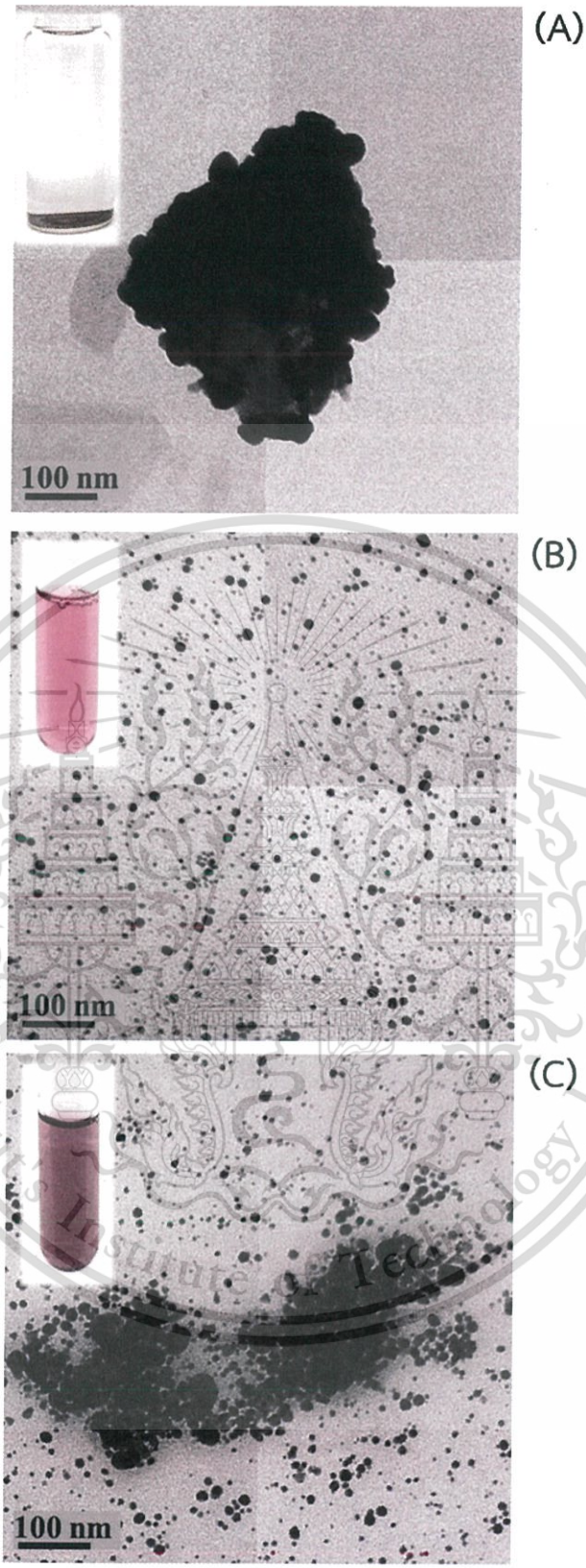

Figure 4.14 TEM images of the reused traditional gold leaf-prepared AuNPs obtained when (A) 0, (B) 2 and (C) 8 % (w/v) PVA are investigated. The concentration of citrate is fixed at 1.2 % (w/v). Inset photos are the corresponded solutions at the different PVA concentrations.

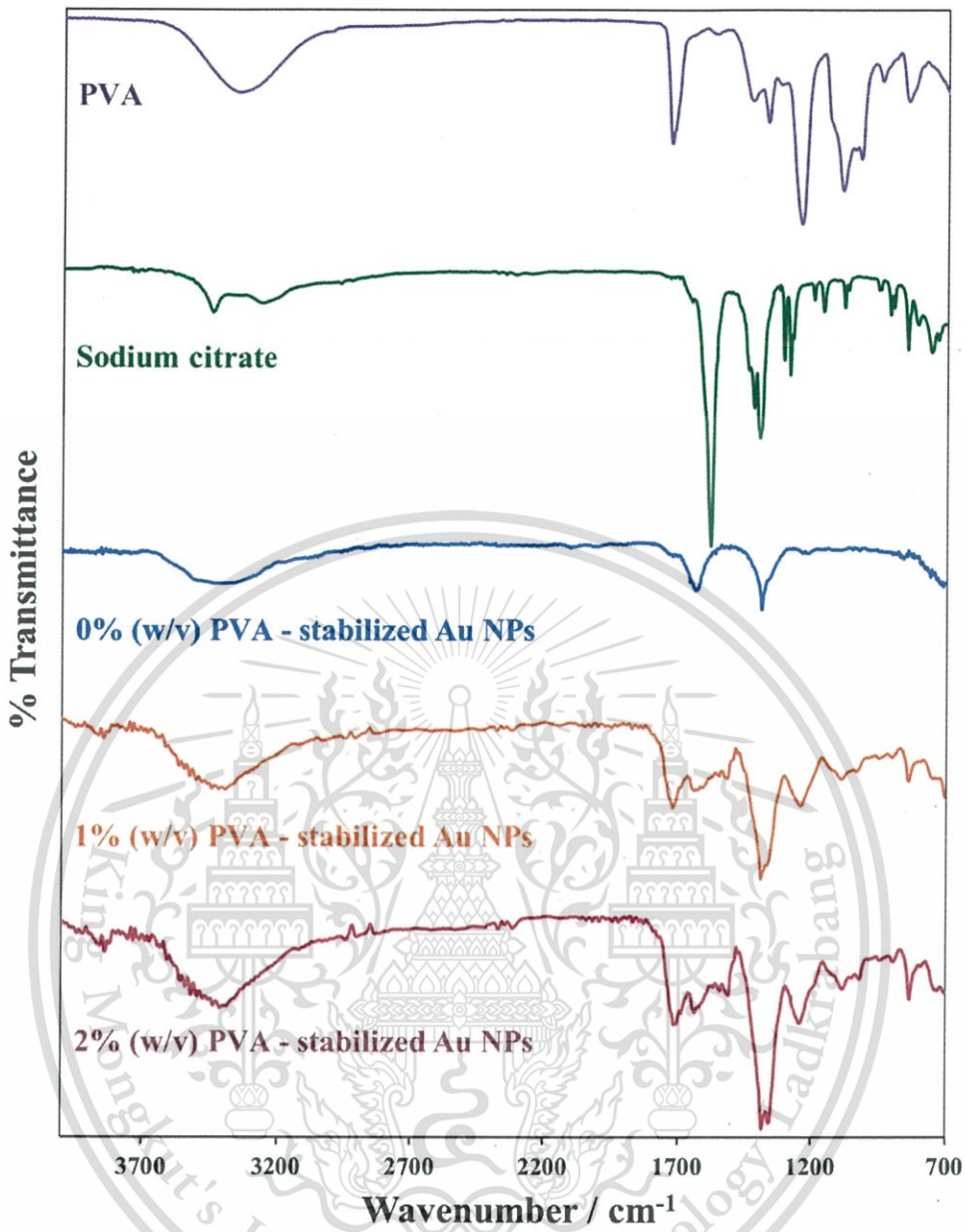

Figure 4.15 Transmission FT-IR spectra of the pristine PVA and the corresponding PVA-stabilized gold leaf-prepared AuNPs at different concentrations of PVA.

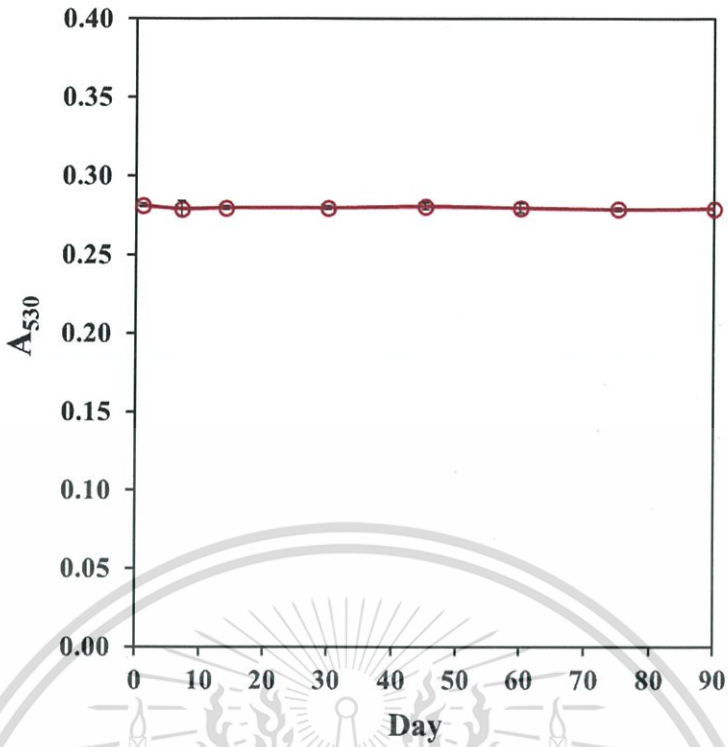

Figure 4.16 Absorbance readings of the traditional gold leaf-prepared AuNPs at 530 nm with increasing days of storage.

4.2.2.3 Colorimetric response of the reused traditional gold leaf-prepared AuNPs to creatinine

Schematic illustration of the principle for colorimetric detection of creatinine using the gold leaf-prepared AuNPs is depicted in Figure 4.17A. After the post-modification of the citrate-capped AuNPs by PVA, facile exchange between the weakly bound surface citrate ions and the polymer is occurred [62]. This enhances the stability of the nanoparticles without self-aggregation (Figure 4.17B). However, the non-covalent interaction of the AuNPs and the polymer is weak because PVA forms physically adsorb to the particles [66]. In the presence of creatinine, the ring nitrogen of hybrid aromatics exhibit much stronger binding affinity to AuNPs [67]. The cross-linking reaction between creatinine and AuNPs is therefore easily achieved via the coordination interaction between the three nitrogen atoms and the AuNPs [68] This promotes aggregation of the nanoparticles (Figure 4.17C) and results in decreasing in the absorbance reading at 530 nm while a new Surface Plasmon peak emerges at 650 nm (Figure 4.17D). The colors of the solutions gradually change from wine-red to blue when the standard creatinine concentrations are increased.

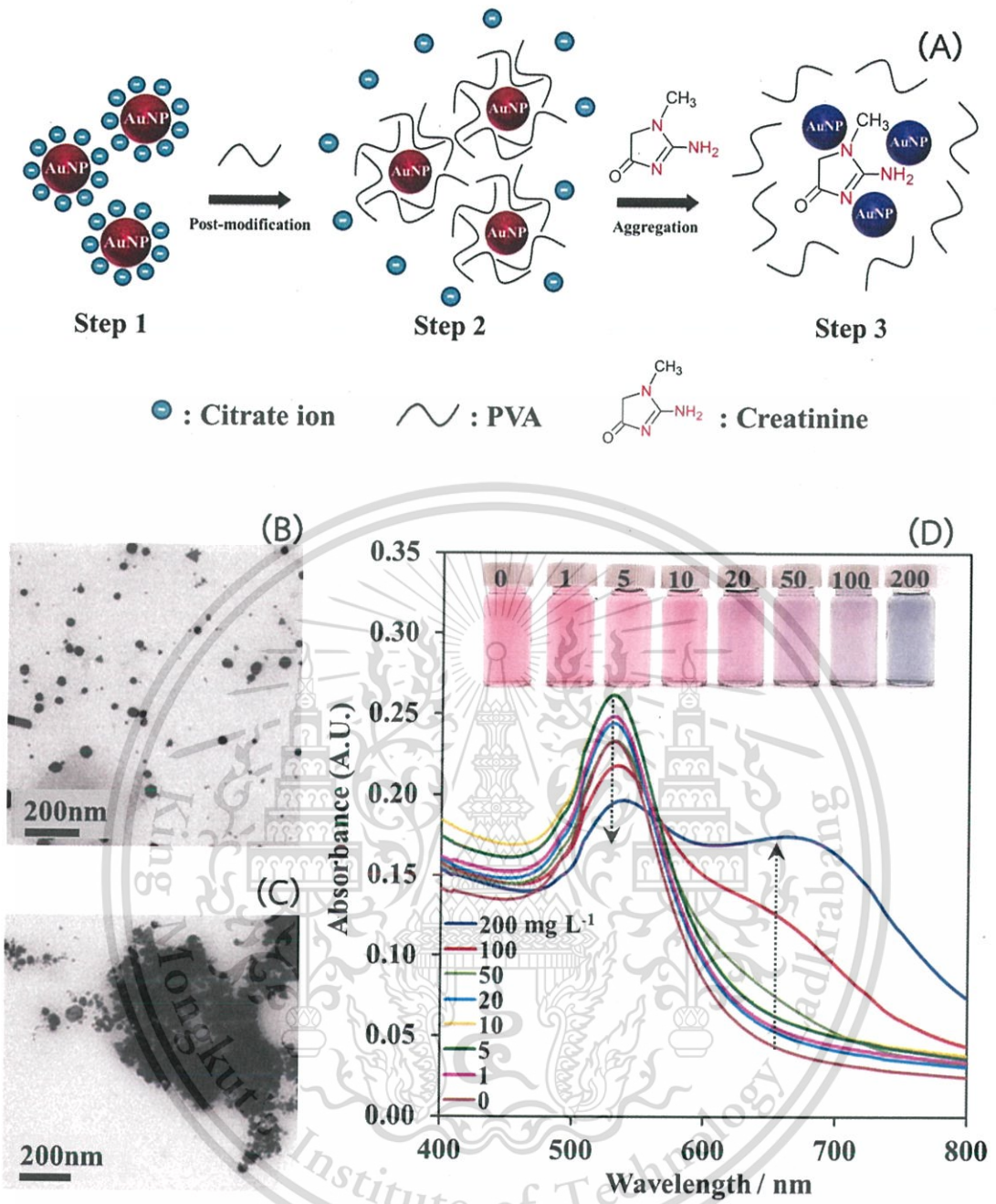

Figure 4.17 (A) Schematic illustration of the proposed mechanism for colorimetric response of the as-prepared AuNPs to creatinine. (B) and (C) are the representative TEM images of the as-prepared AuNPs in the absence and in the presence of 200 mg L^{-1} creatinine, respectively. (D) Surface Plasmon bands of the as prepared-AuNPs with various concentrations of standard creatinine.

4.2.2.4 Effect of reaction time for measurement of creatinine

Effect of reaction time on the aggregation of the as-prepared AuNPs by creatinine was investigated in range 1 to 10 min. The results in Figure 4.18 A indicate that higher concentration of creatinine results in faster response time. Furthermore, the absorbance readings ratios ($A_{650/530}$) are increased as the reaction times are prolonged. In term of linearity of the calibration plot, the reaction time of 3 min provides the better linear response ($r^2 > 0.98$) (Figure 4.18 B). This time is therefore selected as the suitable reaction time.

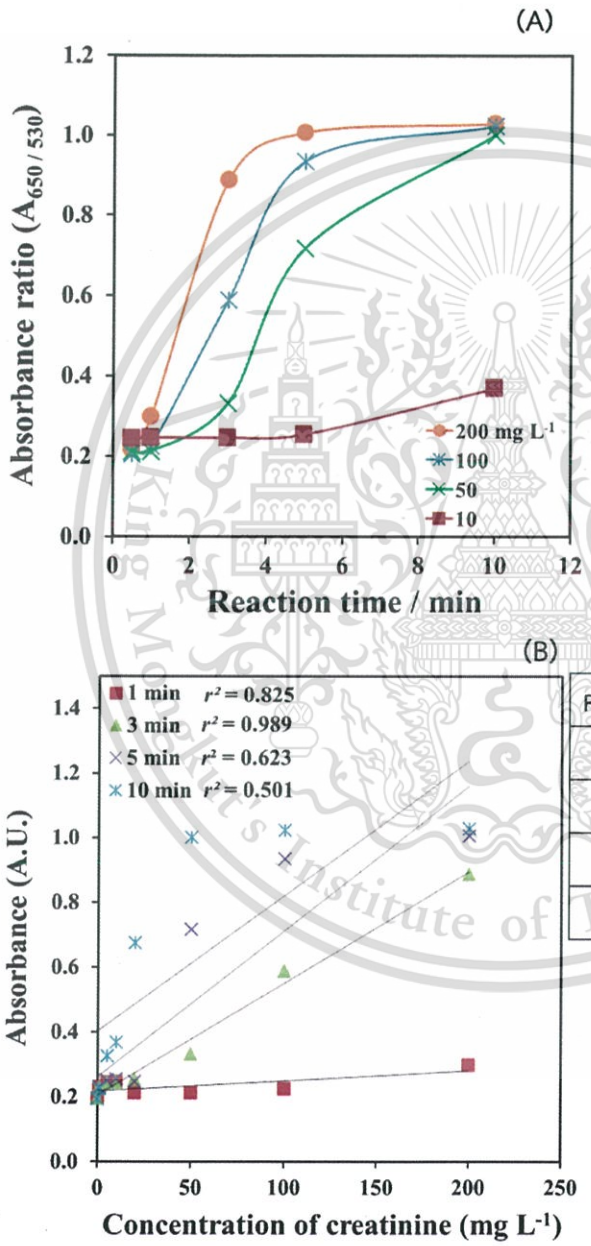

Reaction time	Equations
1 min	y = 0.0003x + 0.218
3 min	y = 0.0034x + 0.206
5 min	y = 0.0045x + 0.263
10 min	y = 0.0042x + 0.404

Figure 4.18 Effect of the reaction time on the aggregation of the as-prepared AuNPs in the presence of creatinine (10 – 200 mg L^{-1}). (A) The plot of the absorbance reading ratio (A650/530) against the reaction times. (B) Calibration plots of standard creatinine.

4.2.2.5 Selectivity study

The selectivity of the gold leaf-prepared AuNPs for the detection of creatinine or the small organic compounds containing nitrogen and the other substances potentially existed in urine (albumin, uric acid and ascorbic acid) was evaluated. Results in Figure 4.19A obviously show that only creatinine causes the solution color change from wine-red to blue and initiates highest absorbance reading ratio (Figure 4.19B). These results indicate that the as-prepared AuNPs are more selective to creatinine than the other small organic compounds and the substances potentially found in urine.

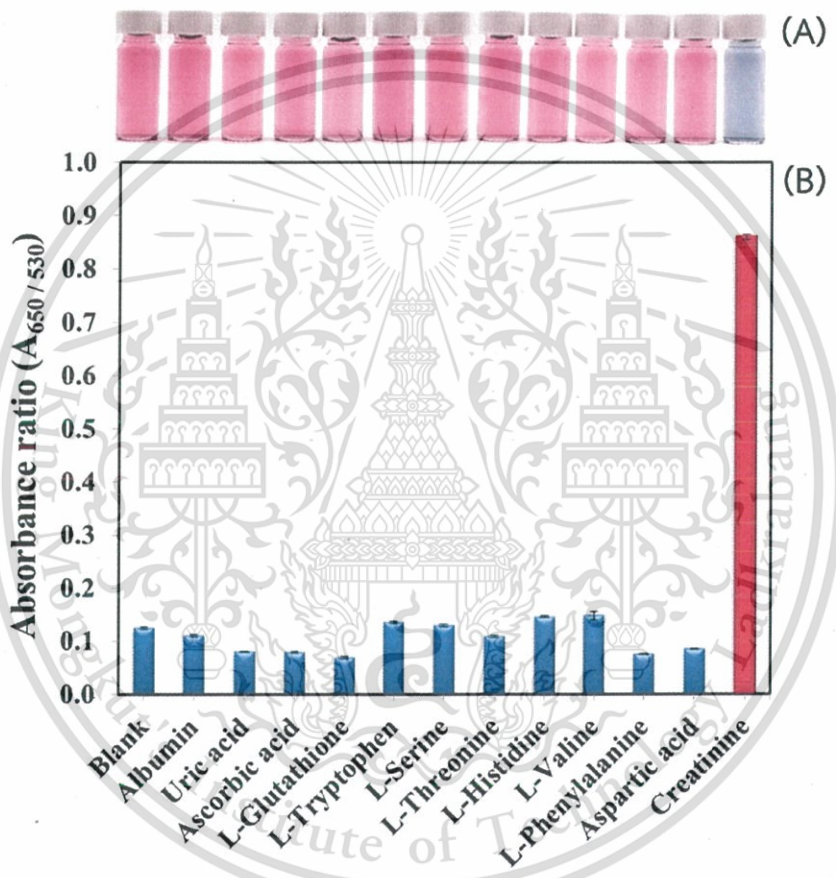

Figure 4.19 The photographs of the as-prepared AuNPs in the presence of creatinine (1.8 mmol L^{-1}), the other small compounds and the substances potentially existed in urine (10 mmol L^{-1} for each foreign species) and (B) their corresponding absorbance reading ratios ($A_{650/530}$).

4.2.2.6 Determination of creatinine using the LED spectrometer

In this part, quantitative measurement of creatinine using the gold leaf-prepared AuNPs with the developed LED spectrometer as detector was investigated. The optimal condition for the detection method was taken from the previous part that is investigated by UV - visible spectrophotometer.

For LED spectrometer, red and blue LED bulb were chosen as a light source for monitoring of the absorption of the product. The result in Figure 4.20 shows that the absorbance readings ratios ($A_{Red/Blue}$) were proportionally increased to the concentration of creatinine with good linearity. Furthermore, performance of the LED spectrometer was compared to the performance of conventional UV - visible spectrophotometer. The results indicate that the sensitivity of LED spectrometer is lower than UV-vis. spectrophotometer about 18 %.

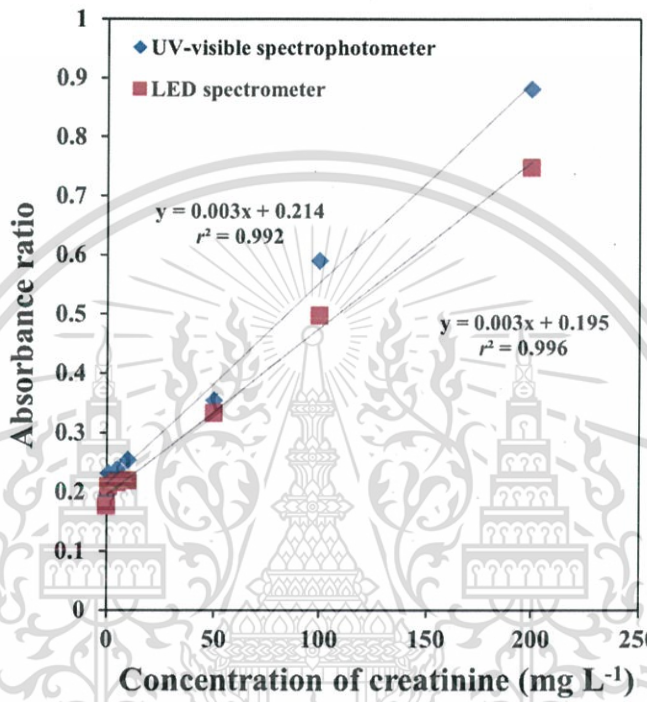

Figure 4.20 The linear plots between the creatinine concentration and the absorbance readings obtained by LED spectrometer and UV-visible spectrophotometer.

4.2.2.7 Validation

The analytical performances were examined and summarized in Table 4.4. The results revealed that the LED spectrometer gave good linearity. The reproducibility was studied by a series of ten repetitive measurements of 10 and 200 mg L^{-1} creatinine, corresponding to the relative standard deviation (RSD) of 4.3 and 3.1 %, respectively. Analytical recoveries were found in the range of 97.0 – 108.0 % (Table 4.5). The device is still applicable for quantitative measurement of creatinine in human urine since the device provides limit of detection (LOD) of 0.23 mg L^{-1} for creatinine which are lower than the indicating concentration of analytes normally found in patient.

Table 4.4 Analytical performances of the method for determination of creatinine.

Analytical performances	Value
Linearity range	1.0 – 200.0 mg L^{-1}
Coefficient of determination (r^2)	0.996
RSD (%) (n = 10)	3.1 - 4.3
Recovery (%)	97.0 – 108.0
LOD ($y_B + 3S_B$)	0.23 mg L^{-1}
LOQ ($y_B + 10S_B$)	0.50 mg L^{-1}

Table 4.5 The recovery study of the urinary creatinine determination.

Sample	Creatinine concentration, mg L^{-1}			Recovery, %
	Original	Added	Found	
1	10.1	10.0	20.6	105
2	9.2	10.0	19.5	103
3	4.9	10.0	15.7	108
4	10.1	50.0	60.1	100
5	9.2	50.0	57.8	97.2
6	4.9	50.0	55.8	102
7	3.5	50.0	52.0	97.0
8	10.1	200.0	211.4	101
9	9.2	200.0	212.7	102
10	4.9	200.0	218.6	107

4.2.2.8 Application to human urine

To demonstrate the capability of the reused traditional gold leaf-prepared AuNPs for real use, they were applied to human urine for colorimetric determination of creatinine. The samples were spot collected from normal volunteers and were 100-fold diluted with water prior to the analysis. Any further sample pretreatment was negligible. The results determined by the developed method and by the validating HPLC method were compared by means of the Bland-

Altman plot. Results in Figure 4.21 showed that all data lay within ±2SD of the mean of their differences, showing that the developed method is equivalent to the HPLC method. Results in Table 4.6 also confirm that the compared methods are not significant different based on the statistical paired *t*-test. This means the developed method offers high accuracy. Advantage of the developed method is that the analytical procedure is simpler and faster than the HPLC method.

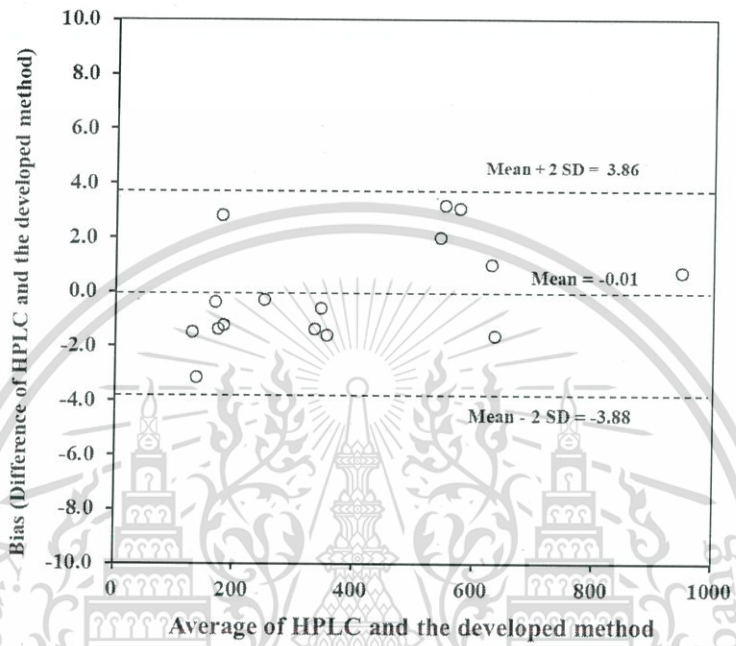

Figure 4.21 The Bland-Altman plot for comparison of the data obtained by the developed method with the validating HPLC method.

Table 4.6 Comparison of the urinary creatinine concentrations determined by the developed method based on use of the reused traditional gold leaf-prepared AuNPs as the colorimetric sensor and by the validating HPLC method. Each contents is reported as mean (± SD) from the triplicate determinations.

Sample code	Urinary creatinine concentrations (mg L^{-1})	
	The developed method	HPLC
S-1	130.3 ± 0.1	128.0 ± 4.4
S-2	137.6 ± 0.3	134.5 ± 3.8
S-3	167.9 ± 0.1	167.5 ± 1.9
S-4	176.7 ± 1.7	171.9 ± 2.1
S-5	177.8 ± 3.2	178.5 ± 7.9

Table 4.6 Cont'd

Sample code	Urinary creatinine concentrations (mg L^{-1})	
	The developed method	HPLC
S-6	182.2 ± 0.6	181.0 ± 2.0
S-7	249.4 ± 1.9	249.2 ± 2.4
S-8	336.3 ± 0.9	333.4 ± 3.8
S-9	345.2 ± 3.3	344.6 ± 1.7
S-10	357.6 ± 3.1	353.8 ± 5.6
S-11	534.8 ± 2.1	543.9 ± 4.5
S-12	549.1 ± 0.2	552.3 ± 2.2
S-13	567.5 ± 1.4	576.0 ± 4.4
S-14	634.2 ± 1.1	629.6 ± 2.3
S-15	653.6 ± 0.5	633.9 ± 2.3
S-16	977.1 ± 2.0	947.7 ± 2.4

4.2.3 A LED spectrometer for measurement of urinary uric acid

4.2.3.1 Study on the principle for colorimetric detection of uric acid by UV - visible spectrophotometer

The detection reaction for uric acid is presented as the following equation.

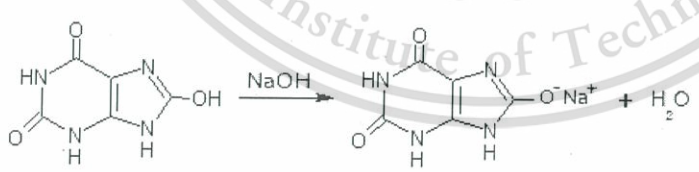

Uric acid — Monosodium urate

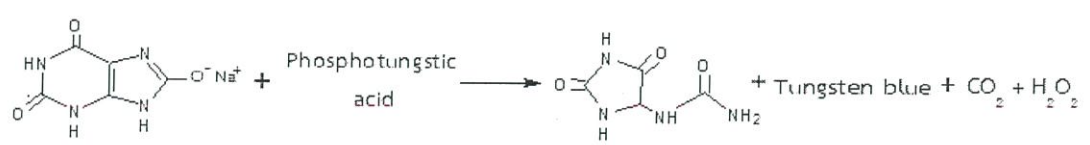

Allantoin

Uric acid reacts with phosphotungstic acid in alkaline medium to form a blue-colored complex (Figure 4.22A). The alkaline medium is provided by sodium carbonate. The absorption spectra of the blue-colored solution were monitored. Results are shown in Figure 4.22B. The intensity of the color is directly proportional to concentration of uric acid. Maximum absorption wavelength is located at 740 nm. For LED spectrometer, Red LED bulb was chosen as a light source for monitoring of the absorption of the product.

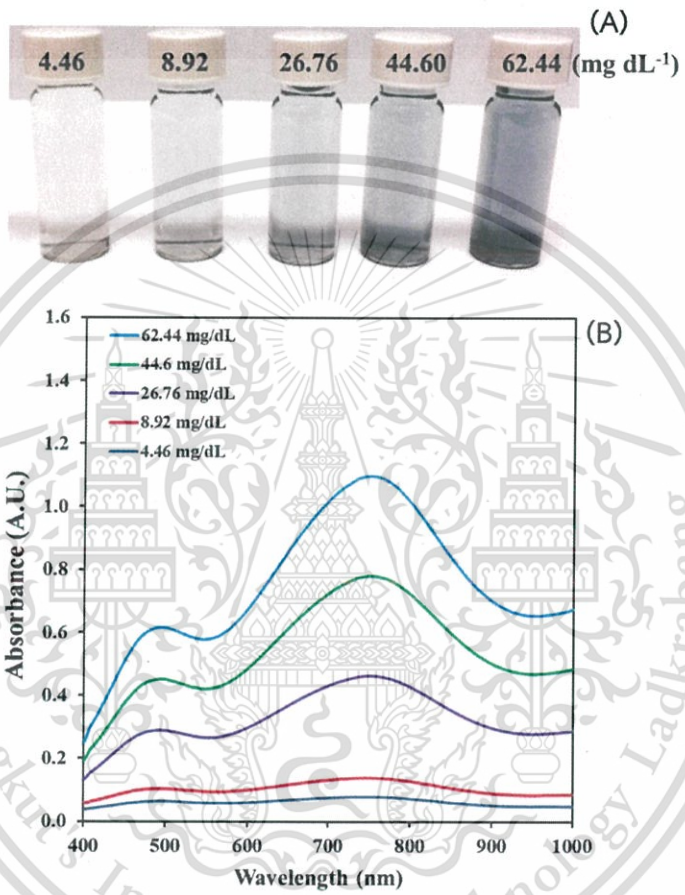

Figure 4.22 (A) Images and (B) absorption spectra of the tungsten blue complex, at various concentrations of uric acid ranging from 4.46 to 62.44 mg dL^{-1}.

4.2.3.2 Optimization study using LED spectrometer

(1) Effect of phosphotungstic acid concentration

Effect of the phosphotungstic acid concentration was studied from 20 to 80 % (w/v). Results in Figure 4.23 demonstrate that the highest sensitivity was obtained when the concentration of 40% (w/v) was used. We observed precipitation of the solution at higher concentration (60% and 80% (w/v)), therefore at 40% (w/v) was selected as optimal concentration.

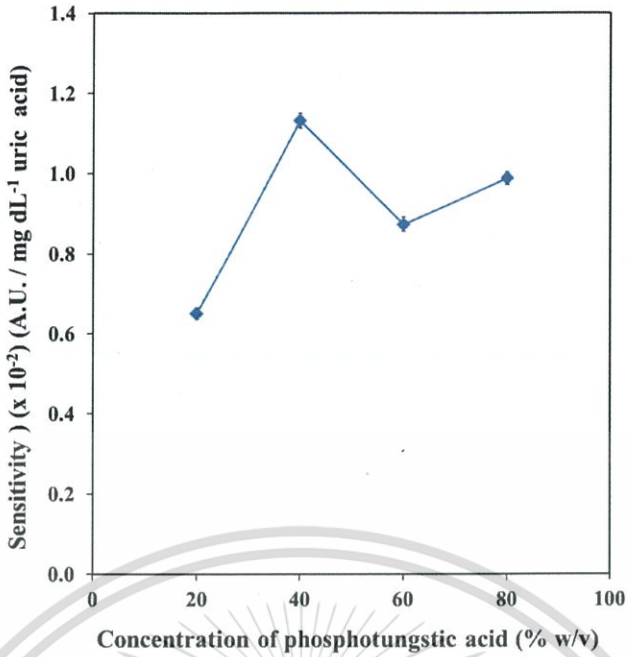

Figure 4.23 Effect of the phosphotungstic acid concentration on sensitivity.

(2) Effect of sodium carbonate concentration

Effect of the concentration of sodium carbonate was studied from 2 to 14 % (w/v). Results are shown in Figure 4.24. When the concentration of sodium carbonate is increased, sensitivity is decreased due to itself precipitation [42]. The concentration of 2 % (w/v) sodium carbonate was selected as appropriate concentration.

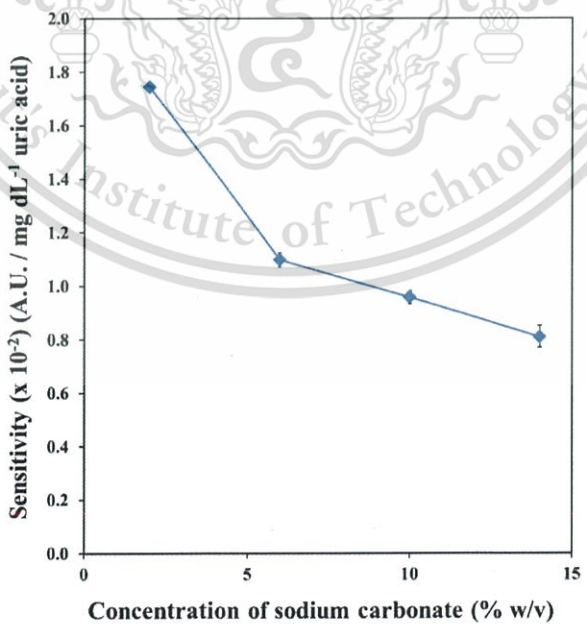

Figure 4.24 Effect of the sodium carbonate concentration on sensitivity.

(3) Appropriate time for measurement

The kinetic reaction of this method was studied by monitoring the absorbance in the function of time. The highest absorbance value when a standard uric acid of 62.44 mg dL^{-1} was studied, observed at 1 min (Figure 4.25). When reaction time is increased, the absorbance value is gradually decreased. It is because the product is unstable. Therefore, the absorbance values were recorded at 1 min in each experiment.

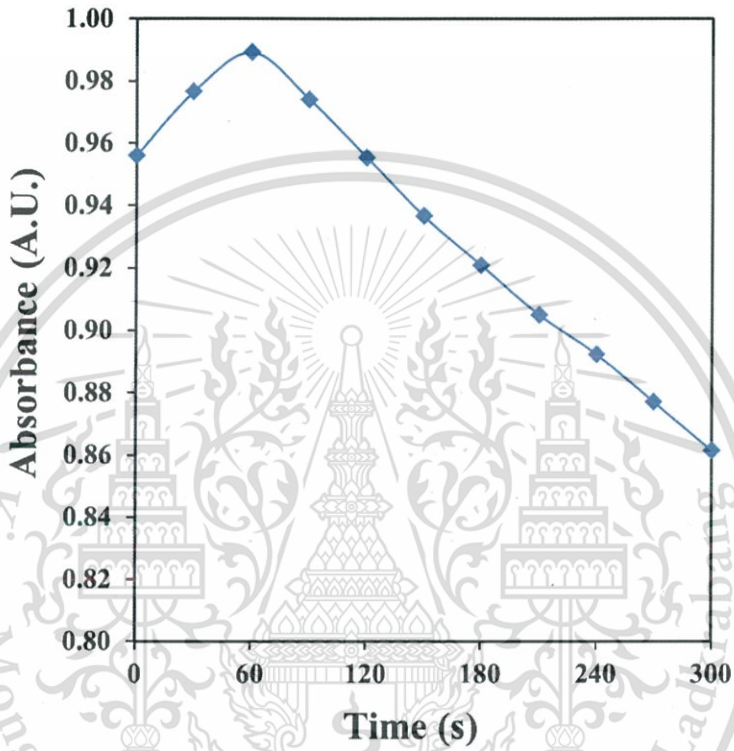

Figure 4.25 Effect of the reaction time.

4.2.3.3 Selectivity study

The effect of interference on determination of uric acid was studied using UV - visible spectrophotometer. The experiments were carried out by mixing of various compounds with phosphotungstic acid in alkaline medium. Results are shown in Figure 4.26. Only uric acid can react with phosphotungstic acid and the blue - colored solution is observed, while glucose, creatinine, cysteine and oxalic acid did not react with phosphotungstic acid, even when their concentrations were extravagantly high [69, 70]. This means that the chromogenic reagent is selective to uric acid.

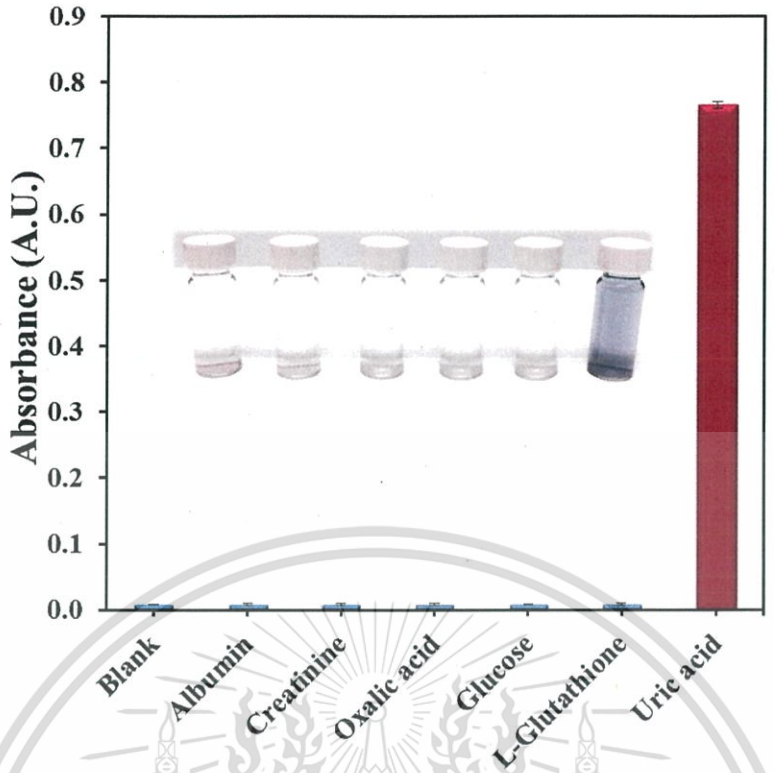

Figure 4.26 Selectivity of the method for the colorimetric detection of uric acid (The concentration of albumin is 300 mg L^{-1}, creatinine is 0.40 mmol L^{-1}, oxalic acid is 0.3 mmol L^{-1}, glucose is 22.0 mmol L^{-1} and L-glutathione is 0.25 mmol L^{-1}).

4.2.3.4 Analytical performances

The results involving in the analytical performances are concluded in Table 4.7. Working range from 4.46 to 62.44 mg dL^{-1} was observed with good linearity (r^2 = 0.998). The method also provided good precision (RSD: 2.9 to 5.7 %) and accuracy (Analytical recovery: 88 to 95 %). The limit of detection (y_B+3S_B) and the limit of quantitation (y_B+10S_B) were found at 2.33 and 7.38 mg dL^{-1}, respectively.

Performance (in term of analytical sensitivity) of the LED spectrometer for measurement of uric acid in urine was compared to the performance of UV - visible spectrophotometer. Results in Figure 4.27 indicated that the sensitivity of LED spectrometer was lower than UV - visible spectrophotometer around 27%. However, the LED spectrometer are still applicable for quantitative measurement of uric acid in human urine since the method provides limit of detection (LOD) of 2.36 mg dL^{-1} which is lower than the indicating concentration of uric acid normally found in gout patient.

Table 4.7 Analytical performances of the LED spectrometer for measurement of uric acid.

Performances	Value
Linearity range	4.46 – 62.44 mg dL^{-1}
Coefficient of determination (r^2)	0.9975
RSD (n = 6)	2.9 – 5.7 %
Recovery	88.3 - 95.0 %
LOD ($y_B + 3S_B$)	2.36 mg dL^{-1}
LOQ ($y_B + 10S_B$)	7.91 mg dL^{-1}

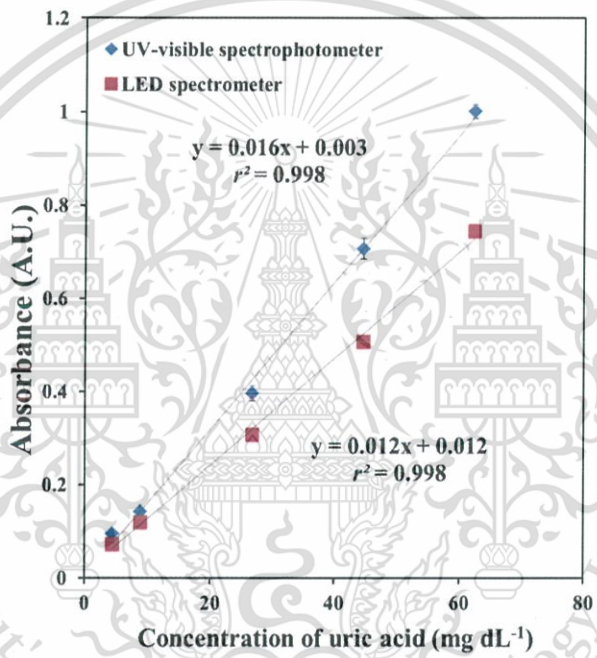

Figure 4.27 The linear plots between the uric acid concentration and the absorbance readings obtained by LED spectrometer and UV-visible spectrophotometer.

4.2.3.5 Application to human urine

The method was applied to determination of uric acid in 10 urine samples that were spot collected from normal volunteers (Table 4.8). The obtained results were analyzed with Bland-Altman test. Result in Figure 4.28 showed that all data lay within ± 2SD of the mean of their differences, indicating that the developed method was equivalent to the conventional spectrophotometer. These results can be concluded that the developed LED spectrometer and the conventional spectrophotometer were well correlated.

Table 4.8 Concentrations of uric acid in urine samples.

Sample	Concentration (mg L^{-1}, mean ± SD)	
	LED spectrometer	UV-visible spectrophotometer
1	4.0 (± 0.3)	3.5 (± 0.8)
2	6.1 (± 0.3)	4.8 (± 0.2)
3	6.4 (± 0.5)	6.4 (± 0.4)
4	6.6 (± 0.3)	5.6 (± 0.7)
5	8.2 (± 0.2)	9.8 (± 1.2)
6	9.3 (± 0.5)	8.9 (± 0.4)
7	13.0 (± 0.1)	11.2 (± 1.1)
8	14.0 (± 0.0)	15.9 (± 1.2)
9	15.3 (± 0.4)	12.6 (± 0.3)
10	16.1 (± 0.4)	13.0 (± 0.3)

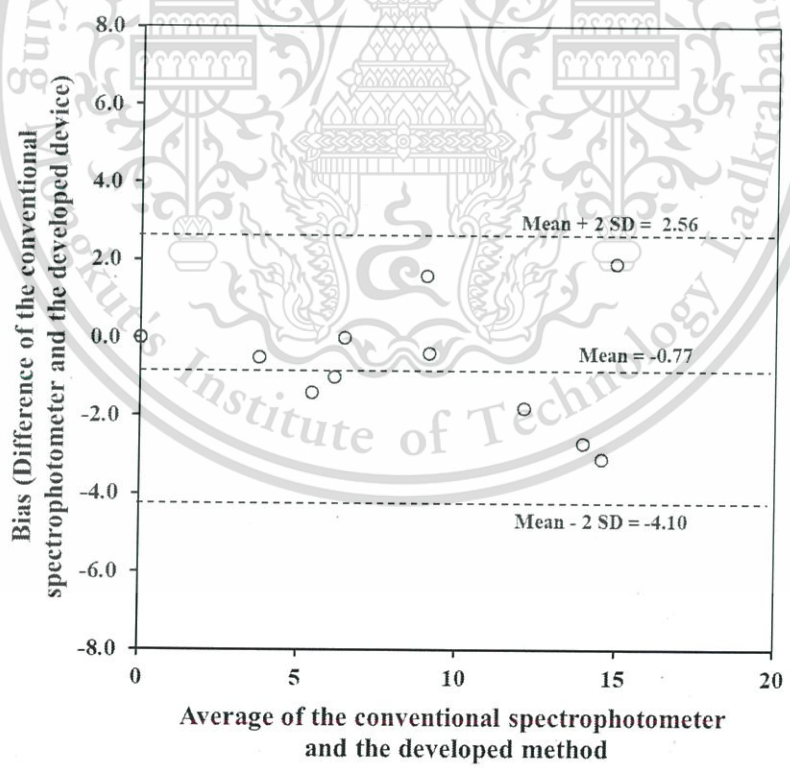

Figure 4.28 The Bland-Altman plot for comparison of the data obtained by the LED spectrometer with the validating spectrophotometric method.

Chapter 5
Conclusions and Suggestions

5.1 Conclusions

5.1.1 Mobile phone-based analyzer for measurement of urinary albumin

The simple method using a mobile phone with the installed application, namely 'Albumin smart test', as the analyzer for quantitative analysis of urinary albumin was developed. As a result, precise and accurate quantitative measurement of the albumin concentration can be accomplished without using any extra module for lighting adjustment during image capturing. Successful validation of the developed method against the spectrophotometric method was achieved. The mobile phone with the installed application showed high proficiency to be utilized as a portable diagnostic analyzer for the microalbuminuria analysis.

5.1.2 A LED spectrometer for measurement of urinary creatinine and uric acid

The LED spectrometer was successfully developed. The performance of the developed device is comparable to as the conventional spectrophotometer. The device is cost-effective, portable and simple to fabricate. The developed device was successfully applied for colorimetric determination of creatinine and uric acid in human urine with high accuracy and high precision.

For determination of creatinine, synthesis of the AuNPs using the reused traditional gold leaf as the starting material was achieved. Benefits of exploiting this kind of gold leaf are that its price is very much cheaper as it is free of charge. It is also more stable at the ambient temperature. The as-prepared AuNPs was successfully applied for colorimetric sensing of creatinine in human urine with high sensitivity and selectivity.

For determination of uric acid, the colorimetric reaction between uric acid and phosphotungstic acid in the presence of sodium carbonate was chosen as detection principle because of its simplicity. The method provides high accuracy and high precision with simple and rapid analysis.

In addition, the developed device shows high efficiency to be employed as an analyzer for 'point-of-care' quantitative analyses of urinary biomarkers for renal dysfunction.

5.2 Suggestions

The developed methods are suitable for 24 - hour urine specimen collection. For accurate clinical diagnosis, the amount of bio-markers (albumin, creatinine and uric acid) in human urine should be reported as albumin to creatinine ratio or uric acid to creatinine ratio.

References

[1] Online available: https://en.wikipedia.org/wiki/Albumin

[2] Online available: https://en.wikipedia.org/wiki/Serum_albumin

[3] Busher, J.T. 1990. "Serum albumin and globulin." Chapter 101. 497-499 in Walker, H.K., Hall. W.D., Hurst, J.W. **Clinical Methods: The History, Physical, and Laboratory Examinations.** 3rd edition. Boston : Butterworths.

[4] National Kidney Foundation. 2007. "KDOQI Clinical practice guidelines and clinical practice recommendations for diabetes and chronic kidney disease." **American Journal of Kidney Diseases.** 49(2) : 850-886.

[5] Satirapoj, B. 2010. "Review on pathophysiology and treatment of diabetic kidney disease." **Journal of the Medical Association of Thailand.** 93(6) : s228-s241.

[6] Online available: https://dtc.ucsf.edu/living-with-diabetes/complications/individual-complications/kidney-complications/

[7] Arndt, T. 2009. "Urine-creatinine concentration as a marker of urine dilution: reflections using a cohort of 45,000 samples." **Forensic Science International.** 186(1-3) : 48-51.

[8] Krimer, P.M. 2012. "Creatinine." 924 In Charles, W. **Clinical Veterinary Advisor: The Horse.** Oxford : Elsevier.

[9] Online available: http://emedicine.medscape.com/article/244255-workup

[10] Maiuolo, J., Oppedisano, F., Gratteri, S., Muscoli, C., and Mollace, V. 2016. "Regulation of uric acid metabolism and excretion." **International Journal of Cardiology.** 213 : 8-14.

[11] Zhang, Q., McGuigan, C.F., Lew, K. and Chris Le, X. 2012. "3.06 - Urine Sample Collection and Handling." **Comprehensive Sampling and Sample Preparation Analytical Techniques for Scientists.** 3 : 123-142.

[12] Ibraheem, N.A., Hasan, M.M., Khan, R.Z. and Mishra, P.K. 2012. "Understanding color models : A Review." **ARPN Journal of Science and Technology.** 2(3) : 265-275.

[13] Cantrell, K., Erenas, M.M., de Orbe-Payá, I. and Capitán-Vallvey, L.F. 2010. "Use of the hue parameter of the hue, saturation, value color space as a quantitative analytical parameter for bitonal optical sensors." **Analytical Chemistry.** 82(2) : 531-542.

[14] Watla-iad, K., Sakai, T., Teshima, N., Katoh, S. and Grudpan, K. 2007. "Successive determination of urinary protein and glucose using spectrophotometric sequential injection method." **Analytica Chimica Acta.** 604 : 139–146.

[15] Tavener, S.J. and Thomas-Oates, J.E. 2007. "Build your own spectrophotometer" **Education in Chemistry.** 44(5) : 151-154.

[16] Zhao, P., Li, N. and Astruc D. 2013 "State of the art in gold nanoparticle synthesis." **Coordination Chemistry Reviews.** 257 : 638-665.

[17] Kumar, S., Gandhi, K. S. and Kumar, R. 2007. "Modeling of formation of gold nanoparticles by citrate method." **Industrial & Engineering Chemistry Research.** 46(10) : 3128-3136.

[18] Horikoshi, S. and Serpone, N. 2013. "Microwaves in nanoparticle synthesis." Chapter 1. 497-499 in Walker, H.K., Hall. W.D., Hurst, J.W. **Introduction to Nanoparticles.** Weinheim : Wiley-VCH Verlag GmbH & Co. KGaA.

[19] Online available: https://nanocomposix.com/pages/the-science-of-plasmonics

[20] Martillo, M.A., Nazzal, L. and Crittenden, D.B. 2014. "The crystallization of monosodium urate." **Current Rheumatology Reports.** 16(2) : 400.

[21] Turek, S. 1974. "Albumin turbidity reaction of blood serum." **Casopis Lékaru Ceských.** 113(14) : 445-446.

[22] Luque, G. L., Ferreyra, N.F., Ferreyra, L. and Rivas, G.A. 2007. "Electrochemical sensor for amino acids and albumin based on composites containing carbon nanotubes and copper microparticles." **Talanta.** 71(3) : 1282-1287.

[23] Contois, J. H., Hartigan, C., Rao, L.V., Snyder, L.M. and Thompson, M.J. 2006. "Analytical validation of an HPLC assay for urinary albumin." **Clinica Chimica Acta.** 367(1-2) : 150-155.

[24] Jiang, C. and Luo, L. 2004. "Spectrofluorimetric determination of human serum albumin using a doxycycline–europium probe." **Analytica Chimica Acta.** 506 : 171-175.

[25] Sakai, T., Kito, Y., Teshima, N., Katoh, S., Watla-lad, K. and Grudpan, K. 2007. "Spectrophotometric flow injection analysis of protein in urine using tetrabromophenolphthalein ethyl ester and triton X-100." **Journal of Flow Injection Analysis.** 24(1) : 23-26.

[26] Moss, G. A., Bondar, R. J. L. and Buzzelli, D. M. 1975. "Kinetic enzymatic method for determining serum creatinine." **Clinical Chemistry.** 21(10) : 1422-1426.

[27] Ogawa, J., Nirdnoy, W., Tabata, M., Yamada, H. and Shimizu, S. 1995. "A new enzymatic method for the measurement of creatinine involving a novel ATP-dependent enzyme *N*-methylhydantoin amidohydrolase." **Bioscience, Biotechnology, and Biochemistry.** 59(12) : 2292-2294.

[28] Ambrose, R.T., Ketchum, D.F. and Smith, J.W. 1983. "Creatinine determined by High-Performance" Liquid Chromatography." **Clinical Chemistry.** 29(2) : 256-259.

[29] Yuen, P.S.T., Dunn, S.R., Miyaji, T., Yasuda, H., Sharma, K. and Star, R.A. 2004. "A simplified method for HPLC determination of creatinine in mouse serum." **American Journal of Physiology-Renal Physiology**. 286 F1116 : F1119.

[30] Jaffé, M. 1886. "Ueber den niederschlag, welchen pikrinsäure in normalem harn erzeugt und über eine neue reaction des kreatinins." **Zeitschrift für physiologische Chemie.** 10(5) : 391-400.

[31] Vasiliades, J. 1976. "Reaction of alkaline sodium picrate with creatinine : I. Kinetics and mechanism of formation of the mono-creatinine picric acid complex." **Clinical Chemistry**. 22(10) : 1664-1671.

[32] Falcó, P.C., Genaro, L.A.T., Lloret, S.M., Gomez, F.B., Cabeza, A.S. and Legua, C. M. 2001. "Creatinine determination in urine samples by batchwise kinetic procedure and flow injection analysis using the Jaffé reaction chemometric study." **Talanta**. 55 : 1079-1089.

[33] Apyari, V. V., Arkhipova, V. V., S. Dmitrienko, G. and Zolotov, Y. A. 2014. "Using gold nanoparticles in spectrophotometry." **Journal of Analytical Chemistry**. 69(1) : 1-11

[34] Hormozi-Nezhad, M.R., Seyedhosseini, E. and Robatjazi, H. 2012. "Detection of urinary creatinine using gold nanoparticles after solid phase extraction." **Scientia Iranica F.** 19(3) : 958-963.

[35] He, Y., Zhang, X. and Yu, H. 2015. "Gold nanoparticles-based colorimetric and visual creatinine assay." **Microchimica Acta.** 182 : 2037-2043.

[36] Sutariya, P.G., Pandya, A., Lodha, A. and Menon S.K. 2016. "A simple and rapid creatinine sensing via DLS selectivity, using calix[4]arene thiol functionalized gold nanoparticles." **Talanta.** 147 : 590-597.

[37] Sittiwong, J. and Unob, F. 2015. "Detection of urinary creatinine using gold nanoparticles after solid phase extraction." **Spectrochimica Acta Part A: Molecular and Biomolecular Spectroscopy**. 138 : 381-386.

[38] Lorentz, K. and Berndt, W. 1967. "Enzymic determination of uric acid by a colorimetric method." **Analytical Biochemistry**. 451(1) : 58–63.

[39] Gochman, N. and Schmitz, J.M. 1971. "Automated determination of uric acid, with use of a uricase-peroxidase system." **Clinical Chemistry**. 17(12) : 1154–1159.

[40] Islam, Md.N., Ahmed, I., Anik, M.I., Ferdous, Md.S., and Khan, M.S. 2018. "Developing paper based diagnostic technique to detect uric acid in urine." **Frontiers in Chemistry.** 6 : 496.

[41] Martinek, R.G. 1965. "Micromethod for the determination of uric acid in biological fluids." **American Journal of Clinical Pathology**. 18 : 777–779.

[42] Henry, R.J., Sobel, C. and Kim, J. 1957. "A modified carbonate-phosphotungstate method for the determination of uric acid and comparison with the spectrophotometric uricase method." **American Journal of Clinical Pathology**. 28(2) : 152–160.

[43] Sumriddetchkajorn, S., Chaitavon, K. and Intaravanne, Y. 2014. "Mobile-platform based colorimeter for monitoring chlorine concentration in water." **Sensors and Actuators B: Chemical**. 191 : 561-566.

[44] Intaravanne, Y. and Sumriddetchkajorn, S. 2015. "Android-based rice leaf color analyzer for estimating the needed amount of nitrogen fertilizer." **Computers and Electronics in Agriculture**. 116 : 228-233.

[45] Coskun, A.F., Nagi, R., Sadeghi, K., Phillips, S. and Ozcan, A. 2013. "Albumin testing in urine using a smart-phone." **Lab on a Chip**. 13(21) : 4231-4238.

[46] Soni, A., Surana, A.K. and Jha, S.K.Y. 2018. "Smartphone based optical biosensor for the detection of urea in saliva." **Sensors and Actuators B: Chemical**. 269 : 346-353.

[47] Chaianantakul, N., Wutthi, K., Kamput, N., Pramanpol, N., Janphuang, P., Pummara, W., Phimon, K. and Phatthanakun, R. 2018. "Development of mini-spectrophotometer for determination of plasma glucose." **Spectrochimica Acta Part A**. 204 : 670–676.

[48] Yeh, T.S. and Tseng, S.S. 2006. "A low cost LED based spectrometer." **Journal of the Chinese Chemical Society**. 53 : 1067-1072.

[49] Albert, D.R., Todt, M.A. and Davis, H.F. 2012. "A Low-cost quantitative absorption spectrophotometer." **Journal of Chemical Education**. 89 : 1432-1435.

[50] Veras, G., Silva, E.C., Lyra, W.S., Soares, S.F.C., Guerreiro, T.B. and Santos, S.R.B. 2009. "A portable, inexpensive and microcontrolled spectrophotometer based on white LED as light source and CD media as diffraction grid." **Talanta**. 77 : 1155–1159.

[51] Puder, A. and Antebi, O. 2013. "Cross-compiling android applications to iOS and windows phone 7." **Mobile Networks and Applications**. 18 : 3–21.

[52] Erenas, M.M. , Cantrell, K., Ballesta-Claver, J., de Orbe-Payá, I. and Capitán-Vallvey, L.F. 2012. "Use of digital reflection devices for measurement using hue-based optical sensors." **Sensors and Actuator B**. 174 : 10–17.

[53] Miller, J.N. and Miller, J. C. 1993. **Statistics and chemometrics for analytical chemistry**. 4th edition. London : Pearson Education.

[54] Glantz, S.A. 2002. **Primer of biostatistics**. 5th edition. USA : McGraw-Hill.

[55] Elomaa, H., Seisko, S., Junnila, T., Sirviö, T., Wilson, P.B., Aromaa, J. and Lundström, M. 2017. "The effect of the redox potential of aqua regia and temperature on the Au, Cu, and Fe dissolution from WPCBs." **Recycling**. 2(14) : 1-9.

[56] Pupanthong, P. 2011. **Gold Refining with Aqua regia and Sulfite Compound**. 2nd edition. Bangkok : Department of primary industries and mines.

[57] Pimpang, P. and Choopun, S. 2011. "Monodispersity and stability of gold nanoparticles stabilized by using polyvinyl alcohol." **Chiang Mai Journal of Science**. 38(1) : 31-38.

[58] Ojea-Jiménez, I. and Campanera, J.M. 2012. "Molecular modeling of the reduction mechanism in the citrate-mediated synthesis of gold nanoparticles." **The Journal of Physical Chemistry C**. 116 : 23682-23691.

[59] Schulz, F., Homolka, T., Bastús, N.G., Puntes, V., Weller, H. and Vossmeyer, T. 2014. "Little adjustments significantly improve the Turkevich synthesis of gold nanoparticles." **Langmuir**. 30 : 10779-10784.

[60] Polyakov, A.Y., Lebedev, V.A., Shirshin, E.A., Rumyantsev, A.M., Volikov, A.B., Zherebker, A., Garshev, A.V., Goodilin, E.A. and Perminova, I.V. 2017. "Non-classical growth of water-redispersible spheroidal gold nanoparticles assisted by leonardite humate." **CrystEngComm**. 19 : 876-886.

[61] Kimling, J., Maier, M., Okenve, B., Kotaidis, V., Ballot, H. and Plech, A. 2006. "Turkevich method for gold nanoparticle synthesis revisited." **The Journal of Physical Chemistry B**. 110 : 15700-15707.

[62] Shan, J. and Tenhu, H. 2007. "Recent advances in polymer protected gold nanoparticles: synthesis, properties and applications." **Chemical Communications**. 0 : 4580-4598.

[63] Baygazieva, E.K., Yesmurzayeva, N.N., Tatykhanova, G.S., Mun, G.A., Khutoryanskiy, V.V. and Kudaibergenov, S.E. 2014. "Polymer protected gold nanoparticles: synthesis, characterization and application in catalysis." **International Journal of Biology and Chemistry**. 7 : 14-23.

[64] Thorat, A.A. and Dalvi, S.V. 2012. "Liquid antisolvent precipitation and stabilization of nanoparticles of poorly water soluble drugs in aqueous suspensions: Recent developments and future perspective." **The Chemical Engineering Journal**. 181-182 : 1-34.

[65] Rahman, S. 2016. "Size and concentration analysis of gold nanoparticles with ultraviolet - visible spectroscopy." **Undergraduate Journal of Mathematical Modeling: One + Two**. 7(1) : Article 2, 1-13.

[66] Uehara, N. 2010. "Polymer-functionalized gold nanoparticles as versatile sensing materials." **Analytical Sciences**. 26 : 1219-1228.

[67] Gittins, D. I. and Caruso, F. 2001. "Spontaneous phase transfer of nanoparticulate metals from organic to aqueous media." **Angewandte Chemie International Edition**. 40(16) : 3001-3004.

[68] Chi, H., Liu, B., Guan, G., Zhang, Z. and Han, M.Y. 2010. "A simple, reliable and sensitive colorimetric visualization of melamine in milk by unmodified gold nanoparticles." **Analyst**. 135(5) : 1070-1075.

[69] Diogo, L. and Fábio, R.P.R. 2010. "A flow-based procedure with solenoid micro-pumps for the spectrophotometric determination of uric acid in urine." **Microchemical Journal**. 94(1) : 53–59.

[70] Breebaart, K. and Haan, A.M.F.H. 1972. "A new automated determination of uric acid." **Zeitschrift für klinische Chemie und klinische Biochemie**. 10(1) : 17–20.

Appendix

Appendix A

ImageJ program for measurement of color intensity

ImageJ program for measurement of color intensity

Presented by

Mr.Arjnarong Mathaweesansurn

Department of Chemistry, Faculty of Science
King Mongkut's Institute of Technology Ladkrabang

Outline

2

1. RGB color model
2. Program for image processing
3. Image processing
   - Gray intensity
   - RGB intensity

RGB Color Model

3

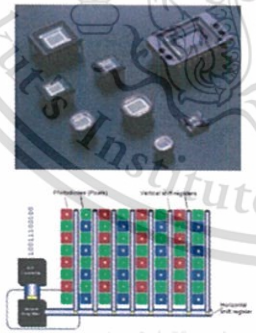

RGB Color Model

4

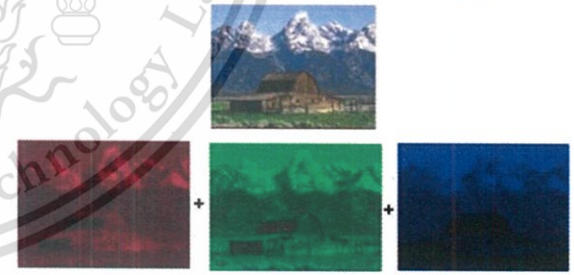

Fig.1 The color of an image is obtained by combining the three elementary colors for each pixel (Three elementary images)

RGB Color Model

5

•The model is based on the 3D Cartesian coordinate system, where the color subspace of interest is the color cube shown below.

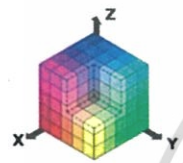

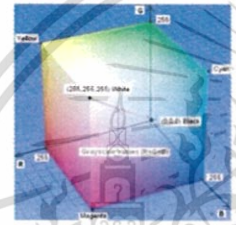

- RGB:
  - ➢ The simplest color space
  - ➢ Axes: Red, green, blue
  - ➢ Advantages: simple

Program for image processing

6

home | news | docs | download | plugins | macros/dev | list | links

ImageJ Search

Image Processing and Analysis in Java

- Features
- News
- Documentation
- Download
- Plugins
- Developer Resources
- Applets WebStart
- Mailing List
- Links

Program for image processing

7

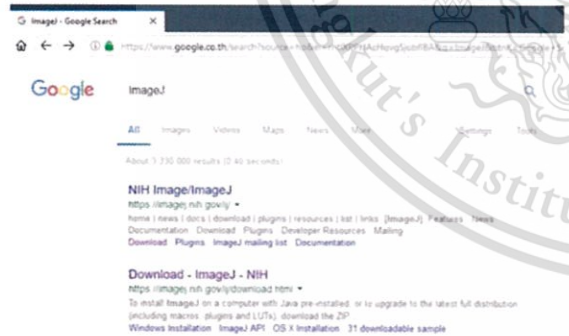

Image J program

8

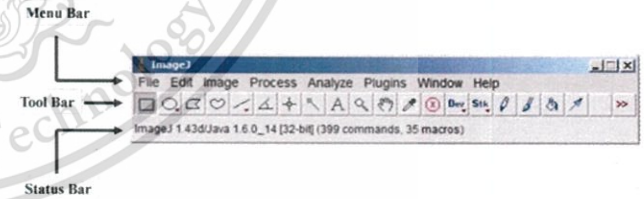

Image J program

9

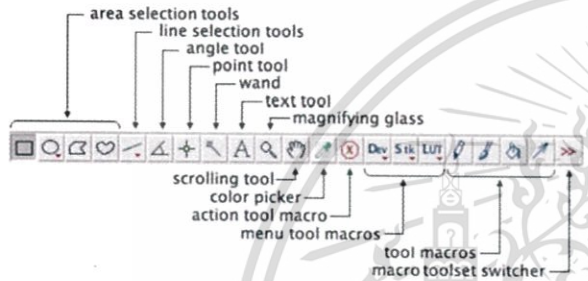

Image processing

10

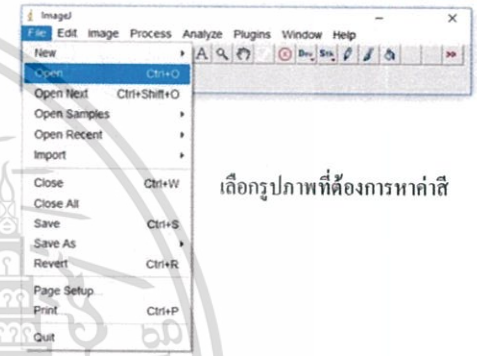

เลือกรูปภาพที่ต้องการหาค่าสี

Image processing

11

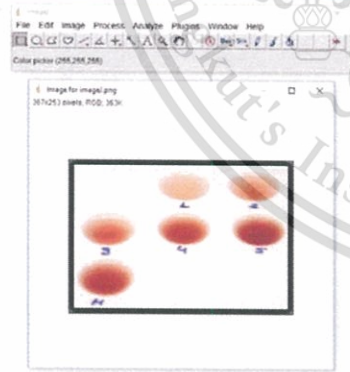

Image processing : gray scale

12

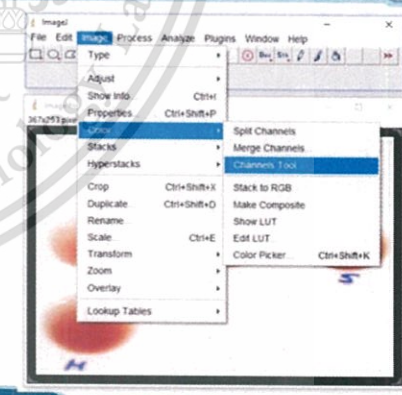

Image processing : gray scale 13

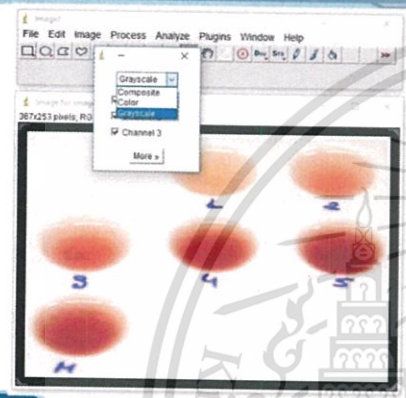

Image processing : gray scale 14

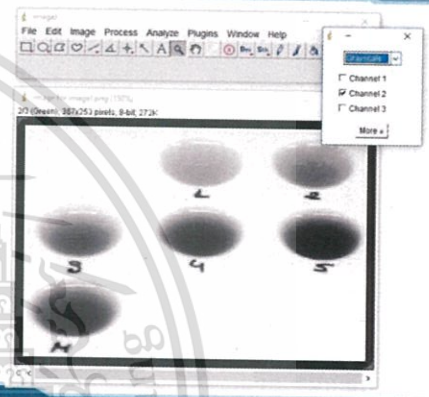

Image processing : gray scale 15

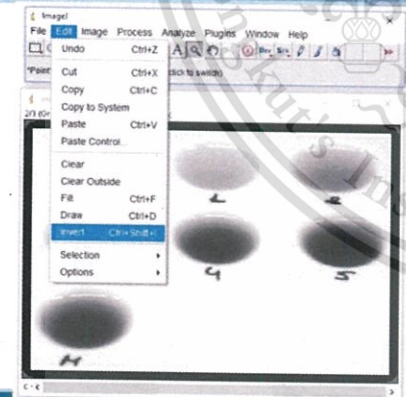

Image processing : gray scale 16

กำหนดพื้นที่ที่จะหาค่าสี

เลือก channel สีที่เหมาะสม
ในการหาค่า Intensity

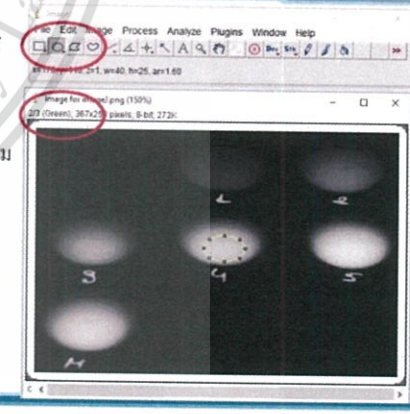

Image processing : gray scale 17

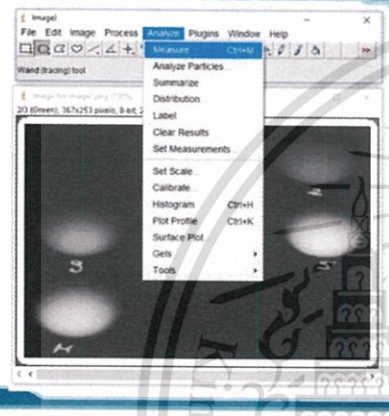

Image processing : gray scale 18

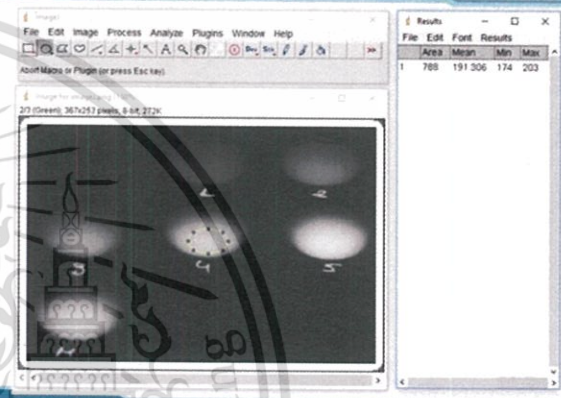

Image processing : Red Green Blue 19

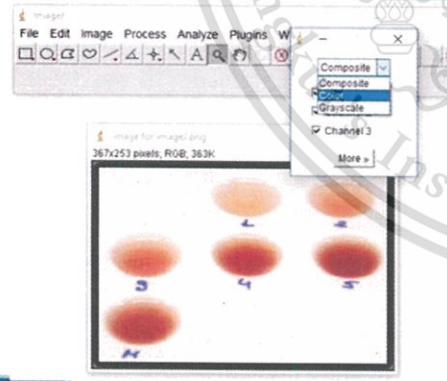

Image processing : Red Green Blue 20

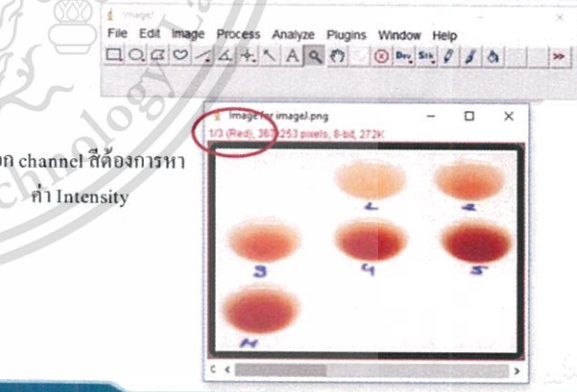

เลือก channel สีต้องการหา

ทำ Intensity

Image processing : Red Green Blue 21

กำหนดพื้นที่ที่จะหาค่าสี

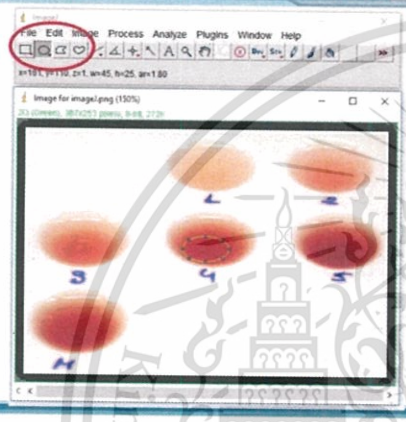

Image processing : Red Green Blue 22

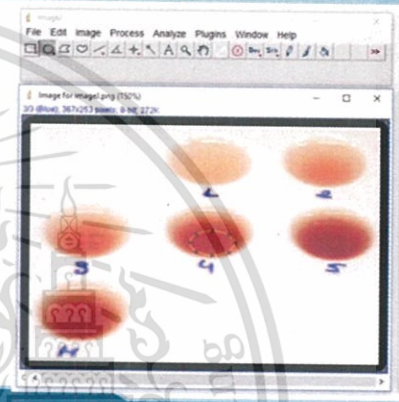

!! The end !!

Appendix B

Price list of the LED spectrometer components

Table B.1 Price list of the LED spectrometer components

No.	Description	Price (Baht) / each
1	Micro-controller	600.00
2	High Power LEDs	720.00
3	PCB	700.00
4	Photo transistor	15.00
5	LCD monitor	240.00
6	Li-ion battery	350.00
7	Switch	100.00
8	USB cable	20.00
9	Resistor	60.00
10	Transistor BC337	10.00
11	PIN	50.00
12	Cable with PIN	50.00
13	Nuts and bolts	100.00
14	Acrylic board	3,500.00

Appendix C

International publications and conference proceedings

Sensors and Actuators B 242 (2017) 476–483

Contents lists available at ScienceDirect

Sensors and Actuators B: Chemical

journal homepage: www.elsevier.com/locate/snb

A mobile phone-based analyzer for quantitative determination of urinary albumin using self-calibration approach

Arjnarong Mathaweesansurn[a,b], Noppadol Maneerat[c], Nathawut Choengchan[a,b,*]

[a] Flow Innovation Research for Science and Technology Laboratrories (FIRST Labs), Faculty of Science, King Mongkut's Institute of Technology Ladkrabang, Chalongkrung Road, Bangkok 10520, Thailand

[b] Applied Analytical Chemistry Research Unit, Department of Chemistry, Faculty of Science, King Mongkut's Institute of Technology Ladkrabang, Chalongkrung Road, Bangkok 10520, Thailand

[c] Department of Control Engineering, Faculty of Engineering, King Mongkut's Institute of Technology Ladkrabang, Chalongkrung Road, Bangkok 10520, Thailand

ARTICLE INFO

Article history:
Received 16 June 2016
Received in revised form 9 November 2016
Accepted 10 November 2016

Keywords:
Mobile phone
Image processing
Self-calibration
Quantitative determination
Albumin
Urine

ABSTRACT

This work demonstrates use of a smart mobile phone installed with an Android application, termed 'Albumin smart test', as an analyzer for quantitative determination of urinary albumin. The reaction between albumin and tetrabromophenolphthalein ethyl ester (TBPE) in the presence of Triton X-100 was employed for detection principle.The mobile phone was exploited with the sample cassette and the test paper. One sample cassette composes of two holders for accommodation of control and test samples. The test paper was designed in order to contain standard colorimetric strip and space for situating the sample cassette. Optical images of the strip and the samples were simultaneously captured in a single shot by a digital camera of the mobile phone and were digitally processed by the developed application for quantification of the albumin concentration based on self-calibration approach. With the advantage of self-calibration, the albumin test by our mobile phone can be performed in ambient light without using any extra module integrated with lighting control device. The other advantages are portability, ease of implementation and rapid analysis (3 min) with high precision (RSD ≤ 2.5%) and high accuracy (Recovery = 98.7% ± 1.6). The mobile device was successfully applied to diagnosis of microalbuminuria.

1. Introduction

Chronic kidney disease (CKD) is one of a major public health problem worldwide [1,2]. In Thailand, data from the Ministry of Health reveal that the prevalence of CKD in adults is around 30% [3]. The major outcomes of CKD include kidney failure, complications of decreased kidney function and cardiovascular disease. In order to prevent or delay these adverse outcomes, early detection and treatment are very important especially for person who has high risk factors with hypertension, hyperlipidemia and diabetes [4]. Early stage of kidney dysfunction can be diagnosed using the test on urinary albumin excretion [5]. The albumin concentration in urine collected from normal people is very low (<30 mg L^{-1}) [6]. In cases of early period of kidney disease, small amount of albumin can leak into urine. This leads to a condition termed as 'microalbuminuria' in which typically exhibits the urinary albumin concentration in the range of 30–300 mg L^{-1} [6]. Therefore, the measurement of albumin in urine can be exploited as an initial method for diagnosis of kidney disease.

A large number of analytical methods are presented for the determination of albumin in urine with various methodologies including separation techniques [7,8], immunology [9,10], spectrofluorometry [11] and spectrophotometry [12–16]. The continuous flow-based methods using flow injection analysis (FIA) [17] and sequential injection analysis (SIA) [18–20] are also reported. Advantages of the FIA and the SIA methods are high speed of analysis and high potential for a fully automatic manipulation. However, the methods are not applicable for point-of-care testing because some bulky and costly bench-top apparatuses are required. This can limit the albumin testing to only in laboratory setting. The test paper impregnating the dye stuff is commonly used for field test with naked eye detection [21]. Nevertheless, it does not provide accurate analytical results. Development of a portable analyzer for quantitative measurement of the urinary albumin is therefore very necessary.

* Corresponding author at: Flow Innovation Research for Science and Technology Laboratrories (FIRST Labs), Faculty of Science, King Mongkut's Institute of Technology Ladkrabang, Chalongkrung Road, Bangkok 10520, Thailand.
E-mail address: nchoengchan@gmail.com (N. Choengchan).

http://dx.doi.org/10.1016/j.snb.2016.11.057
0925-4005/

Nowadays, the improvement of electronics and information technology has brought about the revolution of personal computers to smart mobile devices. With the rapid advancement of cell phones and tablets embedded with digital cameras and central processing units, simple mobile devices are reported as a portable analyzer for many applications [22–28]. However, the main limiting parameter for using the smart phones' camera as analytical instrument is that the response is mainly affected by the ambient light. In order to overcome this problem, employment of external light source and enclosure to place and keep hold the mobile phone is essential. Recently, use of a smart-phone attached with 3D-printed enclosure integrated with lighting control device for the determination of albumin in urine was demonstrated [27]. Although this analyzer was effective, requirement of the extra devices could leads the method to complicated and costly measurement.

In this work, we aim to demonstrate a simple method using a mobile phone with the installed application, namely 'Albumin smart test', as the analyzer for quantitative determination of urinary albumin. The Android application was designed for image capturing of urine sample without using any extra apparatus for illuminating control. Our mobile phone analyzer is employed with the sample cassette and the test paper assigned for self-calibration purpose. The association reaction between albumin and tetrabromophenolphthalein ethyl ester (TBPE) in the presence of Triton X-100 was chosen as detection principle. TBPE is predominantly attractive as it has a large molar absorptivity [18]. Advantage of the test paper in term of self-calibration for suppression of error from fluctuation of environmental illumination was demonstrated. Validation and application of the developed method to human urine for diagnosis of the microalbuminuria were also investigated.

2. Materials and methods

2.1. Standard and reagents preparation

All standard and reagents used were of analytical reagent grade. Deionized-distilled water purified by Milli-Q apparatus (18 MΩ/cm, Millipore, USA) was used throughout all the experiments. An albumin standard stock solution containing 1000 mg albumin L^{-1} was prepared by dissolving 0.1xxx g of solid powder of human serum albumin (Fluka, Switzerland) in 100.00 mL of water. This standard stock solution was kept in refrigerator (4° C) and the working standard solutions (1 to 50 mg albumin L^{-1}) were freshly prepared by appropriate dilution of the standard stock solution with water. The chromogenic reagent solution (2.0×10^{-4} mol L^{-1} TBPE in 0.2% v/v Triton X-100) was daily prepared by dissolving 0.014 g of TBPE (Aldrich, USA) in 5.0 mL of 99.9% ethanol (Carlo Erba, Italy). Into this solution, 2.0 mL of Triton X-100 (Aldrich, USA) was added. The solution was then made up with ethanol to 100.0 mL. Acetate buffer solution (0.1 mol L^{-1}), exploited for maintaining the pH of solutions, was prepared by adding 0.1 mol L^{-1} sodium acetate (Rankem, India) in 0.1 mol L^{-1} acetic acid (Mallinckrodt, Thailand). This solution was adjusted to a final pH of 3.1. The concentrations for all reagents are adapted from P. Inpota et al. [29].

2.2. Apparatuses and analytical workflows

Fig. 1 illustrates key apparatuses exploited for quantitative determination of albumin in urine by our mobile phone-based analyzer. The smart mobile device in Fig. 1A is Samsung Galaxy S5 (Samsung, South Korea) embedded with Android 5.0 operation system. Its specifications are full HD (1920 × 1080 pixel) main

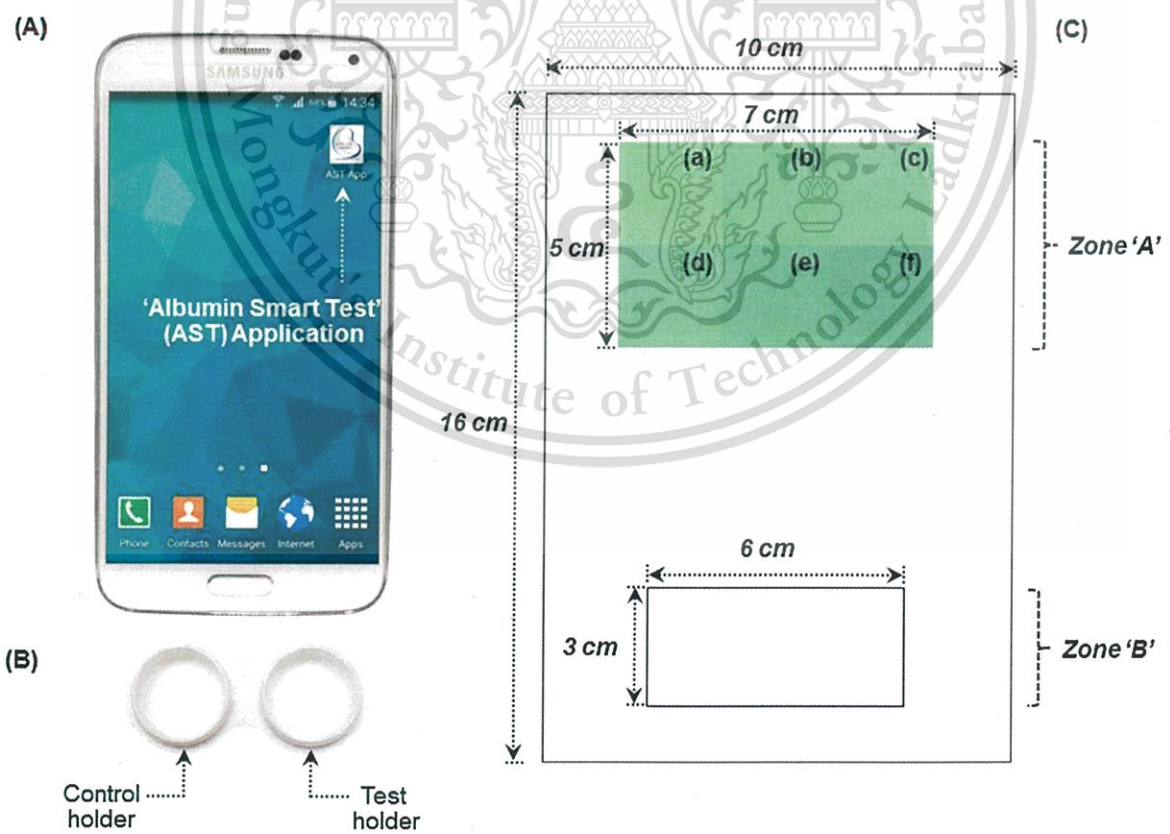

Fig. 1. Key apparatuses exploited with the mobile phone-based analyzer for quantitative determination of urinary albumin. (A) Smart mobile phone, (B) Sample cassette (shown as lids open) and (C) Test paper which contains Zone 'A' and Zone 'B'. Zone 'A': Standard colorimetric strip that composes of printed reference colors representation of (a) 1 mg L^{-1}, (b) 10 mg L^{-1}, (c) 20 mg L^{-1}, (d) 30 mg L^{-1}, (e) 40 mg L^{-1} and (f) 50 mg L^{-1} standard albumin. Zone 'B': Space for situating the sample cassette.

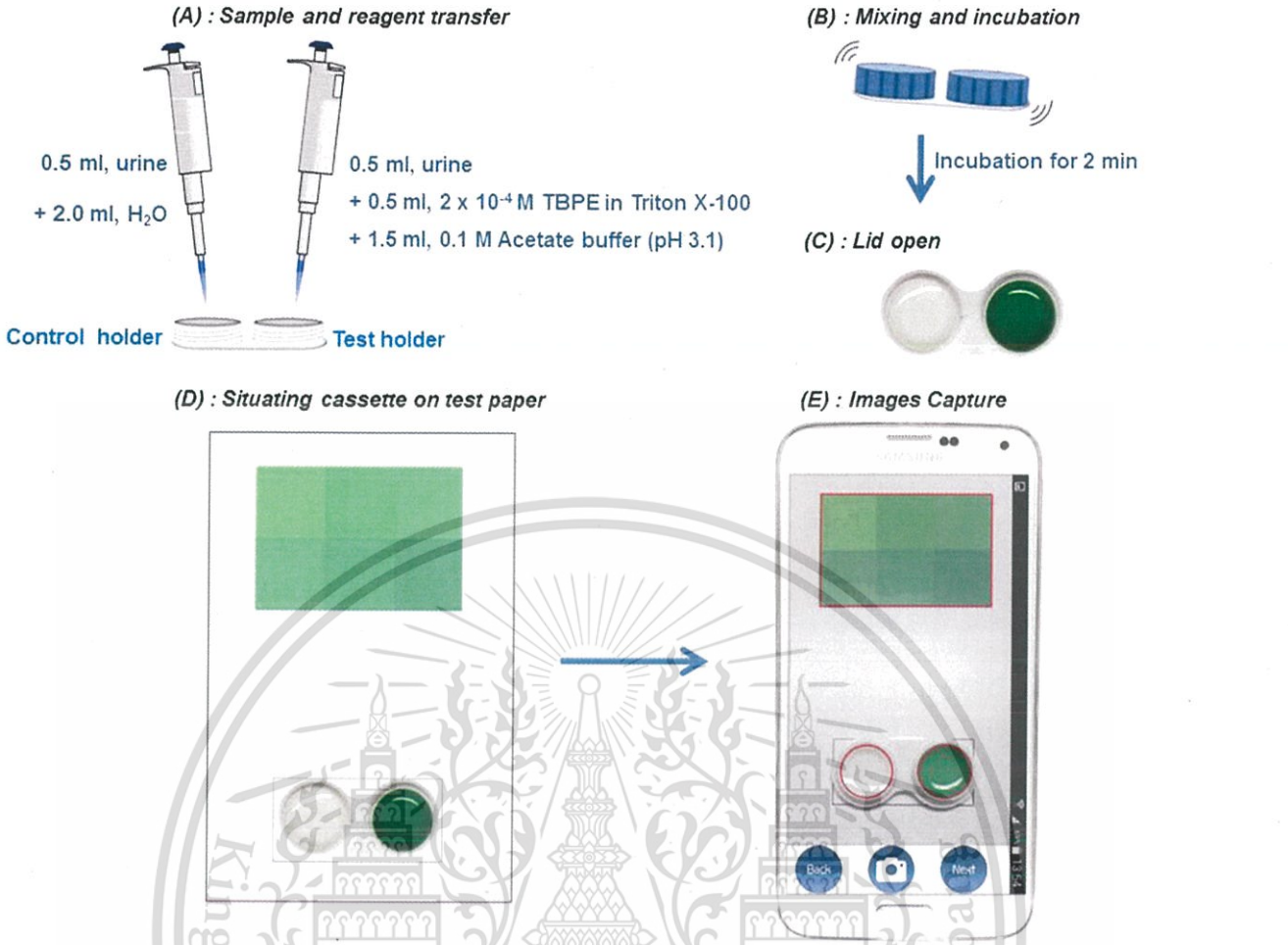

Fig. 2. Summary on the analytical workflows for the albumin measurement in urine sample by the mobile phone-based analyzer. (A): Transferring of sample and reagents into the sample cassette, (B): Mixing and incubation for 2 min, (C): Opening lids of the sample cassette, (D): Placing the sample cassette in the test paper and (E): Capturing the images.

display, 16 M pixel digital camera and 2.5 GHz processing unit. Our developed application (15 MB) namely 'Albumin smart test' or 'AST app' was installed into the mobile phone. Fig. 1B shows the sample cassette that is adapted from a commercially available contact lens container. One cassette is composed of two holders which are employed for accommodating control and test urine samples. Dimension of each holder is 2.2 cm diameter and 1.3 cm depth. The test paper in Fig. 1C, is made of a 270-g, white uniformly photo paper. Two zones are assigned on the paper sheet. Zone 'A' is standard colorimetric strip and zone 'B' is space for situating sample cassette. The standard colorimetric strip was made by printing the reference colors (illustrated as (a)–(f) in Fig. 1C) onto the photo paper using a 2605HP color laser printer.

Analytical workflows for the albumin measurement are summarized in Fig. 2. The measurement is started from transferring of urine sample (without prior pretreatment) and the other reagent solutions into the holders as shown in Fig. 2A. Both holders are covered with their lids and the solutions are mixed by gently shaking of the cassette. After kept standing for incubation (2 min), the lids are opened. The cassette is situated onto the test paper. User can run the application to capture images of standard colorimetric strip and urine sample by touching the camera icon on the screen of the mobile device (Fig. 2E). Parameters of the digital camera of the mobile phone are fixed (ISO: 100, aperture: 2.2 and shutter speed: 1/33). Prior to capture, it is necessary to align the mobile device in order that the images of the standard colorimetric strip and the sample cassette are fixed inside the frames (See Fig. 2E). The acquired images are then automatically processed for converting color intensity into its corresponding albumin concentration. All measurement processes are completed within 3 min.

2.3. Measurement by a validating spectrophotometric method

The spectrophotometric method with the same detection chemistry was chosen as the validating method. Aliquot of 0.5 mL of standard albumin or 10-fold diluted urine sample was pipetted into test tube, followed by adding 0.5 mL of 2.0×10^{-4} mol L^{-1} TBPE in 0.2% v/v Triton X-100 and 1.5 mL of 0.1 mol L^{-1} acetate buffer (pH 3.1). The solution was mixed through a Gennie Z Vortex mixer (Scientific Industries, USA) and was kept standing for incubation (2 min). The solution was then transferred into a 10-mm pathlength quartz cuvette (Helma, Germay). Absorbance reading at 605 nm was monitored using a 630 UV–vis. spectrophotometer (JASCO, USA). The concentration of albumin in urine sample was determined by an external calibration method.

3. Results and discussion

3.1. Design of 'Albumin smart test' application and image processing

'Albumin smart test' application was designed using the Java-based program for Android operating system. Android was chosen because of its ease for programming and the benefit of being free

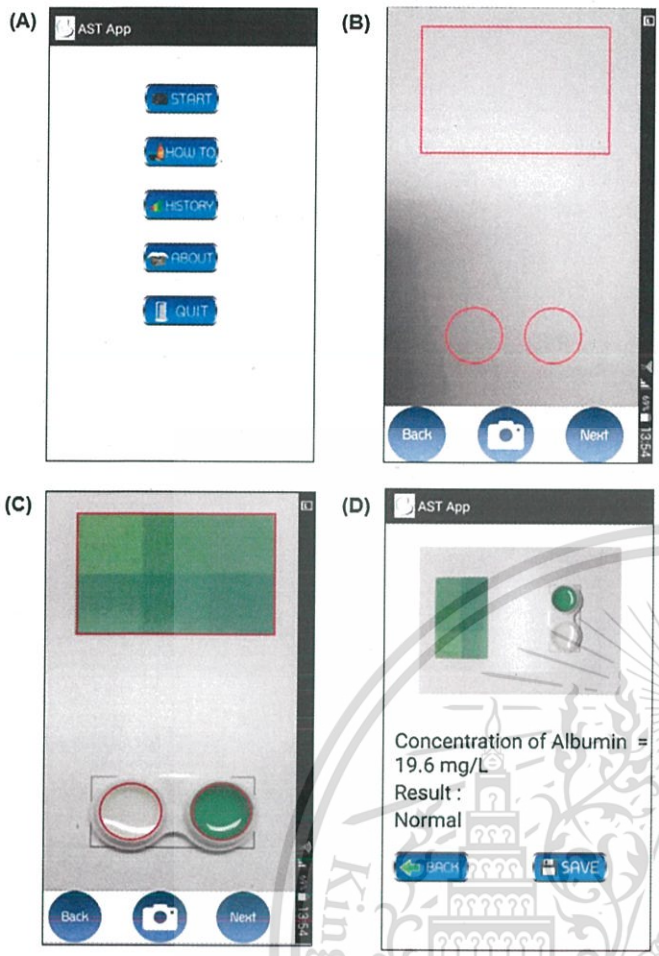

Fig. 3. Screenshots of the 'Albumin smart test' application at difference stages of the image processing. (A): User interface, (B): Power up the digital camera of the smart phone, (C): Simultaneously capturing the images of standard colorimetric strip and the samples and (D): Report on summary of the albumin test.

license. Furthermore, Android currently leads the smart-phone operating system market with almost 75% of the devices [30]. Fig. 3 displays four different screenshots of the developed application at different stages of image processing. User interface is displayed as shown in Fig. 3A. The albumin test is initiated after touching "START". User manual is summarized in "HOW TO". The albumin concentrations for previous diagnoses are recorded in "HISTORY". This information is useful as regarding in term of long-term monitoring of microalbuminuria. General information of the application is concluded in "ABOUT". User can exit the application by touching "QUIT".

After touching on "START", the new window appears and the digital camera of the smart phone is power up as depicted in Fig. 3B. The rectangular frame and the circular frames are exploited to confine the area of the standard colorimetric strip and the samples, respectively. User can conveniently adjust the distance and the orientation of the mobile phone in such a way that the images of the standard colorimetric strip and the samples are clearly observed within these frames (See Fig. 3C). The distance between the digital camera and the objects can be therefore kept constant at every analysis under the same mobile device. Non precise measurement due to the position of the mobile phone is typically shifted or moved away from the objects can be eliminated.

The images of the standard colorimetric strip and the samples are simultaneously captured after touching the camera icon (Fig. 3C). The acquired images are then digitally processed by touching "Next". The image (as JPEG format) with a size of 129 × 129 pixels of each printed reference color are consecutively calculated for its characteristic H (hue) parameter of the HSV color space using the embedded color analysis algorithm as proposed by K. Crantell et al. [31]. The H value is employed as a quantitative analytical parameter in this work as this value is the representation of the cognitive color information in a single parameter [32]. In addition, the H value is stable and easily obtained from the digital camera [31]. The results are exploited for construction of calibration equation against the albumin concentration ranging from 1 to 50 mg L^{-1}. The calibration equation is re-constructed at every measurement. For the next step, the area of the images of the samples (129 × 129

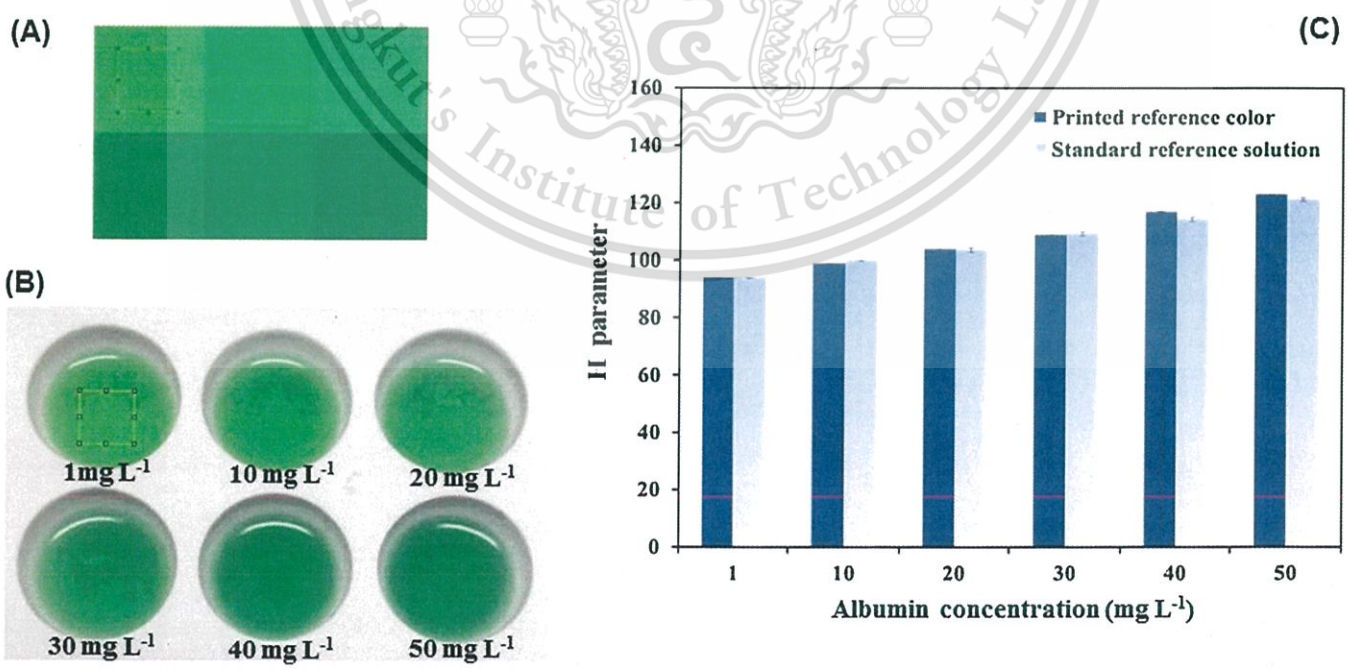

Fig. 4. (A) and (B) Optical images of the printed reference colors on the test paper and the reference standard solution in the plastic spot plate, respectively. The sensing area (depicted as square) is 129 × 129-pixel. (C) Comparison of the H parameters obtained by the printed reference colors and by the reference standard solution.

Table 1
Recovery study of standard albumin added to urine samples.

Sample	Added (mg L^{-1})[a]	Found (Mean (mg L^{-1}) + SD)[b]			Recovery (%)
S1	10	11.4	±	0.24	98.4
S2		11.5	±	0.45	98.4
S3		11.8	±	0.31	100.7
S4		11.7	±	0.28	100.5
S5		11.3	±	0.29	94.4
S6	20	21.9	±	0.10	99.7
S7		21.6	±	0.11	98.6
S8		22.1	±	0.24	100.3
S9		21.8	±	0.41	97.0
S10		21.2	±	0.39	97.3
S11	30	32.1	±	0.29	96.9
S12		32.0	±	0.16	97.9
S13		32.3	±	0.25	97.9
S14		32.4	±	0.41	99.1
S15		31.9	±	0.14	97.5
S16	40	41.9	±	0.29	101.2
S17		41.7	±	0.55	100.9
S18		42.0	±	0.70	101.0
S19		41.5	±	0.58	98.9
S20		41.1	±	0.35	99.6
S21	50	52.0	±	0.16	98.4
S22		51.9	±	0.35	98.3
S23		52.4	±	0.44	99.1
S24		52.1	±	0.23	97.6
S25		51.8	±	0.41	98.4

[a] Concentration of standard albumin added to urine sample solutions.
[b] Measurement was carried out in triplicates.

pixels) in the control and the test holders are evaluated for their H parameters. Result obtained by the test holder is substracted by the one from the control holder for background correction of any perturbation arisen from color of urine sample. The result is converted to its corresponding albumin concentration by the constructed calibration equation. Once the measurement is finished, summary of the result appears in the display of the mobile phone (Fig. 3D). Two different types of labels, either "Normal" or "High Risk to microalbuminuria" is presented for the albumin concentration that fall within a range of lower or greater than 30 mg L^{-1}, respectively. An example of the result in Fig. 3D is observed when urine sample collected from normal volunteer is analyzed. All imaging processes are accomplished within 5 s. User can record the result by touching 'SAVE' or can repeat the measurement by touching 'BACK'.

3.2. Development and verification of the printed reference

Reliability of our developed method is strongly depended on the printed reference colors in the standard colorimetric strip since the H parameters of the printed reference color are employed for constructing the calibration equation. The printed reference colors (Fig. 4A) were developed from the standard reference solutions that were prepared by mixing of the standard working solutions of albumin (1, 10, 20, 30, 40 and 50 mg L^{-1}) with the color developing reagents (2.0×10^{-4} mol L^{-1} TBPE in the presence of 0.2% v/v Triton X-100) and acetate buffer (pH 3.1). Firstly, spectra and absorbance readings at 605 nm of the mixing solutions were monitored. The calibration line as illustrated in Fig. S1 in Supplementary material in the online version at DOI: http://dx.doi.org/10.1016/j.snb.2016.11.057. showed good linearity. The mixed solutions were then transferred into the plastic spot plate (Fig. 4B). The image of the spot plate was captured by the mobile device's camera and was downloaded into personal computer. The sensing area (129 × 129 pixels) of each image of standard reference solution in the spot plate was digitally processed using Mathlab for evaluation of the H parameter. The results were designated as the color indices for printing a pattern of the reference colors in the standard colorimetric strip.

A Criterion to verify the printed reference color is to compare its H parameter to the one obtained by the standard reference solution. The H parameter of each printed reference color was evaluated similarly to the H parameter obtained by the standard reference solution. The results in Fig. 4C are not significant difference by the statistical paired *t*-test [33] ($t_{stat} = -1.08$, $t_{cri} = 2.57$, $d.f. = 5$). This implies that the printed reference colors of the standard colorimetric strip can be employed as the representation of the standard reference solutions for the quantification of albumin .

3.3. Advantage for self-calibration configuration

The 'Albumin smart test' and the test paper are designed in order that the standard colorimetric strip and the sample are simultaneously captured in a single shot. Integration of self-calibration configuration is therefore achieved. The most advantage is that effect of variation of illuminations can be minimized. To demonstrate this advantage, optical images of the mixed solutions between standard albumin (1, 10 30 and 50 mg L^{-1}) and the

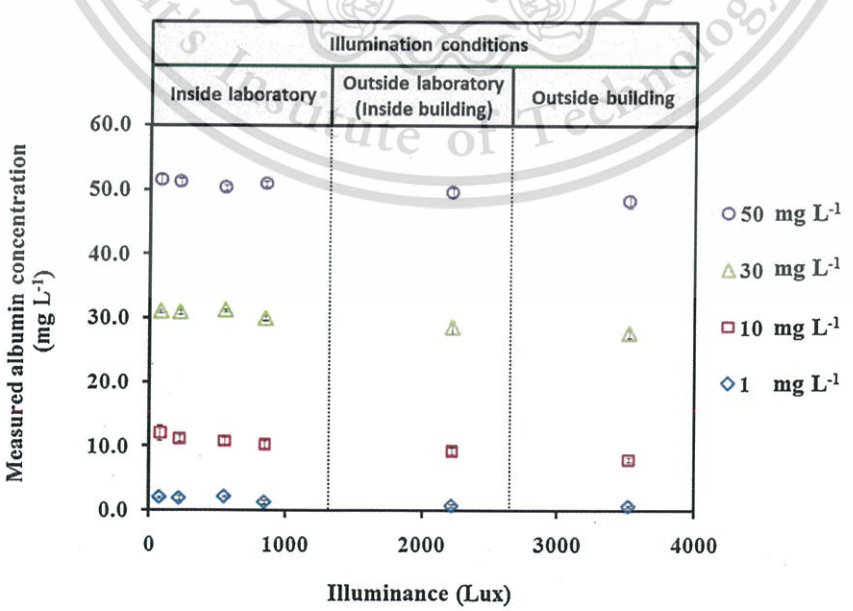

Fig. 5. Effect of different illumination conditions.

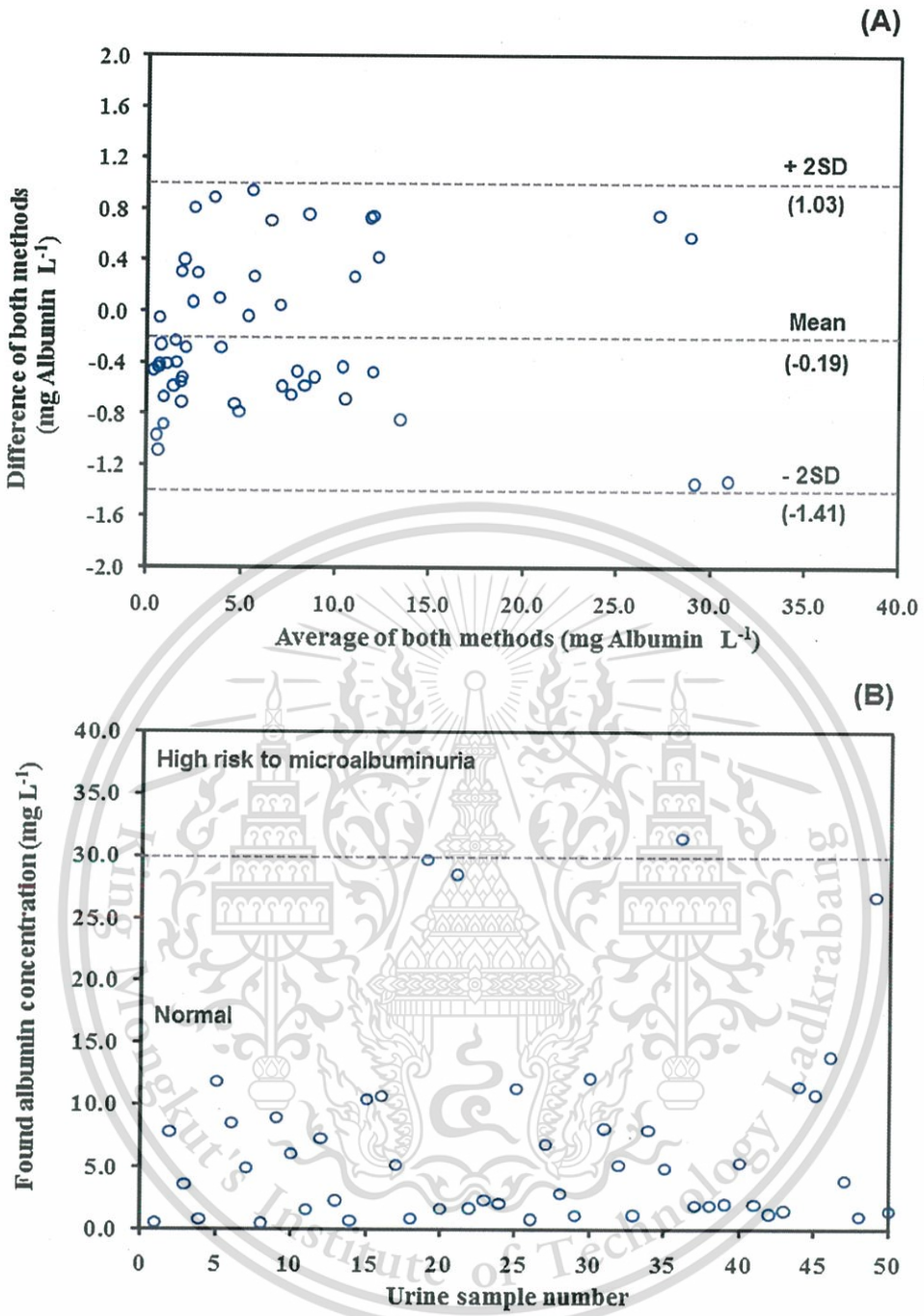

Fig. 6. Validation and application to urine samples (n = 50 samples). (A) The Bland-Altman plot [32] for comparison of the data obtained from our method with the validating spectrophotometric method. (B) Found albumin concentration, determined by our method.

chromomeric reagents were captured and were analyzed by our mobile phone device at various illumination levels. As shown in Fig. 5, the measured albumin concentrations are not difference for all illuminant conditions. The effect of variation of illumination is therefore negligible. This can lead our mobile phone-based to provide high versatility for measurement of the urinary albumin concentration in both typical indoor and outdoor illumination without requirement of any additional lighting control apparatus.

3.4. Recovery study

An experiment was carried out on 50 urine samples to evaluate the recovery of the method. Addition of albumin standards (10 to 50 mg L^{-1}) was made for a sample solution. The samples were analyzed by the mobile phone-based analyzer without any further dilution. The results given in Table 1 demonstrate that the method provides satisfactorily good recovery of the signal.

3.5. Comparison of the albumin content, determined by different mobile devices

The developed application program was installed into the other mobile devices. Comparison of the albumin content in urine samples, determined by different mobile devices is concluded in Table 2. By ANOVA test [33], the results are not significant difference

Table 2
Comparison of the measured albumin concentration in urine samples, determined by different mobile-based devices.

Sample	Concentration of measured albumin[a] (Mean (mg L^{-1}) ± SD)								
	Device 1[b]			Device 2[c]			Device 3[d]		
S1	31.2	±	1.0	31.1	±	0.5	30.6	±	1.3
S2	31.0	±	0.5	32.2	±	0.8	30.1	±	0.5
S3	32.4	±	0.5	33.9	±	1.4	31.3	±	0.8
S4	31.9	±	2.1	33.2	±	0.4	32.4	±	0.3
S5	31.8	±	1.8	32.0	±	1.0	31.2	±	0.5

[a] Measurement was carried out in triplicates.
[b] Samsung Galaxy Table 10.1 (No.1).
[c] Samsung Galaxy Table 10.1 (No.2).
[d] Samsung Galaxy S5.

(F_{stat} = 3.12, F_{crit} = 3.89). This implies that the developed application program is applicable for different devices and models.

3.6. *Application to urine samples: validation and diagnosis of microalbuminuria*

The developed method was applied to the determination of albumin in 50 urine samples that were spot collected from volunteers of various ages (30–60 year-old) with no known history of CKD. The results determined by our mobile phone were compared with results obtained using the validating spectrophotometric method by means of the Bland–Altman plot [34] for validation study. Results in Fig. 6A shows that all data lay within ± 2SD of the mean of their differences, showing that this method was equivalent to the validating method. Pearson's correlation (See Fig. S2 in the online version at DOI: http://dx.doi.org/10.1016/j.snb.2016.11.057) also confirms that our method gave results that did not differ significantly from values using the validating methods (r^2 = 0.9968). Our method also gives high precision (within-day RSD: 0.9–1.2% and between-day RSD: 0.7–2.5%). Fig. 6B shows that some volunteers are of high risk of microalbuminuria. It was observed by our personal interview that these volunteers suffered from hypertension and diabetes.

4. Conclusions

The mobile phone-based analyzer installed with the 'Albumin smart test' application was reported for the first time for the determination of urinary albumin based on self-calibration approach. This is also the first report that the distance between the digital camera of the mobile phone and the object is easily adjusted and is kept constant for all measurement under the same mobile device. As a result, precise and accurate quantitative measurement of the albumin concentration can be accomplished without using any extra module for lighting adjustment during image capturing. Successful validation of the developed method against the spectrophotometric method was achieved. Our mobile phone showed high proficiency to be exploited as a portable diagnostic analyzer for the microalbuminuria analysis. However, measurement of creatinine in the spot urine to correct for the variation in the urine sample volume is necessary. Therefore, future work relates on the extension of our mobile phone-based analyzer prototype for the evaluation of urinary albumin to creatinine ratio is now under developed .

Acknowledgements

Financial supports from King Mongkut's Institute of Technology Ladkrabang Fund, grant no. KREF015201 and from the Thailand Toray Science Foundation, TTSF (for NC) and from the Faculty of Science, King Mongkut's Institute of Technology Ladkrabang (for AM) are gratefully acknowledged. Instrumental supports from Applied Analytical Chemistry Research Unit, Department of Chemistry, Faculty of Science, King Mongkut's Institute of Technology Ladkrabang are also appreciated.

References

[1] A.S. Levey, J. Coresh, E. Balk, A.T. Kausz, A. Levin, M.W. Steffes, R.J. Hogg, R.D. Perrone, J. Lau, G. Eknoyan, National kidney foundation practice guidelines for chronic kidney disease: evaluation, classification, and stratification, Ann. Intern. Med. 139 (2003) 137–147.
[2] P.A. Sarafidis, G.L. Bakris, Microalbuminuria and chronic kidney disease as risk factors for cardiovascular disease, Nephrol. Dial. Transplant. 21 (2006) 2366–2374.
[3] http://social.nesdb.go.th/social/Default.aspx?tabid=131 (written in Thai).
[4] A.S. Levey, S.P. Andreoli, T. DuBose, R. Provenzano, A.J. Collins, Chronic kidney disease: common, harmful and treatable–world kidney day 2007, Am. J. Nephrol. 27 (2007) 108–112.
[5] H. Kramer, M.E. Molitch, Screening for kidney disease in adults with diabetes, Diabet. Care 28 (2005) 1813–1816.
[6] C.E. Mogensen, Microalbuminuria predicts clinical proteinuria and early mortality in maturity-onset diabetes, N. Engl. J. Med. 310 (1984) 356–360.
[7] J.H. Contois, C. Hartigan, L.V. Rao, L.M. Snyder, M.J. Thompson, Analytical validation of an HPLC assay for urinary albumin, Clin. Chim. Acta 367 (2006) 150–155.
[8] E.A. Bessonova, L.A. Kartsova, A.U. Shmukov, Electrophoretic determination of albumin in urine using on-line concentration techniques, J. Chromatogr. A 1150 (2007) 332–338.
[9] J. Woo, M. Floyd, D.C. Cannon, B. Kahan, Radioimmunoassay for urinary albumin, Clin. Chem. 24 (1978) 1464–1467.
[10] H. Thakkar, D.J. Newman, P. Holownia, C.L. Davey, C.C. Wang, J. Lloyd, A.R. Craig, C.P. Price, Development and validation of a particle-enhanced turbidimetric inhibition assay for urine albumin on the Dade aca® analyzer, Clin. Chem. 43 (1997) 109–113.
[11] C. Jiang, L. Luo, Spectrofluorimetric determination of human serum albumin using a doxycycline-europium probe, Anal. Chim. Acta 506 (2004) 171–175.
[12] H. Yatzidis, New colorimetric method for quantitative determination of protein in urine, Clin. Chem. 23 (1997) 811–812.
[13] K.H. Schosinsky, M. Vargas, A.L. Esquivel, M.A. Chavarria, Simple spectrophoto- metric determination of urinary albumin by dye-binding with use of bromphenol blue, Clin. Chem. 33 (1967) 223–226.
[14] Y. Fujita, I. Mori, M. Toyoda, Determination of basic-proteins based on color reaction with the 3 4, 5, 6-tetrachloro-2-carboxyphenylfluorone-manganese(II) complex, Anal. Sci. 8 (1992) 693–694.
[15] M.J. Pugia, J.A. Lott, J.A. Profitt, T.K. Cast, High-sensitivity dye binding assay for albumin in urine, J. Clin. Lab. Anal. 13 (1999) 180–187.
[16] Z.X. Guo, Y.M. Hao, X. Cong, H.X. Shen, Application of the dibromohydroxyphenylfluorone-molybdenum(VI) complex to the sensitive spectrophotometric determination of protein, Anal. Chim. Acta 403 (2000) 225–233.
[17] T. Sakai, Y. Kito, N. Teshima, S. Katoh, K. Watla-iad, K. Grudpan, Spectrophotometric flow injection analysis of protein in urine using tetrabromophenolphthalein ethyl ester and triton X-100, J. Flow Injection Anal. 24 (2007) 23–26.
[18] K. Watla-iad, T. Sakai, N. Teshima, S. Katoh, K. Grudpan, Successive determination of urinary protein and glucose using spectrophotometric sequential injection method, Anal. Chim. Acta 604 (2007) 139–146.
[19] W. Siangproh, N. Teshima, S. Katoh, O. Chailapakul, Alternative method for measurement of albumin/creatinine ratio using spectrophotometric sequential injection analysis, Talanta 79 (2009) 1111–1117.
[20] W. Laiwattanapaisal, U. Kunanuvat, W. Intharachuti, C. Chinvogamorn, S. Hannongbua, O. Chailapakul, Simple sequential injection analysis system for rapid determination of microalbuminuria, Talanta 79 (2009) 1104–1110.
[21] W.L. Gyure, Comparison of several methods for semiquantitative determination of urinary protein, Clin. Chem. 23 (1977) 876–879.
[22] Z. Iqbal, R.B. Bjorklund, Colorimetric analysis of water and sand samples performed on a mobile phone, Talanta 84 (2011) 1118–1123.
[23] A. García, M.M. Erenas, E.D. Marinetto, C.A. Abad, I. de Orbe-Paya, A.J. Palma, L.F. Capitán-Vallvey, Mobile phone platform as portable chemical analyzer, Sens. Actuators B 156 (2011) 350–359.
[24] S. Sumriddetchkajorn, K. Chaitavon, Y. Intaravanne, Mobile-platform based colorimeter for monitoring chlorine concentration in water, Sens. Actuators B 191 (2014) 561–566.
[25] W. Xu, Y. Chen, T. Zhao, Y. Jiang, Y. Wang, X. Chen, Simultaneous color sensing of O_2 and pH using a smartphone, Sens. Actuators B 220 (2015) 326–330.
[26] Y.Y. Wu, A. Boonloed, N. Sleszynski, M. Koesdjojo, C. Armstrong, S. Bracha, V.T. Remcho, Clinical chemistrymeasurements with commercially available test slideson a smartphone platform: colorimetric determination of glucoseand urea, Clin. Chim. Acta. 448 (2015) 133–138.
[27] A.F. Coskun, R. Nagi, K. Sadeghi, S. Phillips, A. Ozcan, Albumin testing in urine using a smart-phone, Lab Chip 13 (2013) 4231–4238.

[28] Y. Intaravanne, S. Sumriddetchkajorn, Android-based rice leaf color analyzer for estimating the needed amount of nitrogen fertilizer, Comput. Electron. Agric. 116 (2015) 228–233.
[29] P. Inpota, S. Teerasong, A. Kongsakphaisal, N. Maneerat, D. Nacapricha, N. Choengchan, Parallel cross injection analysis system for determination of albumin to creatinine ratio in urine, Pure and Applied Chemistry Conference (PACCON) Proceedings (2011) 79–82.
[30] A. Puder, O. Antebi, Cross-compiling android applications to iOS and windows phone 7, Mob. Netw. Appl. 18 (2013) 3–21.
[31] K. Cantrell, M.M. Erenas, I. de Orbe-Payá, L.F. Capitán-Vallvey, Use of the hue parameter of the hue saturation, value color space as a quantitative analytical parameter for bitonal optical sensors, Anal. Chem. 82 (2010) 531–542.
[32] M.M. Erenas, K. Cantrell, J. Ballesta-Claver, I. de Orbe-Payá, L.F. Capitán-Vallvey, Use of digital reflection devices for measurement using hue-based optical sensors, Sens. Actuators B 174 (2012) 10–17.
[33] J.N. Miller, J.C. Miller, Statistics and Chemometrics for Analytical Chemistry, fourth ed., Pearson Education, 1993.
[34] S.A. Glantz, Primer of Biostatistics, fifth ed., McGraw-Hill, USA, 2002.

Biographies

Arjnarong Methaweesansurn received his B. Sc. in industrial chemistry in 2009 and M. Sc. in chemistry (analytical chemistry) in 2012 from King Mongkut's Institute of Technology Ladkrabang (KMITL), Thailand. On his M.Sc. study, he was granted from "Tab Nilaniti Foundation" for student who has excellent score in scientific study. Now he is a Ph.D. student in applied chemistry, KMITL. He received research grant from Faculty of Science, KMITL. In 2014, his work entitled 'Albumin smart test' was awarded 'a gold medal' in the 32th National Graduate Research Conference in Bangkok, Thailand.

Noppadol Maneerat earned his B.Sc. in physics from Srinakharinwirot University, Pitsanulok in 1990. He received his M. Sc. and Ph. D. in electrical engineering from KMITL in 1997 and 2006, respectively. He is now an assistant professor at Department of Control Engineering, Faculty of Engineering, KMITL, Thailand.

Nathawut Choengchan received his B. Sc. (chemistry) and M. Sc. (applied analytical chemistry and inorganic chemistry) from Mahidol University (MU), Thailand, in 1999 and 2002, respectively. During his M.Sc. study, he was granted for the "Staff Development in the Shortage Area scholarship" from KMITL. In 2006, he received his Ph.D. (analytical chemistry) from MU. On the period of Ph.D. study, he earned a fellowship from the "Royal Golden Jubilee Ph.D. Program" for doing one part of his works in Okayama University, Japan for one year (2005–2006). He now works as assistant professor at Department of Chemistry, KMITL, Thailand.

Send Orders for Reprints to reprints@benthamscience.ae

Current Analytical Chemistry, 2018, *14*, 1-11

RESEARCH ARTICLE

Low-cost Synthesis of Gold Nanoparticles from Reused Traditional Gold Leaf and its Application for Sensitive and Selective Colorimetric Sensing of Creatinine in Urine

Arjnarong Mathaweesansurn[a,b], Nathawut Choengchan[*a,b], Putthiporn Khongkaew[c] and Chutima Matayatsuk Phechkrajang[a,d]

[a]*Flow Innovation-Research for Science and Technology Laboratories (FIRST Labs), Bangkok, 10520 Thailand;* [b]*Department of Chemistry and Applied Analytical Chemistry Research Unit, Faculty of Science, King Mongkut's Institute of Technology Ladkrabang, Chalongkrung Road, Ladkrabang, Bangkok, 10520 Thailand;* [c]*Faculty of Pharmaceutical Science, Burapha University, Longhaad Bangsaen Road, Muang, Chonburi, 20131 Thailand;* [d]*Department of Pharmaceutical Chemistry, Faculty of Pharmacy, Mahidol University, Sri-Ayuthaya Road, Rachathevi, Bangkok, 10400 Thailand*

Abstract: ***Background:*** Gold nanoparticles (Au NPs) are normally prepared using standard gold (III) trichloride which is much expensive and irritant. This work is aimed at demonstrating simple and low-cost synthesis of Au NPs from the reused traditional gold leaf which is cost-free and less toxic.

Method: The reused gold leaf was donated by the local temple. It was digested and used as the precursor for the preparation of the Au NPs by Turkevich method. Poly (vinyl alcohol) (PVA) was employed as a stabilizer. The as-prepared Au NPs were applied for the colorimetric determination of creatinine in urine without any sample pretreatment.

Results: Long-term stability of the gold colloids was achieved for at least 3 months. Morphology and purity of the as-prepared Au NPs were the same as the ones prepared from standard gold (III) salt and standard gold foil. Colorimetric response of the Au NPs was linear to the standard creatinine up to 200 mg L^{-1}. The limit of detection (0.16 mg L^{-1} or 1.41 μM) was enough sensitive for urinary creatinine detection in patients with kidney disease. Good recoveries (97-108 %) and fast analysis time (3 min) were achieved. The developed method was successfully validated against the HPLC method.

Conclusion: Facile and cost-effective synthesis of the Au NPs from the reused traditional gold leaf, was accomplished. The as-prepared Au NPs were successfully applied for the determination of urinary creatinine with high sensitivity and selectivity.

ARTICLE HISTORY

Received: August 25, 2018
Revised: September 24, 2018
Accepted: October 03, 2018

DOI:
10.2174/1573411014666181010130631

Keywords: Colorimetric sensing, creatinine, gold nanoparticles, reused traditional gold leaf, urine.

1. INTRODUCTION

To date, metal nanoparticles have drawn a significant attention due to their unique physical and chemical properties different from those of the bulk state or atoms [1]. Gold nanoparticles (Au NPs) are probably the most outstanding metal nanoparticles because of the advantages of chemical inertness, easy modification, simple control of particle size and high extinction coefficient. Its distinct optical property is the clear color change from wine-red to blue after aggregation of the particles. This offers the use of the Au NPs for colorimetric assay in various applications with the benefits of excellent sensitivity, selectivity and simplicity [2-12].

In general, the Au NPs are most widely prepared accordingly to chemical reduction of standard gold (III) trichloride by sodium citrate or the so-called "Turkevich method" [13] due to its easiness. Although the gold (III) salt is normally used as a common precursor, it commercially exists in the chemical formula with trihydrate or tetrahydrate which is highly hygroscopic and leads to easy deterioration. Moreover, its net price is of high cost *e.g.*, 197 USD/g (99.9 %) or 174 USD/g (49 %). In terms of health effect, gold (III) trichloride is a strong eye, skin, and mucous membrane irritant. Some work, [14] therefore, reported the use of a standard gold foil as a less toxic material for the synthesis of the Au NPs by laser ablation technique. However, the laser ablation

*Address correspondence to this author at Department of Chemistry, Faculty of Science, King Mongkut's Institute of Technology Ladkrabang, 10520, Bangkok, Thailand; Tel: +66-2-326-8400-11 Ext. 290, Fax: +66-2-329-8428; E-mail: nchoengchan@gmail.com

1573-4110/18 $58.00+.00

instrument is available in few laboratories in the developing countries including Thailand and price of the standard gold foil is very high (351 USD/g for 99.9 %). These limitations can hinder the applications of the Au NPs.

Herein, we aim to demonstrate the simple and low-cost method for the preparation of the Au NPs. We were interested in exploiting the reused Thai traditional gold leaf as an alternative material. In Thailand, Buddhism always uses the gold leaf to gild into Buddha image for making merit. The gold leaves are removed from the waste when there are a lot of them, covering on Buddha image. It is better to reuse these gold leaves. In this work, the reused gold leaf is donated by the local temple. It is the first acid digested and then the solution is used as the precursor for the preparation of the Au NPs following the Turkevich method with using poly (vinyl alcohol) (PVA) as a stabilizer. Morphology and optical properties of the as-prepared Au NPs are characterized and are compared to the ones which are prepared from standard gold (III) trichloride and standard gold foil. We also proved the capability of the reused traditional gold leaf-prepared Au NPs in real use by applying as the colorimetric sensors for the detection of creatinine in urine for clinical diagnosis of kidney dysfunction. Detection principle is based on the aggregation of the Au NPs by creatinine, where the color of the nanoparticles solution is converted from wine-red into blue. Several analytical methods have been reported for the creatinine determination including the colorimetric Jaffé method [15-17], electrochemical sensor [18], HPLC [19] and capillary zone electrophoresis [20]. Although these methods are powerful and error proof, some of them are laborious, complex and time-consuming. There are some publications that describe the use of the Au NPs for the quantitative analysis of creatinine in biological samples [6-10]. However, standard gold (III) trichloride is employed as the material for preparation of the Au NPs for all the mentioned methods. It is also found in some works that surface modification of the Au NPs by toxic heavy metal ion (Hg(II)) [9] or by macrocyclic oligomer with many steps of modification [10] to achieve high sensitivity is necessary. While the other works require either long reaction time (> 20 min) [6-8] or solid phase extraction of the sample prior to the creatinine analysis [8]. In this work, we therefore consequently intend to not only use the alternative material for low-cost and simple preparation of the Au NPs but also to improve the creatinine measurement by the as-prepared Au NPs much easier and faster. Detection mechanism of the reaction between the as-prepared Au NPs (in the presence of the PVA stabilizer) and creatinine is also proposed.

2. MATERIALS AND METHOD

2.1. Reagents and Chemicals

The reused traditional gold leaf was donated by the local Buddhism temple in Chachoengsao Province, Thailand. Hydrochloric and nitric acids were bought from Carlo Erba (Italy) and were used for the preparation of a stock aqua regia (HCl/HNO_3, 3:1). Sodium citrate tribasic dihydrate and 80 % hydrolysed PVA were purchased from Sigma-Aldrich (USA) and were exploited as the reducing and stabilizing agents, respectively. A 10 mM phosphate buffer (pH 6.0) was prepared from sodium dihydrogen orthophosphate (UNIVAR, New Zealand) and disodium hydrogen phosphate heptahydrate (Panreac, UK). A standard stock creatinine (1000 mg L^{-1}) was prepared by dissolving 0.05xx g of creatinine powder (Sigma-Aldrich, USA) in 50.0 mL of water and was kept at 4°C. The working standards were freshly prepared by appropriate dilution of the stock solution. Deionized-distilled water (18 MΩ cm^{-1}) purified by ZENEER UP 900 (Human corporation, Korea) was used throughout. All glassware used were cleaned with aqua regia, rinsed with deionized-distilled water and air dried prior to use.

2.2. Synthesis and Characterization of the Reused Traditional Gold Leaf-prepared Au NPs

An accurate weight of 0.1xxx g of the reused traditional gold leaf was first digested with 5.0 mL of 70 % (v/v) aqua regia at 75°C with continuous stirring for 30 min. The solution was set aside to room temperature and filtered through Whatman™ No 2. The filtrate was made up to 50.0 mL with water and was exploited as the precursor for preparation of Au NPs based on the Turkevich method with some modifications. Briefly, the filtrate was adjusted to pH 2.0 using 1.0 M NaOH and was heated to 95°C. Then, a solution of 1.2 % (w/v) sodium citrate was rapidly transferred under vigorous stirring. The solution was continuously boiled for 15 min. After cooling, an aliquot of 0.5 mL of 2.0 % (w/v) PVA was added to this solution. The as-prepared colloidal gold solution was then kept at 4.0°C. Optical properties and morphology of the as-prepared Au NPs were characterized using a V-630 UV-visible spectrophotometer (Jasco, USA), a Tracer-100 Fourier transform-infrared (FT-IR) spectrometer (Shimadzu, Japan) and a Tecnai G2 T20 transmission electron microscope (TEM, FEI company, The Netherlands). The Au^0 content was evaluated using an X-MaxN energy dispersive X-ray spectrometer (EDS, Oxford instrument, UK).

2.3. Colorimetric Assay of Creatinine

An aliquot of 1.0 mL of the as-prepared Au NPs was pipetted into the test tube, followed by adding 5.0 mL of 10 mM phosphate buffer (pH 6.0) and 0.05 mL of either standard creatinine or urine samples. Each sample was 100-fold diluted with water before the analysis. The solution was mixed through a Gennie Z Vortex mixer (Scientific Industries, USA) and was incubated for 3 min at an ambient temperature. The surface plasmon band was monitored from 400 to 800 nm using a V-630 UV-visible spectrophotometer (Jasco, USA). Calibration plot between the absorbance reading ratio at 650 nm to 530 nm ($A_{650/530}$) against the standard creatinine concentrations was exploited for the quantification of creatinine in urine.

2.4. The Validating HPLC Conditions

The creatinine contents obtained by the developed method were validated with the results obtained by the reversed-phase HPLC. Conditions for the HPLC experiment are listed as the following parameters: Symmetry TM C18- column (3.9 mm x 150 mm, 5 μm); 100 % of 20 mM ammonium

dihydrogen orthophosphate (Merck, USA), pH 7.4, as the mobile phase; flow rate of 0.8 mL min^{-1}; injection volume of 20 µL; run time of 7 min; photodiode array detector with a fixed wavelength at 210 nm and column temperature of 25°C. Urine samples were diluted with the mobile phase and then were filtered through a 0.22-µm nylon membrane prior to injection.

3. RESULTS AND DISCUSSIONS

3.1. Appropriate Conditions for Digestion of the Reused Traditional Gold Leaf

Gold is resistant to most acids, though it can dissolve in aqua regia (HCl/HNO_3, 3:1). HNO_3 dissolves gold to form Au(III). HCl reacts with Au(III) to produce tetrachloroauric acid ($HAuCl_4$) as written in the following equation [21].

$$2Au\ (s) + 3HNO_3\ (aq) + 11HCl\ (aq) = 2HAuCl_4(aq) + 3NOCl\ (aq) + 6H_2O\ (l) \quad \ldots\ldots\ldots \quad (1)$$

In this work, the parameters affecting the digestion of the reused traditional gold leaf, *i.e.* the concentration of aqua regia and the digestion time are investigated. Criterion for selecting the appropriate conditions is based on the product yield (%) which is calculated from the concentration ratio of $[HAuCl_4]_{observed}$ to $[HAuCl_4]_{theoretical}$. The $[HAuCl_4]_{observed}$ is the concentration of $HAuCl_4$ in the digested gold leaf solution which is evaluated *via* the linear calibration plot between the absorbance reading at 308 nm (the maximum absorption wavelength (λ_{max}) of $HAuCl_4$) against the concentrations of the standard $HAuCl_4$. The $[HAuCl_4]_{theoretical}$ is the concentration of $HAuCl_4$ which is stoichiometrically calculated based on the use of equation (1).

Results in Fig. (**1A**) show that the λ_{max} of the digested gold leaf is located at 310 nm, which is very close to the λ_{max} of the standard $HAuCl_4$. This implies that $HAuCl_4$ is obtained after digestion. Both the absorbance readings and yields increase when the aqua regia concentrations increase up to 70 % (v/v). Therefore, the concentration of 70 % (v/v) is chosen. The absorbance readings and yields also increase, when the digestion times increase up to 30 min (Fig. **1B**). The digestion time of 30 min is selected as compromising between the obtained yield and the consumed time. This digestion time reduces to more than 2 hours, compared to the other reports [22, 23] with the comparable yields.

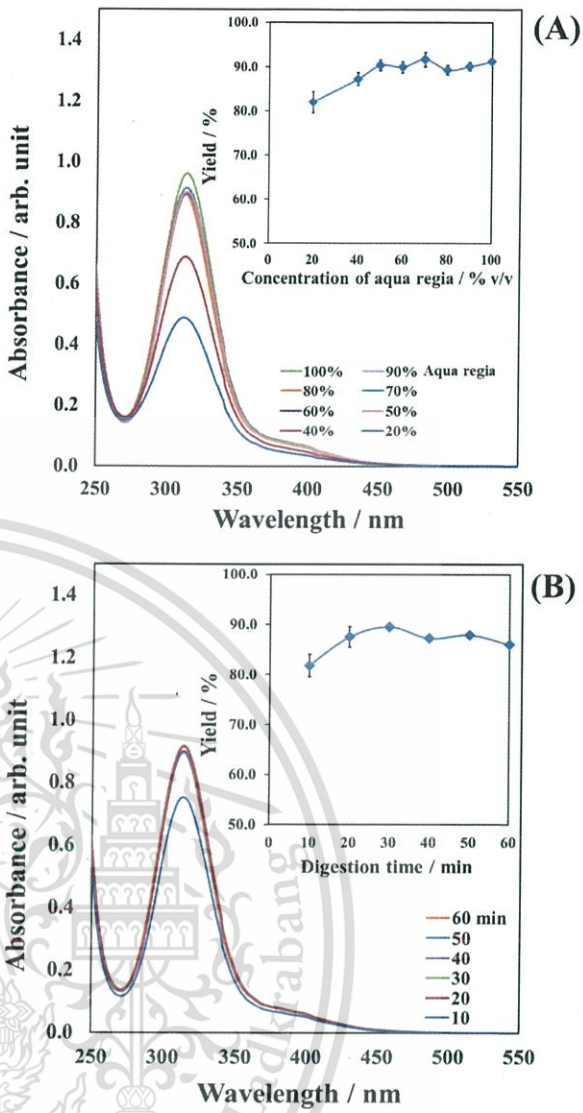

Fig. (1). UV-Visible absorption spectra of the digested gold leaf solutions obtained by **(A)** various concentrations of aqua regia (at fixed acid volume (5.0 mL) and digestion time (30 min)), and **(B)** various digestion times (at fixed acid volume (5.0 mL) and acid concentration (70 % v/v)). Inset graphs are the product yield (%) at various concentrations of aqua regia and digestion times. Note: The product yield is calculated as the following equation; yield = $[HAuCl_4]_{observed}$ / $[HAuCl_4]_{theoretical}$ x 100.

3.2. Influences of Chemical Parameters Affecting the Synthesis of the Reused Traditional Gold Leaf-prepared Au NPs

3.2.1. Effect of pH of the Digested Gold Leaf Solution

Results in Fig. (**2A**) indicate that the characteristic surface plasmon band of the Au NPs does not appear when the original digested gold leaf solution (pH 1.4) is used as the precursor. The color of the prepared solution is still pale yellow and does not change into wine-red (See inset photos of Fig. **2A**). This suggests that the Au NPs does not form. This is because at low pH, the carboxyl group of sodium citrate is protonated to citric acid [24]. Reduction of Au(III) to produce Au^0 nanoparticles does not occur. The pHs of the digested gold leaf solutions were then adjusted to obtain the final pH of 2.0, 3.0 and 4.0 by NaOH (1.0 mol L^{-1}) prior to its use in the synthesis. At pH 2.0, the narrowest surface plasmon band is located at 530 nm and color of the corresponded solution turns into wine-red (Fig. **2A**). This means that Au(III) ions in the digested gold leaf solution are converted into Au^0 particles by citrate ions. The representative TEM image in Fig. (**2B**) also displays that the colloidal and spherical-shaped Au NPs are obtained. At pH 3.0 and 4.0, the dark blue solutions are observed and their surface plasmon bands expand with a decreasing in the absorbance readings at 530 nm (Fig. **2A**). It may be due to the hydrolysis of $AuCl_4^-$. These hydrolyzed auric species are less reactive spe-

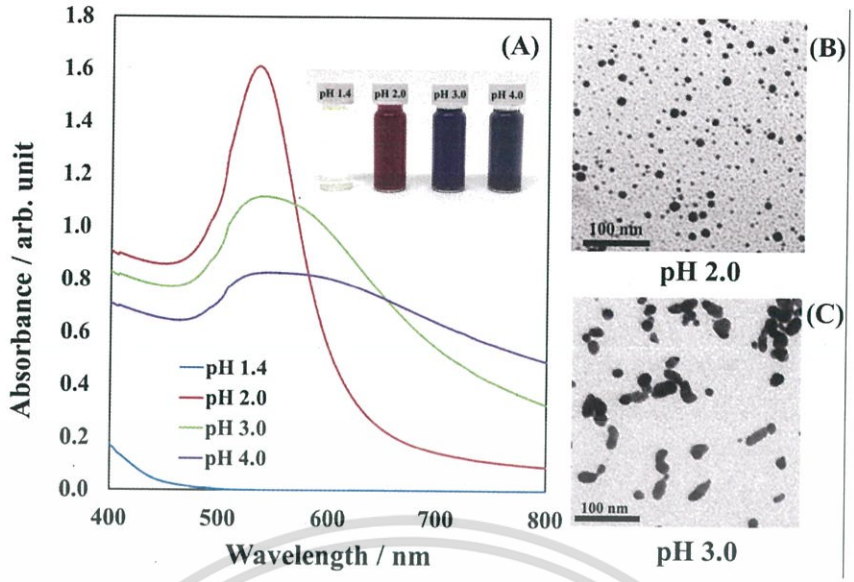

Fig. (2). **(A)** surface plasmon bands obtained when the pH values of the digested gold leaf are varied from 1.4 to 4.0. Inset photos represent colors of the as-prepared solutions at different pH values of the digested gold leaf solutions. **(B)** and **(C)** are the representatives of the TEM images of the reused traditional gold leaf-prepared Au NPs at pH 2.0 and 3.0, respectively. The concentrations of citrate and PVA are fixed at 1.2 and 2.0 % (w/v), respectively.

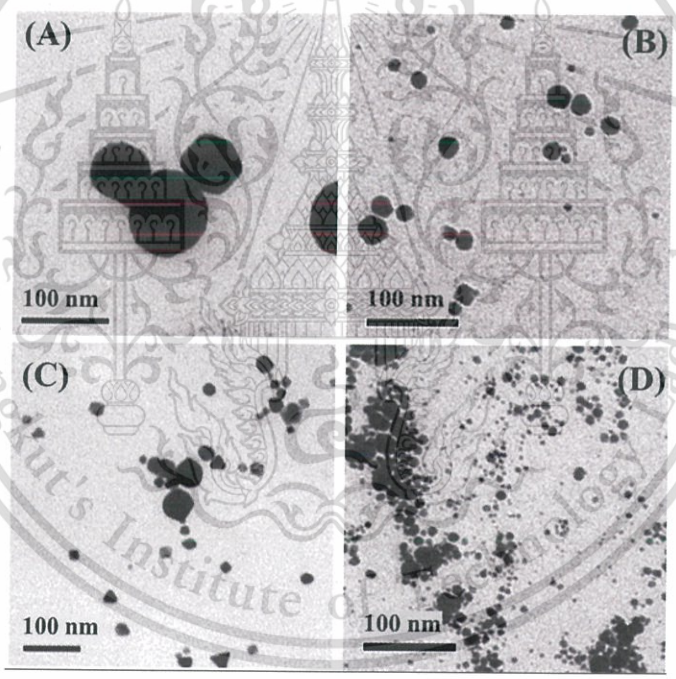

Fig. (3). TEM images of the reused traditional gold leaf-prepared Au NPs obtained when **(A)** 1.1 **(B)** 1.2, **(C)** 1.5 and **(D)** 1.8 % (w/v) citrate are studied. The concentration of PVA is kept at 2.0 % (w/v).

cies and lead to broadening of surface plasmon bands [24-26]. Furthermore, at higher pH, some auric species (Au(I) and Au(III)) can adsorb on the surface of the formed gold colloids and this results in the ellipsoidal-shaped Au NPs [26] as depicted in the representative TEM image in Fig. (**2C**). The pH value of 2.0 is, therefore, regarded as the suitable pH of the digested gold leaf solution.

3.2.2. Effect of the Concentrations of Citrate

Results in Fig. **3** (**A** to **D**) indicate that when the citrate concentrations increase, the size of the particles is decreased. Self-aggregation of the nanoparticles tends to be observed at 1.5 and 1.8 % (w/v) (Fig. **3C** and **D**). This effect is promoted due to the compression of the double layers contributed by the high concentration of the counter sodium ion [27, 28]. In this work, the concentration of 1.2 % (w/v) is chosen as the appropriate concentration because the colloidal Au NPs are obtained without any observation of self-aggregation (Fig. **3B**).

3.2.3. Effect of the Concentrations of PVA

Result of the representative TEM image as displayed in Fig. (**4A**) shows that without using any stabilizer, the Au

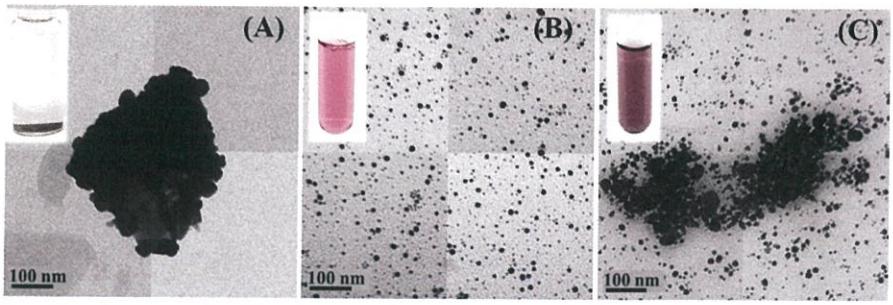

Fig. (4). TEM images of the reused traditional gold leaf-prepared Au NPs obtained when **(A)** 0, **(B)** 2 and **(C)** 8 % (w/v) PVA are investigated. The concentration of citrate is fixed at 1.2 % (w/v). Inset photos are the corresponded solutions at the different PVA concentrations.

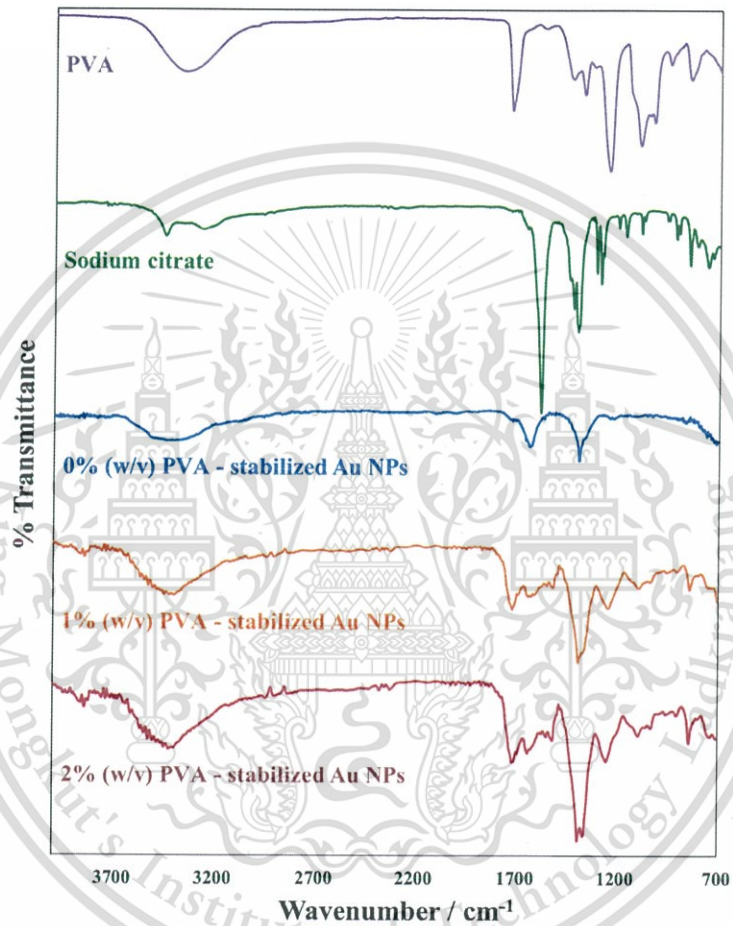

Fig. (5). Transmission FT-IR spectra of the pristine PVA and the corresponding PVA-stabilized gold leaf-prepared Au NPs at different concentrations of PVA.

NPs precipitates are observed, and the solution becomes colorless. It is, therefore, necessary to add the stabilizer for enhancement of the long-term stability of the gold colloids. In this work, PVA which is the non-ionic hydrophilic polymer, is selected for preventing the assembly of the Au NPs as it can inhibit the contact between the individual nanoparticles. Mixing of the Au NPs and PVA was carried out accordingly to the post-modification approach which is simple, and the preformed-Au NPs offer surface, where the exchange of the citrate ions with the polymer is easily attained [29].

At 2 % (w/v) PVA, the spherical-shaped Au NPs are suspended, and this results in the wine-red color solution as shown in Fig. (**4B**). The stabilization mechanism of the Au NPs by PVA is based on the steric effect achieved by the adsorbing polymer onto the surface of particles. However, the nanoparticles tend to be self-aggregated at 8 % (w/v) PVA (Fig. **4C**). It is because when the polymer concentration is greater, it initiates bridging flocculation of the nanoparticles [30, 31]. The concentration of 2 % (w/v) PVA is therefore selected. By this concentration, long-term stability of the as-prepared Au NPs is obtained without precipitation for at least 3 months (Fig. **S1**).

To confirm the modification, the transmission FT-IR spectra of the as-prepared Au NPs were studied. Results in Fig. (**5**) show the following observations: (i) the spectra of the PVA-stabilized Au NPs are similar to that of the pristine

Table 1. Summary of the characteristics of the Au NPs, prepared from reused traditional gold leaf, standard gold foil and standard gold (III) trichloride.

Characteristics	Starting Materials for Preparation of Au NPs		
	Reused Traditional Gold Leaf (99.9 %)	Standard Gold Foil [a, b] (99.9 %)	Standard gold (III) Trichloride [b] (99.9 %)
1 .Morphology (average size/nm)	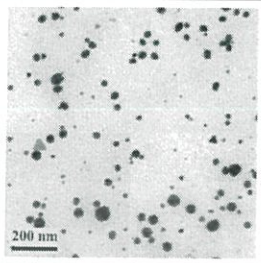	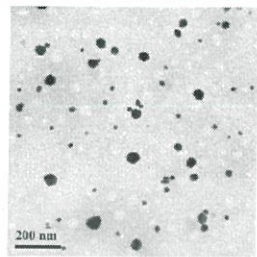	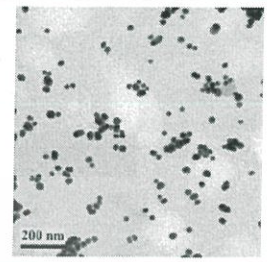
	(24.3 ± 2.3)	(28.3 ± 3.8)	(21.0 ±3.0)
2. Au^0 content (% wt) [c]	94.80	94.82	97.12
3. Cost of the starting materials	Cost-free	351 USD / g	197 USD / g
4. Stability of the starting materials	Stable	Stable	Non-stable (easily moisture absorption)
5. Toxicity of the starting materials	Non-irritant	Non-irritant	Irritant

Note: [a] The standard gold foil was digested under the same conditions for digestion of the reused traditional gold leaf (70 % (v/v) aqua regia and 30 min-digestion time).
[b] Conditions for preparation of the Au NPs from standard gold foil and standard gold (III) trichloride were the same conditions as for preparation of the reused traditional gold leaf-prepared Au NPs.
[c] The percentage of Au^0 content is evaluated by using EDS technique (The representative EDS spectra are demonstrated in Fig. **S2**).

PVA, where the characteristic OH stretching bands emerge at 3200 - 3600 cm^{-1} and (ii) the intensity of this identical band increases when the PVA concentration increases from 1 to 2 % (w/v). This information confirms that the Au NPs are successfully modified with PVA.

3.3. Characteristics of the Reused Traditional Gold Leaf-prepared Au NPs

Under the most appropriate conditions for synthesis, the as-prepared Au NPs offer the spherical shape with an average size of 24.3 (± 2.3) nm as presented in Table **1**. The concentration of these Au NPs is 0.83 nM, which is calculated accordingly to Beer's law using an extinction coefficient of 8.42 x 10^9 M^{-1} cm^{-1} at 530 nm [32]. Characteristics of the reused traditional gold leaf-prepared Au NPs, were also compared to the ones prepared from standard gold foil and standard gold (III) trichloride. It must be noted that (1) standard gold foil was digested by the same conditions for the digestion of the reused traditional gold leaf and (2) the conditions for synthesis of the reused traditional gold leaf-prepared Au NPs were adapted for preparation of the Au NPs from standard gold foil and gold (III) salt. It can be clearly observed from the results in Table **1** that the morphology and purity (% Au^0 content) of the Au NPs, prepared from the different starting materials are comparable. The outstanding benefits of the reused traditional gold leaf-prepared Au NPs are that the synthesis cost is very much cheaper as the raw material is cost-free by donation. In addition, the gold leaf is more stable at ambient temperature, less hygroscopic and less toxic to the user than gold (III) trichloride. The reused traditional gold leaf, therefore, can be exploited as an alternative and effective material for low-cost synthesis of the Au NPs.

3.4. Colorimetric Response of the Reused Traditional Gold Leaf-prepared Au NPs to Creatinine

3.4.1. Proposed Detection Mechanism

In this work, the mechanism of the interaction between the as-prepared Au NPs and creatinine, is proposed as depicted in Fig. (**6A**). Based on the simple Turkevich method, reduction of Au(III) by citrate ions to become the citrate-capped Au NPs was achieved (step 1). By the post-modification, the facile exchange between the weakly bound surface citrate ions and PVA occurred (step 2). This led the colloidal gold to be suspended in the solution without self-aggregation (Fig. **6B**). However, the non-covalent interaction of the Au NPs and PVA was weak because the polymer formed physically was adsorbed by the particles. In the presence of creatinine, the ring nitrogen of hybrid aromatics exhibited much stronger binding affinity to the Au NPs. The cross-linking reaction between creatinine and the Au NPs was therefore easily achieved *via* the coordination interaction between the three nitrogen atoms and the Au NPs (step 3). This promoted aggregation of the nanoparticles (Fig. **6C**) and resulted in decreasing in the absorbance reading at 530 nm while a new surface plasmon peak emerged at 650 nm (Fig. **6D**). Colors of the solutions gradually changed from wine-red to blue when the standard creatinine concentrations increased. The linear response of the as-prepared Au NPs to

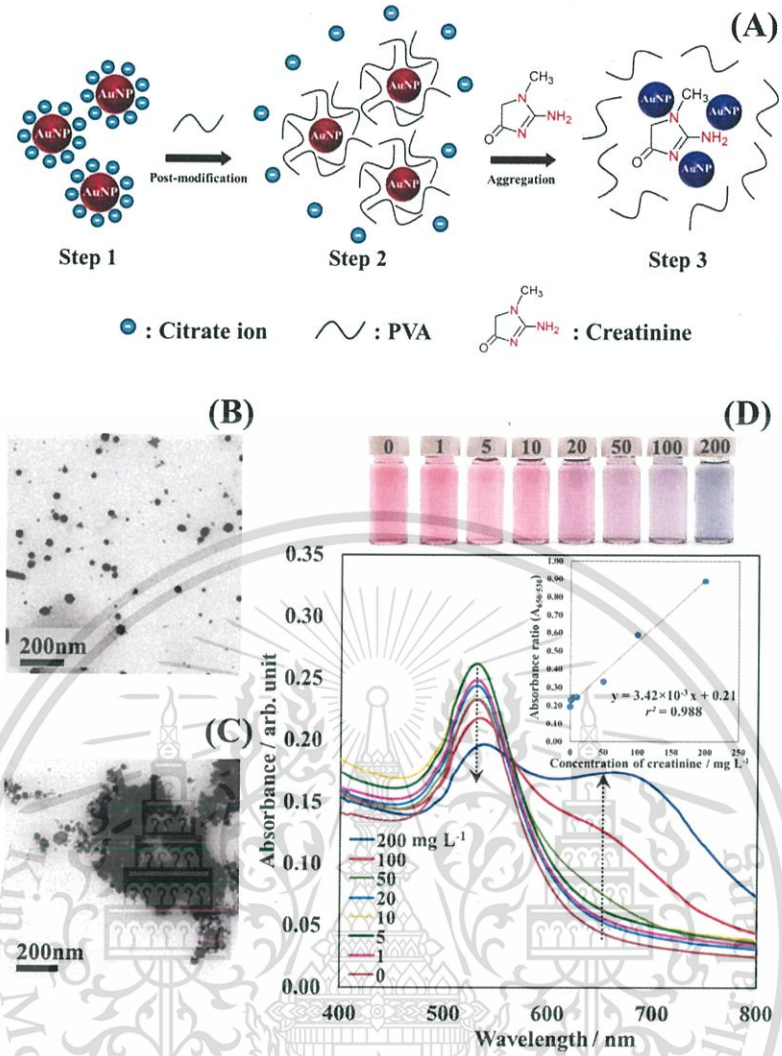

Fig. (6). **(A)** Schematic illustration of the proposed mechanism for colorimetric response of the as-prepared Au NPs to creatinine. **(B)** and **(C)** are the representative TEM images of the as-prepared Au NPs in the absence and in the presence of 200 mg L^{-1} creatinine, respectively. **(D)** surface plasmon bands of the as prepared-Au NPs with various concentrations of standard creatinine. Inset figure of **(D)** is an example of linear calibration plot between the absorbance reading ratio ($A_{650/530}$) and the standard creatinine concentrations (0 to 200 mg L^{-1} creatinine).

the standard creatinine concentration up to 200 mg L^{-1} was also achieved (Inset of Fig. **6D**).

3.4.2. Effect of Reaction Time

Effects of reaction time on the aggregation of the as-prepared Au NPs by creatinine were investigated from 30 s to 10 min. The results in Fig. (**7A**) indicate that higher concentration of creatinine results in faster response time. Furthermore, the absorbance readings ratios ($A_{650}/_{530}$) increase as the reaction times prolong. In terms of linearity of the calibration plot, the reaction time of 3 min provides the better linear response ($r^2 > 0.98$) (Fig. **7B**). This time is therefore selected as the suitable reaction time which is useful for routine analysis of a large number of samples.

3.4.3. Selectivity Study

Results in Fig. (**8A**) obviously show that only creatinine causes the solution color change from wine-red to blue and initiates the highest absorbance reading ratio as presented in Fig. (**8B**). These results indicate that the as-prepared Au NPs are more selective to creatinine than the other small organic compounds and the substances potentially found in urine (albumin, uric acid and ascorbic acid).

3.5. Application to Human Urine: Validation and Recovery Study

To demonstrate the capability of the reused traditional gold leaf-prepared Au NPs for real use, they were applied to human urine for colorimetric determination of creatinine. The samples were spot collected from normal volunteers and were 100-fold diluted with water prior to the analysis. Any further sample pretreatment was negligible. The results determined by the developed method and by validating the HPLC method were compared by means of the Bland-Altman plot [33]. Results in Fig. (**9**) show that all data lay within ±2SD of the mean of their differences, showing that the developed method is equivalent to the HPLC. Results in Table **S1** also confirm that the compared methods are not

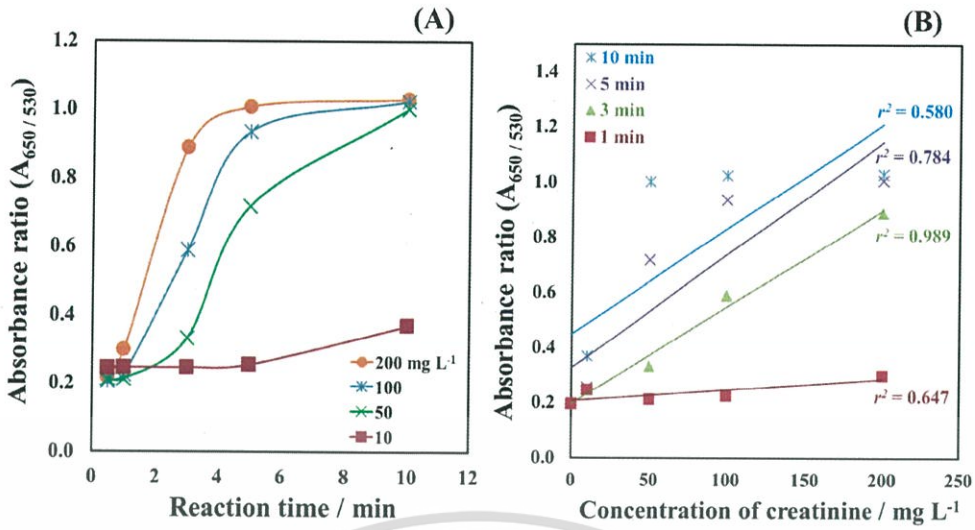

Fig. (7). Effect of the reaction time on the aggregation of the as-prepared Au NPs in the presence of creatinine (10 - 200 mg L^{-1}). **(A)** The plot of the absorbance reading ratio ($A_{650/530}$) against the reaction times. **(B)** Calibration plots of standard creatinine and their corresponded linear correlation coefficients (r^2) obtained by different reaction times.

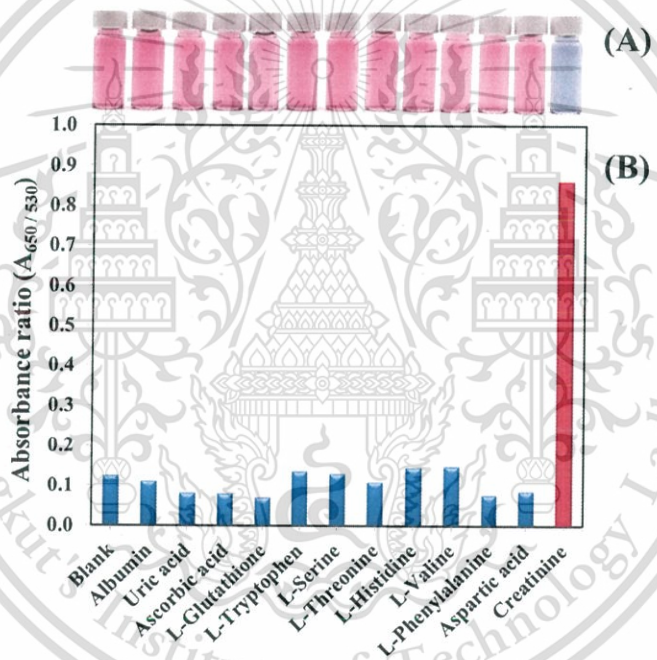

Fig. (8). (A) The photographs of the as-prepared Au NPs in the presence of creatinine (1.8 mmol L^{-1}), the other small compounds and the substances potentially existed in urine (10 mmol L^{-1} for each foreign species) and **(B)** their corresponding absorbance reading ratios ($A_{650/530}$).

significantly different based on the statistical paired *t*-test [34]. This means that the developed method offers high accuracy. The advantage of the developed method is that the analytical procedure is simpler and faster than the HPLC method. Analytical recoveries ranging from 97 - 108 % are obtained (Table **S2**). These results indicate that the developed method is free from sample matrix effect.

3.6. Comparison of the Developed Method with the Other Creatinine Assays

A comparison of the developed method with the other creatinine assays is carried out as shown in Table **2**. The results indicate that the calculated detection limit (3SD of blank/slope [34]) of this method is superior to the colorimetric Jaffe-based method [17], the electrochemical sensor [18] and the separation techniques [19, 20]. This value is sensitive enough to detect the creatinine content in the urine of kidney dysfunction patient as it is much lower than the value of 530 mM which is a sign of having kidney disease [10]. Even though some works [9, 10], based on use of the Au NPs for colorimetric determination of creatinine, provided ultra-high sensitivity, surface modification of the Au NPs by toxic heavy metal (Hg(II)) [9] or by calix[4]arene with several steps of modification [10] is required. Contrary to this work, the Au NPs preparation is simpler, faster and mercury-free. Among the reported Au NPs based-methods as summarized in Table **2**, the analytical procedure of this method is more rapid and easier as serious sample pretreatment is not essential.

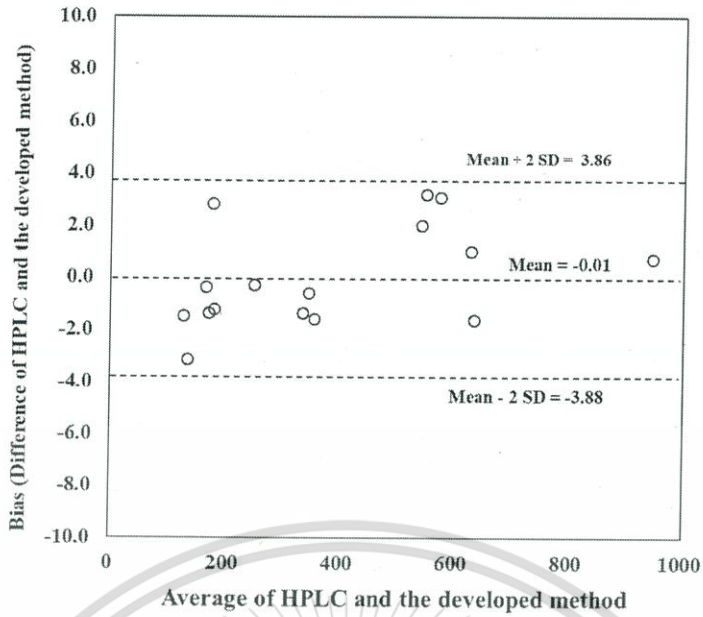

Fig. (9). The Bland-Altman plot [33] for comparison of the data obtained by the developed method with the validating HPLC method.

Table 2. Comparison of the developed method with the other creatinine assays in literatures.

Methods	Starting Material[a]	Sample	Detection limit (μM)	Sample Pretreatment	Analysis Time (min)[b]	Ref.
1. Colorimetric Jaffé-based method	-	Urine	26.5	Dilution with water	3	[17]
2. Electrochemical sensor	-	Serum	40	-	< 5	[18]
3. Cation-exchange HPLC	-	Serum	10	Centrifugation (10 min)	3.2	[19]
4. Capillary zone electrophoresis	-	Urine	50	Dilution with water	1	[20]
5. Resonance light scattering Au NPs-based method (Glutathione-protected Au NPs)	$AuCl_3$[c]	Serum	1.21	Dilution with Britton-Robin buffer	25	[7]
6. Colorimetric Au NPs-based methods						
6.1 Uric acid and Hg(II)-modified Au NPs	$AuCl_3$[c]	Urine/ Serum	1.60×10^{-3}	Dilution with water	5	[9]
6.2 Calix[4]arene thiol-functionalized Au NPs	$AuCl_3$[c]	Urine	2.16×10^{-3}	Centrifugation (5 min) and solvent extraction	4	[10]
6.3 Citrate-stabilized Au NPs	$AuCl_3$[c]	Urine	80	Dilution with Britton-Robin buffer	24	[6]
6.4 Citrate-stabilized Au NPs	$AuCl_3$[c]	Urine	121	Solid phase extraction	10	[8]
6.5 PVA-stabilized Au NPs	Reused traditional gold leaf	Urine	1.41	Dilution with water	3	This work

Note: [a] Starting material for the preparation of the Au NPs.
[b] Not including the interval time for sample pretreatment procedure.
[c] Standard gold (III) trichloride as the chemical formula of $AuCl_3 \cdot 3H_2O$

The reproducibility of this method was studied by a series of ten repetitive measurements of 10 and 200 mg L^{-1} creatinine, corresponding to the relative standard deviation (RSD) of 4.3 and 3.1 %, respectively. One outstanding merit of this method is that the synthesis cost of the Au NPs is much cheaper as the reduced traditional gold leaf is free of charge.

CONCLUSION

Facile and cost-effective synthesis of the Au NPs, using the reused traditional gold leaf as the starting material, is achieved. The characteristics of the as-prepared Au NPs are the same as the Au NPs which are prepared from standard

gold (III) trichloride and standard gold foil. Benefits of exploiting the reused gold leaf are low cost for the Au NPs synthesis, and it is also more stable at the ambient temperature and less toxic than standard gold (III) trichloride. Therefore, the reused traditional gold leaf is an alternative and effective material for the preparation of the gold colloids

The as-prepared Au NPs are successfully applied for colorimetric sensing of creatinine with high sensitivity and selectivity. This is the first report on an achievement of using the gold nanoparticles (Au NPs), prepared from the reused traditional gold leaf, for colorimetric sensing of creatinine in human urine. The developed method provides high accuracy and high precision with simple and rapid analysis (3 min samples^{-1}).

ETHICS APPROVAL AND CONSENT TO PARTICIPATE

Not applicable.

HUMAN AND ANIMAL RIGHTS

The authors would like to thank the National Doping Control Centre, Mahidol University, Bangkok, Thailand, for providing human urine samples.

CONSENT FOR PUBLICATION

Not applicable.

CONFLICT OF INTEREST

The authors declare no conflict of interest, financial or otherwise.

ACKNOWLEDGEMENTS

This work was financially supported by the research grant from Faculty of Science, King Mongkut's Institute of Technology Ladkrabang (KMITL) (Grant no. 2561-01-05-72). The authors would like to thank D. Payungtung, P. Yosbantueng, P. Praiwan (KMITL) and F. Kai (Harbin Institute of Technology, China) for their contributions on doing some preliminary experiments. The authors would also like to thank Wat Sothonwararam, Chachoengchansao Province, Thailand, for donation of the reused traditional gold leaf.

SUPPLEMENTARY MATERIAL

Supplementary material is available on the publisher's website along with the published article.

REFERENCES

[1] Ng, S.M.; Koneswaran, M.; Narayanaswamy, R. A review on fluorescent inorganic nanoparticles for optical sensing applications. *RSC Adv.*, **2016**, *6*, 21624-21661.

[2] Zhang, F.X.; Han, L.; Israel, L.B.; Daras, J.G.; Maye, M.M.; Ly, N.K.; Zhong, C.J. Colorimetric detection of thiol-containing amino acids using gold nanoparticles. *Analyst*, **2002**, *127*, 462-465.

[3] Wei, X.; Qi, L.; Tan, J.; Liu, R.; Wang, F. A colorimetric sensor for determination of cysteine by carboxymethyl cellulose-functionalized gold nanoparticles. *Anal. Chim. Acta*, **2010**, *671*, 80-84.

[4] Li, L.; Li, B. Sensitive and selective detection of cysteine using gold nanoparticles as colorimetric probes. *Analyst*, **2009**, *134*, 1361-1365.

[5] Apyari, V.V.; Arkhipova, V.V.; Dmitrienko, S.G.; Zolotov, Y.A. Using gold nanoparticles in spectrophotometry. *J. Anal. Chem.*, **2014**, *69*, 1-11.

[6] He, Y.; Zhang, X.; Yu, H. Gold nanoparticles-based colorimetric and visual creatinine assay. *Microchim. Acta*, **2015**, *182*, 2037-2043.

[7] Huang, X.P.; Li, Y.J.; Pan, J.H.; Lu, F.S.; Chen, Y.W.; Gao, W.H. Glutathione-protected hierarchical colorimetric response of gold nanoparticles: a simple assay for creatinine rapid detection by resonance light scattering technique. *Plasmonics*, **2015**, *10*, 1107-1114.

[8] Sittiwong, J.; Unob, F. Detection of urinary creatinine using gold nanoparticles after solid phase extraction. *Spectrochim. Acta, Part A*, **2015**, *138*, 381-386.

[9] Du, J.; Zu, V.; Leow, W.R.; Chen, S.; Sum, T.C.; Peng, X.; Cheng, X. Colorimetric detection of creatinine based on plasmonic nanoparticles *via* synergistic coordination chemistry. *Small*, **2015**, *11*, 4104-4110.

[10] Sutariya, P.G.; Pandya, A.; Lodha, A.; Menon, S.K. A simple and rapid creatinine sensing *via* DLS selectivity, using calix[4]arene thiol functionalized gold nanoparticles. *Talanta*, **2016**, *147*, 590-597.

[11] Rasouli, Z.; Ghavami, R. Colorimetric sensing of iodide by the competitive interactions in the surface of gold nanoparticles with the simultaneous aggregation/anti-aggregation mechanisms in edible salts. *Curr. Anal. Chem.*, **2018**, *14*, 1-9.

[12] Ballerini, D.R.; Ngo, Y.H.; Jarujamrus, P.; Garnier, G.; Ladewig, B.P.; Shen, W. Gold nanoparticle-functionalized thread as a substrate for SERS study of analytes both bound and unbound to gold. *AIChE.*, **2014**, *60*, 1598-1605.

[13] Turkevich, J.; Stevenson, P.C.; Hillier, J. A study of the nucleation and growth processes in the synthesis of colloidal gold. *Discussions of the Faraday Society*, **1951**, *11*, 55-75.

[14] Wender, H.; Andreazza, M.L.; Correia, R.R.B.; Teixeira, S.R.; Dupont, J. Synthesis of gold nanoparticles by laser ablation of an Au foil inside and outside ionic liquids. *Nanoscale*, **2011**, *3*, 1240-1245.

[15] Jaffe, M. Ueber den Niederschlag, welchen Pikrinsäure in normalem Harn erzeugt und über eine neue Reaction des Kreatinins. *Z. Phys. Chem.*, **1886**, *10*, 391-400.

[16] Vasiliades, J.; Andreazza, M.L.; Correia, R.R.B.; Teixeira, S.R.; Dupont, J. Reaction of alkaline sodium picrate with creatinine: I. Kinetics and mechanism of formation of the mono-creatinine picric acid complex. *Clin. Chem.*, **1976**, *22*, 1664-1671.

[17] Falcó, P.C.; Genaro, L.A.T.; Lloret, S.M.; Gomez, F.B.; Cabeza, A.S.; Légua, C.M. Creatinine determination in urine samples by batchwise kinetic procedure and flow injection analysis using the Jaffe reaction: chemometric study. *Talanta*, **2001**, *55*, 1079-1089.

[18] Wei, F.; Cheng, S.; Korin, Y.; Reed, E.; Gjertson, D.; Ho, C.; Gritsch, H.; Veale, J. Serum creatinine detection by a conducting-polymer-based electrochemical sensor to identify allograft dysfunction. *Anal. Chem.*, **2012**, *84*, 7933-7937.

[19] Ambrose, R.T.; Ketchum, D.F.; Smith, J.W. Creatinine determined by "high-performance" liquid chromatography. *Clin. Chem.*, **1983**, *29*, 256-259.

[20] Liotta, E.; Gottardo, R.; Bonizzato, L.; Pascali, J.P.; Bertaso, A.; Tagliaro, F. Rapid and direct determination of creatinine in urine using capillary zone electrophoresis. *Clin. Chim. Acta*, **2009**, *409*, 52-55.

[21] Elomaa, H.; Seisko, S.; Junnila, T.; Sirviö, T.; Wilson, P.B.; Aromaa, J.; Lundström, M. The Effect of the Redox Potential of Aqua Regia and Temperature on the Au, Cu, and Fe Dissolution from WPCBs. *Recycling*, **2017**, *2*, 1-9.

[22] Pupanthong, P. *Gold Refining with Aqua regia and Sulfite Compound*, 2nd ed.; Department of primary industries and mines: Bangkok, Thailand, **2011** (written in Thai).

[23] Pimpang, P.; Choopun, S. Monodispersity and Stability of Gold Nanoparticles Stabilized by Using Polyvinyl Alcohol. *Chiang Mai J. Sci.*, **2011**, *38*, 31-38.

[24] Ojea-Jiménez, I.; Campanera, J.M. Molecular Modeling of the Reduction Mechanism in the Citrate-Mediated Synthesis of Gold Nanoparticles. J. *Phys. Chem. C*, **2012**, *116*, 23682-23691.

[25] Schulz, F.; Homolka, T.; Bastús, N.G.; Puntes, V.; Weller, H.; Vossmeyer, T. Little adjustments significantly improve the Tur-

kevich synthesis of gold nanoparticles. *Langmuir*, **2014**, *30*, 10779-10784.

[26] Polyakov, A.Y.; Lebedev, V.A.; Shirshin, E.A.; Rumyantsev, A.M.; Volikov, A.B.; Zherebker, A.; Garshev, A.V.; Goodilin, E.A.; Perminova, I.V., Non-classical growth of water-redispersible spheroidal gold nanoparticles assisted by leonardite humate. *Cryst. Eng. Comm.*, **2017**, *19*, 876-886.

[27] Kimling, J.; Maier, M.; Okenve, B.; Kotaidis, V.; Ballot, H.; Plech, A. Turkevich Method for Gold Nanoparticle Synthesis Revisited. *J. Phys. Chem. B*, **2006**, *110*, 15700-15707.

[28] Kumar, S.; Gandhi, K.S.; Kumar, R. Modeling of Formation of Gold Nanoparticles by Citrate Method. *Ind. Eng. Chem. Res.*, **2007**, *46*, 3128-3136.

[29] Shan, J.; Tenhu, H. Recent advances in polymer protected gold nanoparticles: synthesis, properties and applications. *Chem. Commun.*, **2007**, 4580-4598.

[30] Baygazieva, E.K.; Yesmurzayeva, N.N.; Tatykhanova, G.S.; Mun, G.A.; Khutoryanskiy, V.V.; Kudaibergenov, S.E. Polymer Protected Gold Nanoparticles: Synthesis, Characterization and Application in Catalysis. *International Journal of Biology and Chemistry*, **2014**, *7*, 14-23.

[31] Thorat, A.A.; Dalvi, S.V. Liquid antisolvent precipitation and stabilization of nanoparticles of poorly water-soluble drugs in aqueous suspensions: Recent developments and future perspective. *Chem. Eng. J.*, **2012**, *182*, 1-34.

[32] Rahman, S. Size and Concentration Analysis of Gold Nanoparticles with Ultraviolet-Visible Spectroscopy. *UJMM: One + Two*, **2016**, 7.

[33] Glantz, S.A. *Primer of biostatistics*, 5th ed.; McGraw-Hill: USA, **2002**.

[34] Miller, J.; Miller, J.C. *Statistics and Chemometrics for Analytical Chemistry*, 6th ed.; Pearson Education Limited: Harlow, England, **2010**.

Appendix A2

Proceedings

PACCON 2017
Pure and Applied Chemistry International Conference

Method development for *'point-of-care'* analysis of uric acid in urine using an *'in-house'* LED spectrometer

Arjnarong Mathaweesansurn[1,2*], Natthaphon Surapanworawate[1,2], Treerat Troangjaroensub[1,2], Napasporn Chatapattama[1,2], Noppadol Maneerat[3] and Nathawut Choengchan[1,2*]

[1]*Flow Innovation-Research for Science and Technology Laboratories (FIRST Labs),*
[2]*Applied Analytical Chemistry Research Unit, Department of Chemistry, Faculty of Science, King Mongkut's Institute of Technology Ladkrabang, Bangkok 10520 Thailand*
[3]*Department of Control Engineering, Faculty of Engineering, King Mongkut's Institute of Technology Ladkrabang, Bangkok 10520 Thailand*

*e-mail: a.mathawee@live.com and nchoengchan@gmail.com

Abstract: In this work, the method for *'point-of-care'* analysis of uric acid in urine using the *'in-house'* light emitting diode (LED) spectrometer was presented. Detection chemistry was based on the colorimetric reaction between uric acid and phosphotungstic acid in the presence of sodium carbonate. Blue-colored product was developed and its corresponded absorbance was monitored by the LED spectrometer. Analytical performances of the method using the LED spectrometer were investigated. Working range from 4.46 to 62.44 mg dL^{-1} was observed with good linearity ($R^2 > 0.99$). The method also provided good precision (RSD: 2.9 to 5.7 %) and accuracy (Analytical recovery: 88 to 95 %). The limit of detection (y_B+3S_B) and the limit of quantitation (y_B+10S_B) were found at 2.33 and 7.38 mg dL^{-1}, respectively. The method was applied to spiked urine samples collected from normal volunteers. The results obtained by the LED spectrometer and by the UV-Vis spectrophotometer were not significant difference by paired *t*-test at 95 % confidence ($t_{stat.} = 1.44$, $t_{cri.} = 2.26$). These results implied that the method based on using LED spectrometer suitable and high precision for the quantitative *'point-of-care'* analysis of uric acid in urine sample.

1. Introduction

Gout is a kind of arthritis, results from the deposition of monosodium urate crystals in a joint space. Clinical manifestations of the disease include acute attacks of severe pain and inflammation affecting peripheral joints.[1,2]

Uric acid is a key marker for clinical diagnosis of gout. It is the end product of the degradation of purines and excreted in the urine. Determination of uric acid in body fluids (e.g: serum and urine) is a clinically valuable diagnostic indicator. Normally, uric acid is excreted in urine in 150 to 200 mg dL^{-1}.[4] The presence of elevated levels in urine is a sign of gout.[3] Therefore, the quantitative measurement of uric acid in urine is very important.

Conventional method for determination of uric acid is based on using an enzyme assay with spectrophotometric detection. K. Lorentz and W. Berndt presented an enzymic method for determination of uric acid. Detection was based on quantitative development of hydrogen peroxide by uricase and following oxidation of a chromogenic O_2 acceptor by peroxidase. An absorbance of product could be measured between 510 and 550 nm.[5] Although the conventional method provides high accuracy and selectivity, cost of analysis is quite expensive because enzyme

reagents and spectrophotometer are exploited.

Non-enzymatic method based on reduction of phosphotungstic acid by uric acid to tungsten blue, followed by spectrophotometric detection was also reported.[6] However, this method is not suitable for point-of-care testing due to use of bulky device. This can limit the uric acid testing to only in laboratory setting.

Therefore the aim of this work was to develop the point-of-care method for quantitative analysis of uric acid in urine using the 'in-house' and 'portable' LED spectrometer. The reaction between uric acid and phosphotungstic acid in the presence of sodium carbonate was chosen as detection principle because of its simplicity. Validation and application of the method to human urine were also investigated.

2. Materials and Methods

2.1 Standard and reagents preparation

All chemicals were analytical reagent grade and deionized – distilled water was used throughout this work. Standard stock solution of 100 mg dL^{-1} uric acid (Sigma Aldrich, USA) was prepared by dissolving 0.1xxx g of uric acid powder in water. Into this solution, 3.0 mL of 1.0 mol L^{-1} sodium hydroxide was added. The solution was then made up with water to 100.00 mL. Working standards were appropriated diluted from this stock solution to provide final concentration range of 4.75 – 62.44 mg dL^{-1}. Phosphotungstic acid solution (40 % (w/v)) was prepared by dissolving 4.0 g of phosphotungstic acid (lobachemic, India) in 10.00 mL of water. Sodium carbonate solution (2 % (w/v)) was prepared by dissolving 0.5 g of sodium carbonate (Quality Reagent Chemical Produc, Malaysia) in 25.00 mL of water.

2.2 Sample preparation

Human urine samples were spot collected from normal volunteers. All samples were diluted with water (10-fold) prior to use. Any further pretreatment was not necessary.

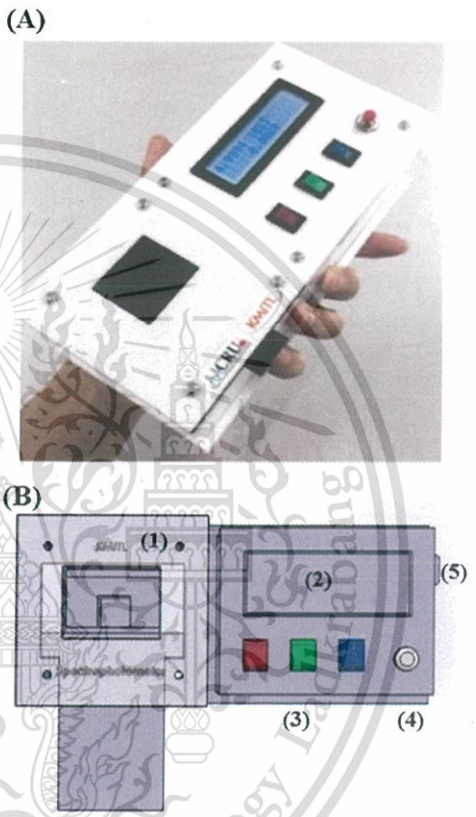

Figure 1. **(A)** Photograph of the LED spectrometer. **(B)** Components of the LED spectrometer which is consisted of (1) sample holder, (2) LCD display, (3) Buttons for Red-Green-Blue LED lamp, (4) Button for auto zero, (5) Switch on / off.

2.3 Design of the 'in-house' and 'portable' LED spectrometer

The photographs of the device and its compartment were illustrated in Figure 1. Hardware of the device was consisted of Red-Green-Blue LED bulbs (as light source), a micro-controller (for evaluation of the absorbance based on Beer's law) and photo transistor (as light detector). The

absorbance was displayed on an LCD screen. Dimension of the LED spectrometer is 9 x 20 x 8 cm^3 (width x length x height).

2.4 Procedure for determination of uric acid

Aliquot of 5.0 mL of the standard solution or sample was transferred to a test tube. 3.0 mL of 2 % (w/v) sodium carbonate solution and 3.0 mL of 40 % (w/v) phosphotungstic acid solution were then added. The absorbance readings were recorded at 1 min after adding the phosphotungstic acid solution via Jasco V-630 UV-visible spectrophotometer (USA) or the LED spectrometer.

3. Results & Discussion

3.1 Study on detection principle by UV-visible spectrophotometer

The detection reaction for uric acid is presented as the following simple equation.[7]

uric acid + phosphotungstate + O_2 + H_2O

$\xrightarrow{OH^-}$ allantoin + CO_2 + tungsten blue..(1)

Uric acid reacts with phosphotungstic acid in alkaline medium to form a blue-colored complex. The alkaline medium is provided by sodium carbonate. The absorption spectra of the blue-colored solution (Figure 2A) were monitored. Results were illustrated in Figure 2B. The intensity of the color is directly proportional to amount of uric acid. Maximum absorption wavelength was located at 740 nm. For LED spectrometer, Red LED bulb was chosen as a light source for monitoring of the absorption of the product.

3.2 Optimization study using LED spectrometer

Optimization study was carried out using univariate method. Summary on the optimization study was concluded in table 1.

3.2.1 Effect of phosphotungstic acid concentration

Effect of the phosphotungstic acid concentration was studied from 20 to 80 % (w/v). Results in Figure 3 demonstrated that the highest sensitivity was obtained when the concentration of 40% (w/v) was used. We observed precipitation of the solution at higher concentration (60% and 80% (w/v)) therefore at 40% (w/v) was selected as optimal concentration.

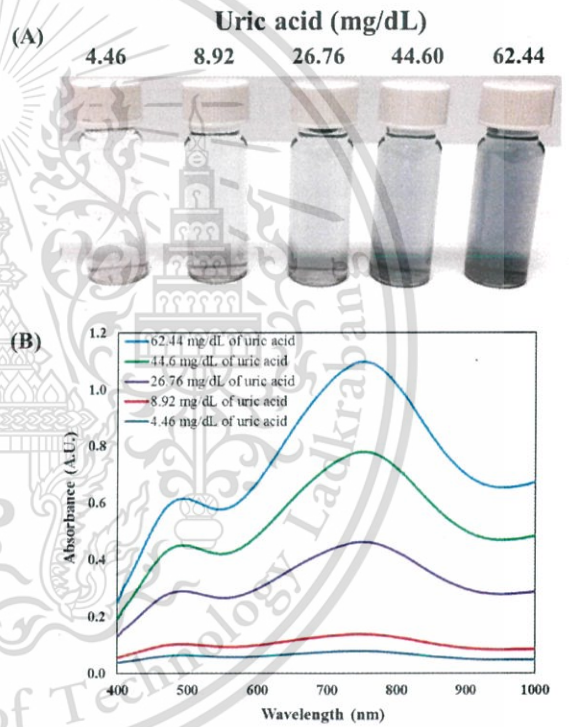

Figure 2. (A) Images and (B) absorption spectra of the tungsten blue complex, at various concentrations of uric acid ranging from 4.46 to 62.44 mg dL^{-1}.

3.2.2 Effect of sodium carbonate concentration

Effect of the concentration of sodium carbonate was studied from 2 to 14 % (w/v). Results are shown in Figure 4. When the concentration of sodium carbonate was increased, sensitivities were decreased due

to itself precipitation.[8] The concentration of 2 % (w/v) was selected as appropriate concentration.

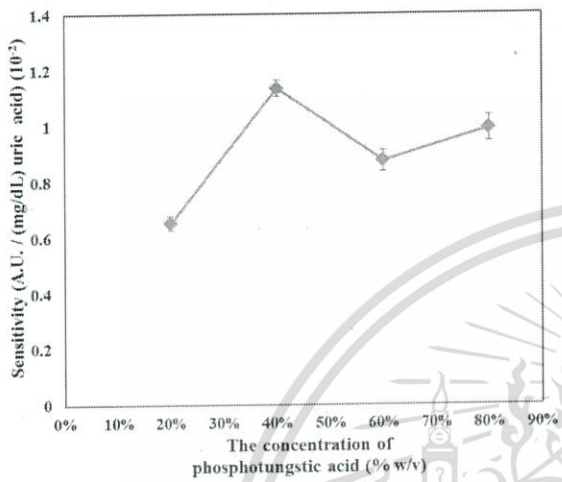

Figure 3. Effect of the phosphotungstic acid concentration on sensitivity.

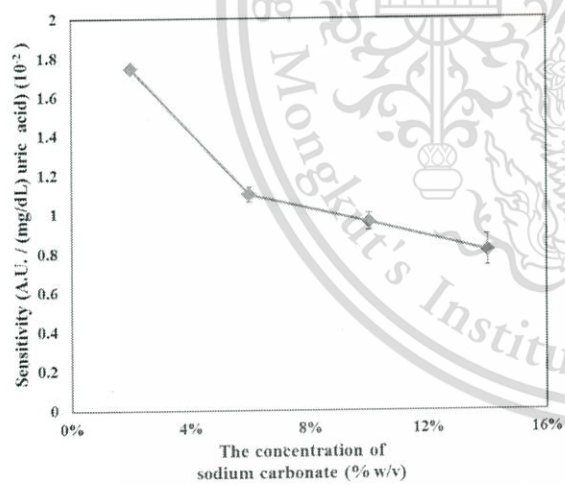

Figure 4. Effect of the sodium carbonate concentration on sensitivity

3.2.3 Appropriate time for measurement

The kinetic reaction of this method was studied by monitoring the absorbance vs time. The highest absorbance value when a standard of 62.44 mg dL^{-1} uric acid was studied at 1 min. Therefore, the absorbance values were recorded at 1 min in each experiment.

Table 1. Summary on optimization of the method for determination of uric acid.

Parameter	Optimal value
Phosphotungstic acid (% w/v)	40
Sodium carbonate (% w/v)	25
Appropriate time for measurement (min)	1

3.3 Analytical performances

The analytical performances were also examined and the results were concluded in Table 2. The linearity range of 4.46 to 62.44 mg dL^{-1} was achieved with good linearity. The method gave high precision and high accuracy. This limit allowed the method for clinical diagnosis.

Performance of the LED spectrometer of uric acid in urine was compared to the performance of UV-visible spectrophotometer. Results in Figure 6 indicate that the sensitivity of LED spectrometer was lower than UV-vis. spectrophotometer around 27%.

However, our method with the LED spectrometer are still applicable for quantitative measurement of uric acid in human urine since the method provides limit of detection (LOD) of 2.36 mg dL^{-1} which is lower than the indicating concentration of uric acid normally found in gout patient.

Table 2. Analytical performances of the method for determination of uric acid.

Performances	Value
Linearity range (mg dL^{-1})	4.46 – 62.44
Regression coefficients (r^2)	0.9975
RSD (%) (n = 6)	2.9 – 5.7
Recovery (%)	88.3 - 95.0
LOD[a] (mg dL^{-1})	2.36
LOQ[b] (mg dL^{-1})	7.91

[a]$LOD = y_B + 3S_B$
[b]$LOQ = y_B + 10S_B$

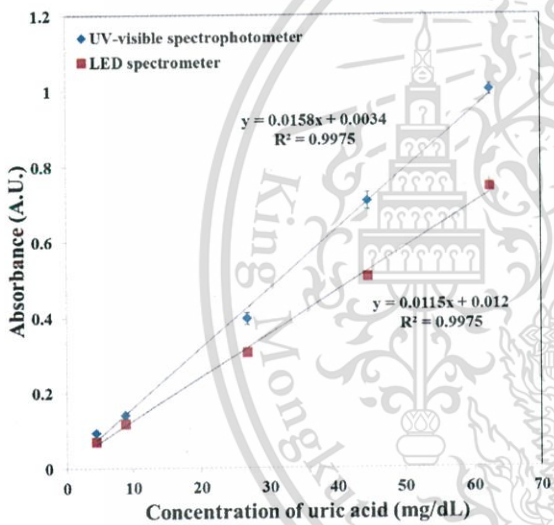

Figure 6. The linear plots between the uric acid concentration and the absorbance readings obtained by LED spectrometer and UV-visible Spectrophotometer.

3.4 Effect of interference

The effect of interference on determination of uric acid was studied. The experiments were carried out by mixing of various compounds with phosphotungstic acid in alkaline medium. Results are shown in Figure 7. Glucose, creatinine, cysteine and oxalic acid did not react with phosphotungstic acid, even when their concentrations were extravagantly high.[9,10] This means that the chromogenic reagent is selective to uric acid.

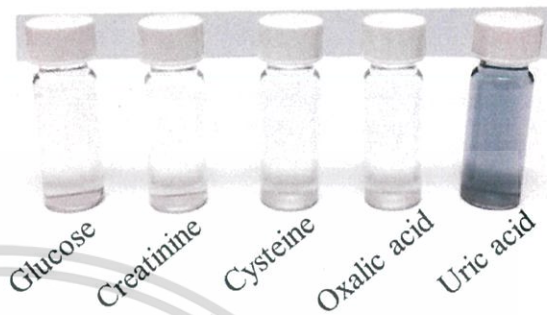

Figure 7. Images of the product solutions from various interferences (The concentration of glucose is 22.0 mM, creatinine is 0.40 mM, cysteine is 0.25 mM and oxalic acid is 0.3 mM).

3.5 Application to urine samples

The developed method was applied to determine the uric acid content in urine of normal volunteers. Results in Table 3 were not significantly difference from the results obtained by UV-visible Spectrophotometer, at 95 % confidence level (t_{stat} = 1.44, t_{crit} = 2.26). There results implied that the method was successfully validated.

Table 3. Concentrations of uric acid in urine samples.

Sample	Concentration (mg L^{-1}, mean ± SD)	
	LED spectro.	UV-vis.spectro
1	4.0 (± 0.3)	3.5 (± 0.8)
2	6.1 (± 0.3)	4.8 (± 0.2)
3	6.4 (± 0.5)	6.4 (± 0.4)
4	6.6 (± 0.3)	5.6 (± 0.7)
5	8.2 (± 0.2)	9.8 (± 1.2)
6	9.3 (± 0.5)	8.9 (± 0.4)
7	13.0 (± 0.1)	11.2 (± 1.1)
8	14.0 (± 0.0)	15.9 (± 1.2)
9	15.3 (± 0.4)	12.6 (± 0.3)
10	16.1 (± 0.4)	13.0 (± 0.3)

4. Conclusion

In this work, the method for quantitative analysis of uric acid in urine using the LED spectrometer was successfully developed. This method provided high accuracy and high precision. Since the fabricated LED spectrometer is portable, the developed method showed high efficiency to be employed as an analyzer for 'point-of-care' of gout testing.

Acknowledgements

Applied Analytical Chemistry Research Unit and Department of Chemistry, Faculty of Science, King Mongkut's Institute of Technology Ladkrabang are grateful acknowledged for equipments and financial supports.

References

1. Hainer, B.L.; Matheson, E.; Wilkes R.T. *American Family Physician* **2014**, *90*, 831-836.
2. Akyilmaz, E.; Sezgintürk, M.K.; Dinçkaya E. *Talanta* **2003**, *61*, 73-79.
3. Chauhan, N.; Pundir, C.S. *Analytical Biochemistry* **2011**, *413*, 97–103.
4. http://emedicine.medscape.com/article/244255-workup
5. Lorentz, K.; Berndt, W. *Analytical Biochemistry* **1967**, *451*, 58–63.
6. Martinek, R.K. *American Journal of Clinical Pathology* **1965**, *18*, 777–779.
7. Shen, Y.S.; Hsieh, C.L.; Wu, K.L. Non-enzymatic disposable uric acid detecting electrode strip, method for producing the same and its use. US 6258230 B1, July 10, 2001.
8. Henry, R.J.; Sobel, C.; Kim, J. *American Journal of Clinical Pathology* **1957**, *28*, 152–160.
9. Diogo, L.; Fábio, R.P.R. *Microchemical Journal* **2010**, *94*, 53–59.
10. Breebaart, K.; Haan, A.M.F.H. *Zeitschrift für klinische Chemie und klinische Biochemie* **1972**, *10*, 17–20.

PACCON
PURE AND APPLIED CHEMISTRY INTERNATIONAL CONFERENCE 2018

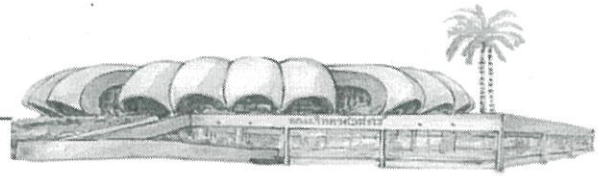

Label-free gold nanoparticles for spectrophotometric determination of creatinine in urine

Arjnarong Mathaweesansurn[1,2]*, Kanisa Tipanantakun[2], Parinya Thaothong[2], Pimmada Ooybumrung[2], Nathawut Choengchan[1,2]*

[1]*Flow Innovation-Research for Science and Technology Laboratories (FIRST Labs),*
[2]*Applied Analytical Chemistry Research Unit, Department of Chemistry, Faculty of Science, King Mongkut's Institute of Technology Ladkrabang, Bangkok 10520, Thailand*
**E-mail: a.mathawee@live.com, nchoengchan@gmail.com*

Abstract:

A simple method for quantitative analysis of creatinine in urine using label-free gold nanoparticles (AuNPs) is presented. In the presence of creatinine, the AuNPs are aggregated and this effect results in a color change from wine-red to purple. The surface plasmon resonance peak is shifted from 522 to 650 nm. Calibration curve between absorbance ratio and standard creatinine concentration was made with linearity of 0 to 200 mg L^{-1} ($Abs_{650/522}$ = 0.004[Creatinine] + 0.103, r^2 = 0.995) was obtained. Other analytical characteristics are listed as the followings: RSD ≤ 5 %, LOD (3SD of blank/slope) = 0.5 mg L^{-1} and LOQ (10SD of blank/slope) = 1.6 mg L^{-1}. The method was successfully applied to determination of creatinine in spiked urine without any complex pretreatment, only simple dilution with water was performed. The results obtained by this method and by Jaffé reaction method were not significant difference when paired *t*-test at 95 % confidence (t_{stat} = -0.13 and t_{cri} = 2.26) was used. All the results implied that the method gave high accuracy and high precision for the quantitative analysis of creatinine in urine sample.

1. Introduction

Creatinine is a metabolite formed from creatine and phosphocreatine and it is excreted in urine by the kidney at a relatively constant rate. The creatinine concentration in urine is an important parameter for kidney diagnosis. The normal range of creatinine concentration in urine are 3.6 to 27 mmol L^{-1} and 3.3 to 22.5 mmol L^{-1} for men and women, respectively.[1] Therefore, creatinine level in urine is an important marker for renal disease.

The traditional method for creatinine determination is the colorimetric Jaffé reaction.[2,3] The method is fast and easy. However, this method is non-specific. The other reported methods are enzymatic method,[4,5] capillary electrophoresis (CE),[6] high performance liquid chromatography (HPLC)[7,8] and amperometric biosensor.[9] Although these methods are high specificity, they are complicated and expensive.

Nowadays, due to the unique optical properties (surface plasmon resonance, SPR), gold nanoparticles (AuNPs) have been widely exploited as colorimetric sensors.[10] Several studies have been reported on the synthesis of AuNPs and their applications in colorimetric detection various of biological molecules. J. Sittiwong *et al.* proposed a utilization of AuNPs as sensor for determination of creatinine in urine after an extraction of sample using sulfonic acid functionalized silica gel.[11]

The aim of this work is to develop a simple method for determination of creatinine in urine using label-free AuNPs as chemical sensor without any serious sample pretreatment. Detection principle is based on the aggregation of the AuNPs in the presence of creatinine. This results in a color change from wine-red to purple and surface plasmon peak shift from 522 to 650 nm. Validation and application of the method to human urine were also investigated.

2. Materials and Methods

2.1 Chemicals

All standard and reagents used were of analytical reagent grade. Deionized-distilled water purified by ZENEER UP 900 (18 MΩ/cm, human corporation, Korea) was used throughout. Tetrachloroauric(III) acid, sodium citrate tribasic dihydrate and creatinine were purchased from Sigma-Aldrich, USA. Sodium dihydrogen ortho phosphate (Analytical UNIVAR reagent, New Zealand) and Disodium hydrogen phosphate heptahydrate (Panreac, E.U.) were used to prepare phosphate buffer (pH 6.0).

2.2 Synthesis of AuNPs

The AuNPs was synthesized accordingly to Turkevich's method.[12] Briefly, the 100.0 mL of 1.0 mM Tetrachloroauric(III) acid ($HAuCl_4$) solution was heated. At the boiling point, 7.0 mL of 38.8 mM sodium citrate was added to this solution. The mixture was heated under vigorous stirring for 15 min. Finally, the solution was cooled down to room temperature and stored at 4°C for further utilization.

2.3 Standard and sample preparation

A creatinine stock standard solution of 1000 mg L^{-1} was prepared by dissolving 0.0500 g of creatinine powder in 50.0 mL of DI water. Working standards were appropriated diluted from stock solution to provide final concentration range of 1.0 to 200.0 mg L^{-1}. Human urine samples were spot collected from normal volunteers. All samples were diluted with water (100-fold) prior to analysis. Any further pretreatment was not necessary.

2.4 Procedure for determination of creatinine

Aliquot of 1.0 mL of AuNPs was transferred to a test tube. 5.0 mL of 10.0 mmol L^{-1} phosphate buffer (pH 6.0) and 0.05 mL of standard creatinine or urine sample were then added. The solution was mixed through a Gennie Z Vortex mixer (Scientific Industries, USA) and was kept standing for incubation (3 min). The surface plasmon band were monitored by scanning wavelength from 400 to 800 nm via Jasco V-630 UV–visible spectrophotometer (USA).

3. Results and Discussion

3.1 Detection principle

The detection reaction between AuNPs and creatinine is presented in Figure 1A. Firstly, the AuNPs is capped with citrate ion because the as-prepared particles are synthesized accordingly to the Turkevich's method, where sodium citrate is used for reduction of Au(III) to Au^0 nanoparticles. The citrate ions are regarded as the stabilizer for preventing the AuNPs from self-aggregation (Figure 1B). However, the interaction between the AuNPs and citrate ions is week. In the presence of creatinine, facile exchange between creatinine and citrate ion is easily occurred. Creatinine can strongly bind with the AuNPs and this result in aggregation of the AuNPs and the solution color change from wine-red to blue (Figure 1C).

Figure 2 shows the surface plasmon band of the synthesized AuNPs with top peak at 522 nm and after addition of creatinine the peak at 522 nm decrease and a new surface plasmon band emerged at around 650nm.

3.2 Appropriate time for measurement

The effect of the mixing time between AuNPs and creatinine was varied from 1 to 10 min (Figure 3). In the presence of 50 mg L^{-1} creatinine, the absorption peak at 650 nm of AuNPs gradually increased with increasing reaction time. A good linearity of the calibration curve was obtained when 3 min was used, this time was therefore selected.

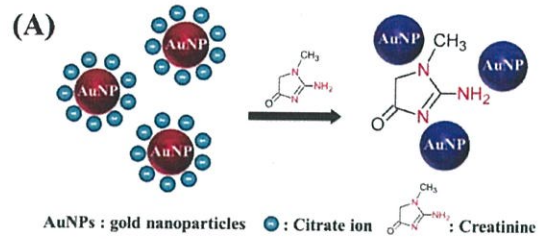

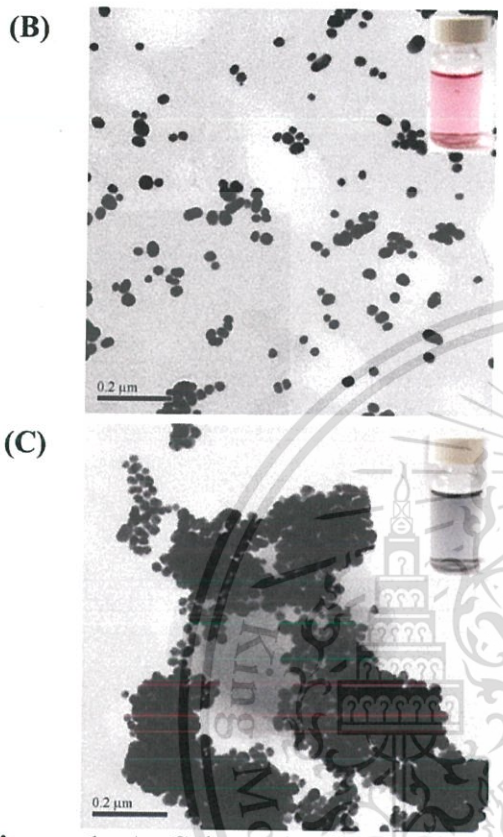

Figure 1. A: Schematic illustration of the interaction of creatinine with AuNPs. B: TEM image of 1.04 nM AuNPs without creatinine and C: TEM image of 1.04 nM AuNPs with 200 mg L^{-1} creatinine. Inset photos present bottles of solutions of B and C, respectively.

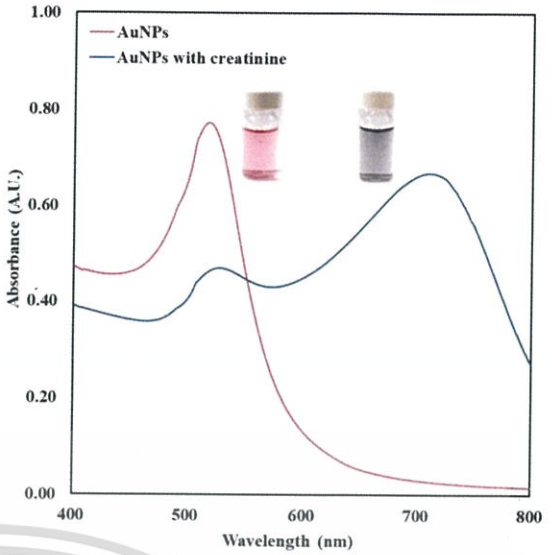

Figure 2. The surface plasmon band of AuNPs solution the in the absence and presence of 200.0 mg L^{-1} creatinine

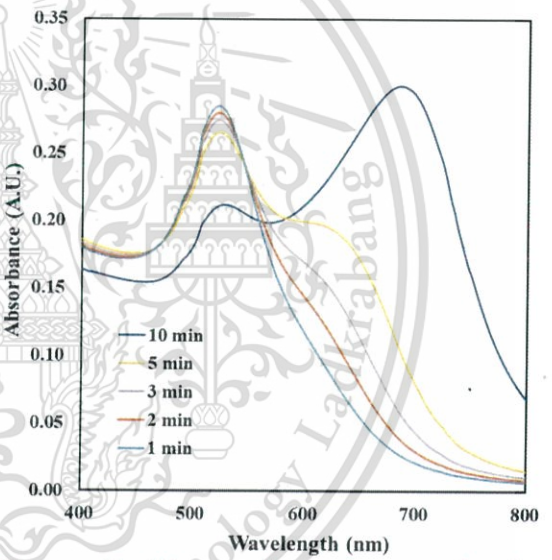

Figure 3. The surface plasmon band of AuNPs solution in the presence of 50.0 mg L^{-1} creatinine recorded at 1 to 10 min

3.3 Effect of the AuNPs concentration

Effect of the concentration of the AuNPs was studied from 0.52 nM to 1.04 nM. Results are shown in Figure 4. The absorbance ratio at 650 and 522 nm (A650/A522) was used to assess the degree of aggregation. When the concentrations were increased, sensitivities and linear relationship were increased. The optimal AuNP concentration of 1.04 nM was selected for further study as it gave the highest sensitivity and linearity.

3.4 Selectivity study

The selectivity of this method was evaluated using other organic small compounds (albumin, uric acid, ascorbic acid, L-glutathione, L-tryptophen, L-serine, L-threonine, L-histidine, L-valine, L-phenylanine and aspartic acid). The interferences concentration was 10-fold higher than that of creatinine. Figure 5A clearly illustrated that only creatinine cause a solution color change from wine-red to blue. The corresponding surface plasmon

bands (Figure 5B) also show that only creatinine cause an increase of absorbance at 650 nm. This suggests that this method is very selective to creatinine.

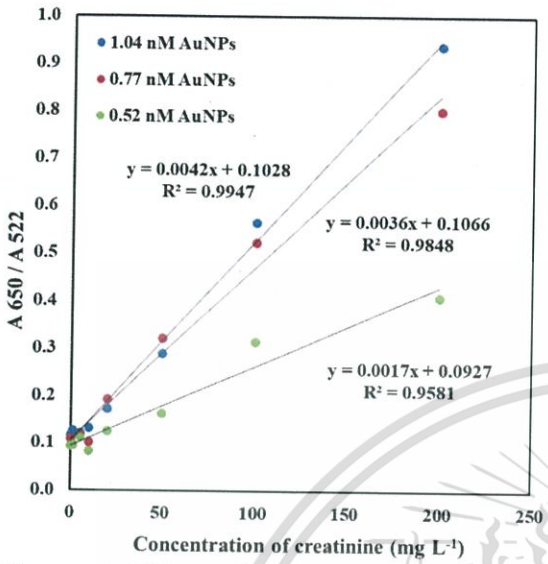

Figure 4. Effect of AuNPs concentration on sensitivity

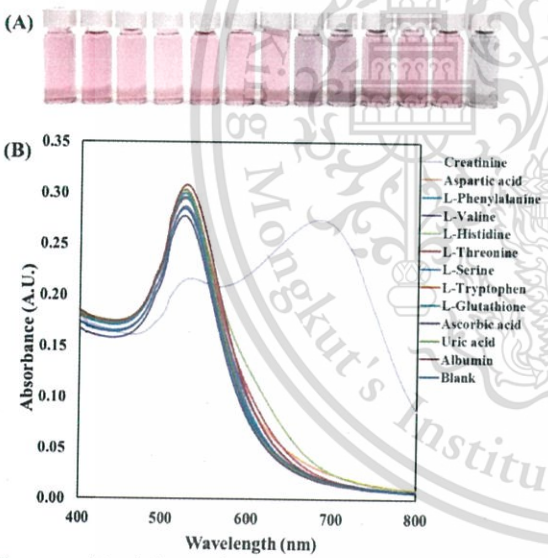

Figure 5. (A): The photograph of AuNPs solutions and (B): The surface plasmon bands of AuNPs solution in the presence of creatinine (200 mg L^{-1}) or interferences (2000 mg L^{-1})

3.5 Colorimetric detection of creatinine

Figure 6 displays the surface plasmon band of the synthesized AuNPs with various concentrations of standard creatinine and the corresponding calibration plot between the absorbance ratio and the standard conditions. It is clearly observed that good linearity is obtained from 0 to 200 mg L^{-1} creatinine.

3.6 Analytical performances

The analytical performances are summarized in Table 1. It gives a good analytical performance.

3.7 Determination of creatinine in urine sample

The developed method was applied to determine the creatinine content in urine of normal volunteers. Urine samples were diluted with water. Any further sample pretreatment is not required. Results in Table 2 are not significantly difference under the statistical paired *t*-test[14] at 95% confidence level (t_{stat} = -0.13, t_{crit} = 2.26). There results imply that the method was successfully validated.

Table 1. Analytical performances of the method for determination of uric acid

Parameter	Value
Linearity range (mg L^{-1})	0 – 200
Regression coefficients (r^2)	0.9947
RSD (%) (n = 5)	2.6 – 4.9
LOD[a] (mg L^{-1})	0.5
LOQ[b] (mg L^{-1})	1.6

[a]LOD = 3SD of blank / slope
[b]LOQ = 10SD of blank / slope

Table 2. Concentrations of creatinine in urine samples

Sample	Concentration (mg L^{-1}, mean ± SD)	
	This work	The Jaffé method
1	233.6 ± 1.3	243.0 ± 4.0
2	256.9 ± 9.7	256.1 ± 8.8
3	150.5 ± 2.0	137.2 ± 0.9
4	121.8 ± 1.8	128.0 ± 1.3
5	107.4 ± 3.9	104.9 ± 6.0
6	228.4 ± 1.8	206.5 ± 4.4
7	171.6 ± 7.8	192.6 ± 10.2
8	226.8 ± 0.1	227.2 ± 7.3
9	197.4 ± 2.3	197.4 ± 9.5
10	94.7 ± 3.2	91.3 ± 5.7

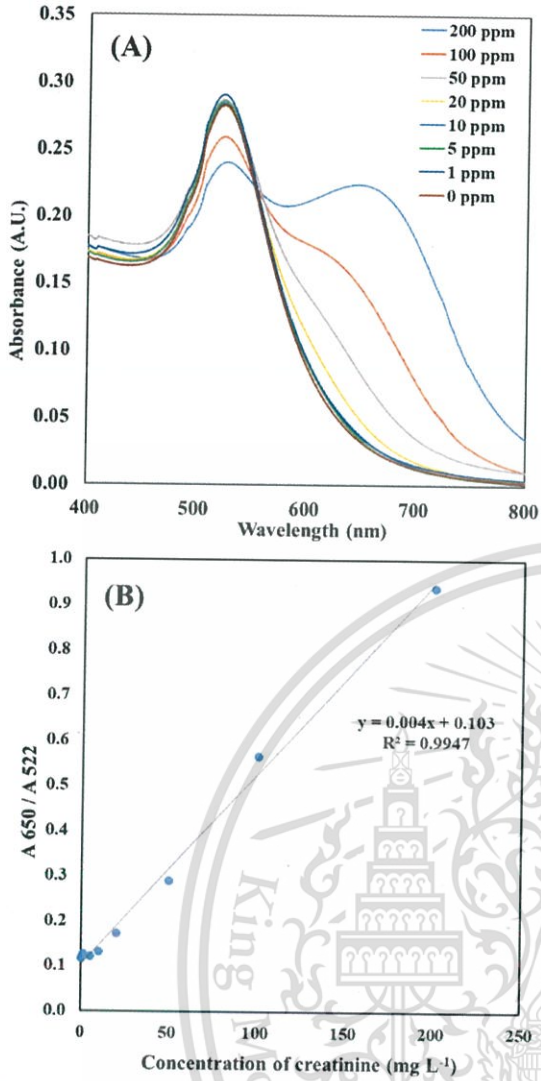

Figure 6. (A): The surface plasmon bands of AuNPs solution in the presence of different creatinine standard solution, (B): The linear plots between the absorbance ratio and the creatinine concentration

4. Conclusion

In this work, a simple method for quantitative analysis of creatinine in urine using label-free gold nanoparticles was accomplishedly developed. Good analytical performance was obtained. As a result, precise and accurate quantification of the creatinine concentration can be obtained. The proposed method was also successfully applied for the creatinine determination in urine samples without any sample pretreatment.

Acknowledgements

Financial supports from the Faculty of Science, King Mongkut's Institute of Technology Ladkrabang is gratefully acknowledged. Instrumental supports from Applied Analytical Chemistry Research Unit, Department of Chemistry, Faculty of Science, King Mongkut's Institute of Technology Ladkrabang are also appreciated.

References

1. Debus, B.; Kirsanov, D.; Yaroshenko, I.; Sidorova, A.; Piven, A.; Legin, A. *Anal. Chim. Acta* **2015**, *895*, 71-79.
2. Vasiliades, J. *Clin. Chem.* **1976**, *22*, 1664-1671.
3. Falcó, P. C.; Genaro, L. A. T.; Lloret, S. M.; Gomez, F. B.; Cabeza, A. S.; Legua, C. M. *Talanta* **2001**, *55*, 1079-1089.
4. Moss, G. A.; Bondar, R. J. L.; Buzzelli, D. M. *Clin. Chem.* **1975**, *21*, 1422-1426.
5. Ogawa, J.; Nirdnoy, W.; Tabata, M.; Yamada, H.; Shimizu, S. *Biosci. Biotech. Biochem.* **1995**, *59*, 2292-2294.
6. Liotta, E.; Gottardo, R.; Bonizzato, L.; Pascali, J. P.; Bertaso, A.; Tagliaro, F. *Clin. Chem.* **2009**, *409*, 52-55.
7. Ambrose, R. T.; Ketchum, D. F.; Smith, J. W. *Clin. Chem.* **1983**, *29*, 256-259.
8. Yuen, P. S. T.; Dunn, S. R.; Miyaji, T.; Yasuda, H.; Sharma K.; Star, R. A. *Am. J. Physiol. Renal. Physiol.* **2004**, *286*, F1116- F1119.
9. Nieh, C. H.; Tsujimura, S.; Shirai, O.; Kano, K. *Anal. Chim. Acta* **2013**, *767*, 128–133.
10. Apyari, V. V.; Arkhipova, V. V.; Dmitrienko, S. G.; Zolotov, Y. A. *J. Anal. Chem.* **2014**, *69*, 4-15.
11. Sittiwong, J.; Unob, F. *Spectrochim. Acta Mol. Biomol. Spectrosc.* **2015**, *138*, 381-386.
12. Turkevich, J.; Stevenson, P. C.; Hillier, J. *Discuss. Faraday Soc.* **1951**, *11*, 55-75.

13. He, Y.; Yu, X. H. *Microchim. Acta* **2015**, *182*, 2037-2043

14. Miller, J. N.; Miller, J. C. Statistics and Chemometrics for Analytical Chemistry, 5th. ed., Pearson Education: Harlow, UK, **2005**

Author Biography

Name	Mr. Arjnarong Mathaweesansurn
Date of Birth	7 January 1988
Address	18/37 Moo. 1, Sothorn, Mueang District, Chachoengsao, 24000 Thailand
Education	(2009) Bachelor of Science in Industrial Chemistry - Analytical Instrumentation, GPA 3.17 King Mongkut's Institute of Technology Ladkrabang. (2012) Master of Science in Analytical Chemistry, GPA 3.75 King Mongkut's Institute of Technology Ladkrabang.

International Publications

1. **A. Mathaweesansurn**, N. Maneerat and N. Choengchan. *A Mobile Phone-based Analyzer for Quantitative Determination of Urinary Albumin using Self-Calibration Approach*, Sensors and Actuators B 242 (2017) 476–483.
2. N. Choengchan, B. Poonthong, **A. Mathaweesansurn**, N. Maneerat, S. Motomizu, N.Ratanawimarnwong and D.Nacapricha. *A 'Dual-acceptor Channel' Membraneless gas-diffusion Unit for Simultaneous Determination of Ethanol and Acetaldehyde in Liquors using Reverse Flow Injection*, Analytical Sciences 34 (2018) 169-175.
3. **A. Mathaweesansurn** , N. Choengchan, P. Khongkaew and C.M. Phechkrajang. *Low-cost Synthesis of Gold Nanoparticles from Reused Traditional Gold Leaf and Its Application for Sensitive and Selective Colorimetric Sensing of Creatinine in Urine*, Current Analytical Chemistry (Accepted). DOI: 10.2174/1573411014666181010130631.

Conference Proceedings

1. **A. Mathaweesansurn**, S. Janyapoon and N. Choengchan. *Separation of Phenolic Compounds in Wood Vinegar using Sequential Injection Chromatography*, Proceedings of Pure and Applied Chemistry International Conference, pp. 57-60, 2013.

2. **A. Mathaweesansurn**, N. Surapanworawate, T. Troangjaroensub, N. Chatapattama, N. Maneerat and N. Choengchan. *Method development for 'point-of-care' analysis of uric acid in urine using an 'in-house' LED spectrometer,* Pure and Applied Chemistry International Conference, pp. 156-161, 2017.
3. K. Phongern, **A. Mathaweesansurn**, N. Maneerat and N. Choengchan. *A design of colorimeter for chemical quantitative analysis based on a web-camera,* 5th International Electrical Engineering Congress, 2017.
4. **A. Mathaweesansurn**, K. Tipanantakun, P. Thaothong, P. Ooybumrung and N. Choengchan. *Label-free gold nanoparticles for spectrophotometric determination of creatinine in urine*, Pure and Applied Chemistry International Conference, pp. AN48-AN52, 2018.
5. S. Thongrod, **A. Mathaweesansurn** and N. Choengchan. *A 'contact stamping' microfluidic paper-based analytical device for determination of creatinine using camera phone and standard addition approach*, Pure and Applied Chemistry International Conference, pp. AN58-AN62, 2018.